University of Trento
University of Brescia
University of Padova
University of Trieste
University of Udine
University IUAV of Venezia

Mariano Angelo Zanini (Ph. D. Student)

MANAGEMENT OF BRIDGE INFRASTRUCTURAL NETWORKS IN SEISMIC AREAS

Prof. Carlo Pellegrino (Tutor)
Prof. Claudio Modena (Tutor)

April, 2015

UNIVERSITY OF TRENTO
Engineering of Civil and Mechanical Structural Systems

Head of the Ph. D. School Prof. Paolo Scardi

Final Examination 22/04/2015

Board of Examiners:
Prof. Jiří Máca (Czech Technical University of Prague)
Prof. Maria Rosaria Pecce (Università degli Studi del Sannio)
Prof. Daniele Zonta (Università degli Studi di Trento)
Dott. Paolo Clemente (UTPRA – Unità Tecnica Caratterizzazione, Prevenzione e Risanamento Ambientale ENEA CRE Casaccia)
Dott. Loris Vincenzi (Università degli Studi di Modena e Reggio Emilia)

SUMMARY

This study deepens key issues related to the seismic emergency management and deterioration state assessment of roadway and railway infrastructural networks by proposing a series of procedures and methodologies through the use of scientific-based analyses in the field of optimal management of infrastructural assets.

This thesis is subdivided in several chapters, in which, the issues of quantification of the bridge structures' deterioration state are intertwined with those related to the estimation of the seismic vulnerability assessment, from punctual level (single bridge) to territorial scale (infrastructural network).

The key topics discussed in this work are, at punctual level, statistical analyses on the effectiveness of *in-situ* investigations for the bridges' seismic fragility estimation, sensitivity analyses on the influence of geometrical parameters on the seismic vulnerability assessment and the construction of fragility curves for bridges subjected to deterioration of key structural components.

At territorial scale, analyses of the restoring costs for bridge stocks, construction of life-cycle curves for bridges subjected to deterioration, simulations of time-dependent earthquake scenarios for infrastructural networks and procedures for the management of seismic emergency for railway networks are presented.

SOMMARIO

Questo studio approfondisce molteplici tematiche inerenti alla gestione dell'emergenza sismica e alla valutazione dello stato di deterioramento delle reti infrastrutturali stradali e ferroviarie proponendo una serie di procedure per la risoluzione delle principali problematiche nel campo della gestione ottimale di *assets* infrastrutturali.

Il lavoro si articola in più capitoli, nei quali, le tematiche della quantificazione dello stato di degrado delle strutture da ponte si intrecciano con gli aspetti legati alla stima della vulnerabilità sismica passando dal livello puntuale (singolo manufatto) a quello territoriale (analisi di rete infrastrutturale).

Tra i vari argomenti chiave toccati in questo lavoro menzioniamo, a livello puntuale, analisi statistiche sull'efficacia dello svolgimento di indagini *in-situ* per la valutazione della vulnerabilità sismica, analisi di sensitività sull'influenza di parametri geometrici sulla vulnerabilità sismica, valutazioni della vulnerabilità sismica per opere soggette a degrado delle componenti strutturali principali.

A livello territoriale, sono stati condotti studi di valutazione dei costi di ripristino e adeguamento strutturale su stock di ponti, valutazioni di curve di ciclo di vita per strutture soggette a deterioramento, simulazioni di scenari sismici-tempo dipendenti di reti infrastrutturali, procedure per la gestione dell'emergenza sismica per reti ferroviarie.

DEDICATION

“Un esercito di cervi guidati da un leone è molto più temibile di un esercito di leoni guidati da un cervo.”
Plutarco

Alla mia cara famiglia

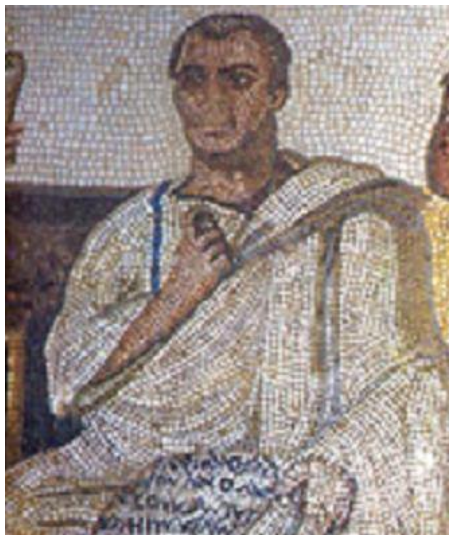

CONTENTS

1 INTRODUCTION

1.1 Background

The fast socio-economic development of many urban areas has often been characterized by the construction of new infrastructures to meet the increasing demands of mobility. Transport networks are indeed essential for carrying out various economic and strategic activities immediately following a catastrophic event mainly to allow initially rescue operations.

Infrastructural networks can experience various natural hazards like earthquakes, floods, windstorms, icing, tsunamis, debris flow and consequently suffer significant economic losses. In particular, lifelines such as transport networks, gas, water, telecommunication facilities subjected to natural hazards can be affected by severe disruptions and a long recovery time to regain complete operability. For this reason, infrastructural networks play a key-role in the social context, and in such way their resilience is fundamental for ensuring their functions, in particular during the emergency and post-emergency phases.

Focusing on transport lifelines, bridges are the most vulnerable singular elements both for roadway and railway systems, and thus major attentions must be directed by public authorities/private companies dealing with their maintenance and retrofit planning.

Another fundamental issue is the evaluation of the effects of ageing due to environmental conditions: concrete cover damage that exposes bars to atmosphere, steel corrosion, concrete damage by icing cycles, ageing of structural materials, etc. can indeed lead to the reduction of the structural capacity of horizontal and vertical structural elements, thus making ageing bridges more vulnerable to natural hazards. In some cases structural deterioration can play a crucial role in the failure of bridge structures subjected to hazardous events. The international scientific community has jet recently deepened this specific combination of factors, trying to estimate in quantitative terms the incidence of deterioration phenomena on the capacity of the main structural elements. These literature studies aimed to better understand the above phenomena, providing procedures for the rational resolution of such problems, which are of great relevance, in particular for European countries,

where the infrastructural network has grown exponentially in the decades following the IInd World War.

1.2 Objectives and scope of the research

This thesis aims to deepen different aspects related to the deterioration assessment and seismic vulnerability estimation of existing bridge structures and provide useful outcomes and insights for authorities dealing with the management of bridge structures. Different analyses are conducted on various bridge stocks belonging to Italian roadway and railway networks starting to the single-structure level and subsequently moving to the network level with the simulation of seismic scenarios. Statistical techniques are used to derive equations and correlations between deterioration indexes, seismic assessment outcomes and cost-benefit parameters. A discussion on the management of the post-earthquake operation of railway networks is illustrated proposing a methodology for the rational control of the railway traffic safety, aimed to minimize the out-of-service time interval.

1.3 Thesis organization

The thesis illustrates in the first part different key issues related to the management and seismic assessment at the bridge level whereas the second part focuses on the management at network level also taking into account economical and transportation models. In particular:

- ***Chapter 2*** briefly describes structural and functional deficiencies, related to natural ageing, degradation processes, poor maintenance, increased traffic loads and upgraded safety standards with nowadays affect existing bridge structural typologies;
- ***Chapter 3*** illustrates a proposal of an integrated procedure for the evaluation of the maintenance condition state and the seismic vulnerability assessment of existing road bridges;

- ***Chapter 4*** presents a statistically-based algorithm for the prediction of bridges' remaining service-life on the basis of the outcomes deriving from the execution of the visual inspection surveys;
- ***Chapter 5*** shows some insights on planning of seismic vulnerability assessment of large stocks of bridges with a real application to the road network of the Veneto region, Italy;
- ***Chapter 6*** illustrates an example of practical estimation of analytical seismic fragility curves for a common existing bridge typology in the Italian transportation network;
- ***Chapter 7*** explores the effects of degradation phenomena on the seismic vulnerability of existing bridges and benefits related to some types of common retrofitting interventions;
- ***Chapter 8*** presents a simplified methodology for estimating the vulnerability of an entire transport network and its time evolution;
- ***Chapter 9*** illustrates *Br.I.N.S.E. v2.0*, a specific tool for the simulation of scenario earthquakes and the evaluation of potential damages on bridge portfolios;
- Finally, ***Chapter 10*** reports main conclusions and recommendations for further studies are suggested.

2 TYPICAL DETERIORATION PROCESSES IN REINFORCED CONCRETE, STEEL AND MASONRY BRIDGES

2.1 Introduction

In recent years the condition appraisal and refurbishment of existing bridges has become a standing problem for bridge owners and administrators in all developed countries. A lot of in-service bridges exhibit in fact dimensional, structural and functional deficiencies as they were designed for performances levels that were progressively made inadequate by more and more demanding traffic conditions and structural safety requirements. Increasing number of vehicles, heavier weight/axle loads, higher traffic volumes, increasing speeds of vehicles and related dynamic effects are in fact reflected in the updating process of codes and standards for road and railway bridges. In addition, deterioration and damage propagation effects are undermining the efficiency of all components in any existing bridge typology.

Existing bridges, which are under-designed for such service conditions, typically would need on one side interventions, to widen the deck and protect different types of lanes, in order to enhance the safety of users, and, on the other side, measures to counteract different phenomena of “mechanical damage”. These processes are emphasized by, and/or emphasize, decay connected to environmental (chemical or physical) actions, in a general context of poor or completely lacking maintenance procedures.

Such situation is made even more complicated in Italy, where in addition to the above mentioned types of “vulnerabilities” affecting existing bridge structures, also the fragility connected to seismic actions is to be taken into account. The fact that the national territory is subject to significant, if not high, seismic hazard, in fact has been only recently recognized (*Ordinance of the Presidency of the Council of Ministers* n. 3274, 2003) by the national structural codes, so that in many cases bridges are very vulnerable to seismic actions as they have been designed and constructed completely ignoring seismic design specifications. What makes such situation particularly engaging is the fact that the new generation of national structural codes makes it compulsory to perform seismic verification, and correspondingly to plan adequate retrofitting interventions, of

“strategic” - in terms of Civil Protection purposes- structures, such as bridges usually are (Modena et al. 2004).
Strengthening can often be a cost-effective alternative to the replacement of the old structures, especially if indirect and social costs related to the closure of the corresponding road connections are evaluated in relation to the traffic demand.
In this context what is crucial from a structural engineering point of view is to define adequate, reliable assessment procedures, capable of recognizing and taking into account the specific sources of “vulnerability” of each structure typology to any type of action. This is the basis of both unavoidable ranking procedures, establishing priority of intervention and allowing for the optimum use of “limited resources”, and of design strategies really able to fulfill the above mentioned scope of devising “ways for extending the life of structures whilst observing tight cost constraints.
Prior to a detailed evaluation of the vulnerability characteristics of a single structure, a general recognition has to be carried out at network level. In every *Bridge Management System* (*BMS*) the definition of the bridge inventory represents the starting point, and concerns the identification of the bridge (geographical position, road, etc.), the description of the technical data (geometry, materials, structural system etc.) and of the maintenance data (condition, inspections, monitoring, etc.).
The database arranged at the University of Padova, *I.Br.I.D.* (*Italian Bridge Interactive Database, http://ibrid.dic.unipd.it*), gathering information about nearly 500 bridges, belonging to the Veneto region road network (in the North-Eastern part of Italy), is an example (Figure 2.1). The statistical distribution of construction material for existing road bridges obtained by this database, is in line with other European databases, and shows the prevalence of *RC* and *PRC* structures, secondly a relevant percentage of masonry arch bridges and finally a small number of steel-composite structures, (generally more recent, built from the beginning of the *90’s*), while a residual percentage of structures is not classified.
A preliminary condition rating of reinforced concrete-prestressed reinforced concrete (*RC-PRC*), steel and masonry bridges is generally done at network level by means of simple visual inspection (e.g. among others, Pellegrino et al. 2011). On the basis of this preliminary information, the network managing authority can define a priority plan and allocate the available resources for the detailed assessment, verification and intervention on structures in the worst state of condition.

The condition assessment of an existing bridge requires a complex comprehensive approach. The detailed knowledge of the structure can involve both the use of standard procedures, like *in-situ* and laboratory tests, by which the characterization of material properties and of the principal effects of deterioration phenomena are obtained, and of less conventional tools, such as structural monitoring and dynamic identification techniques.

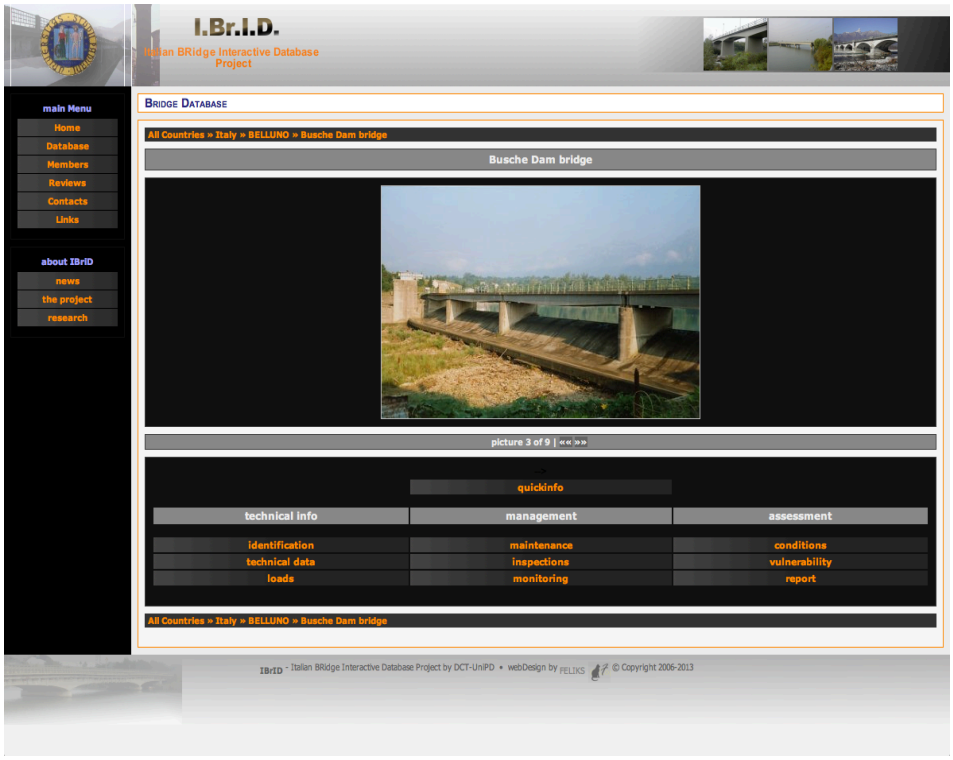

Fig. 2.1 The I.Br.I.D. database developed by the University of Padova.

In addition to the more commonly addressed issues of static strength and stability, consideration should also be given to a broad range of factors including, dynamic and seismic behavior, long-term deformations, fatigue effects, durability (functional efficiency) and possibly other aspects too.

In this chapter, the main degradation processes and typical defects of the original design are briefly described with reference to the most usual bridge typologies: *RC* and *PRC* bridges, masonry/stone bridges and steel/composite girder bridges.

2.2 Deterioration processes in *RC*/*PRC* bridge typologies

In Italy most common types of existing road bridges are represented by *RC* and *PRC* bridges, as already said with reference to the *I.Br.I.D.* database. Many of them were built in the period 1945-1960 in conditions of general shortage of construction materials, and without any motivation for quality control.
Deterioration processes affecting *RC* bridges are due to environmental actions, whose effects are in most of cases accelerated over time by poor maintenance. Environmental actions can be classified respectively in chemical, physical and biological degradation mechanisms (SB-ICA 2007):

- *physical actions* are typically due to the freeze-thaw action, water penetration, thermal variations, environmental vibrations;
- *chemical actions* in bridges are carbonation (carbon dioxide, from the atmosphere, enters to concrete and reacts with the hydroxides to form carbonates and water), corrosion (oxidation of metal causing losses of material), salt actions, alkali-silica reaction, sulphate attacks;
- *biological degradation* is due to accumulation of dirt and rubbish and the activity of living organisms.

Among physical actions, in addition to accidental damages from impacts and cracks due to thermal effects, freezing and thawing cycles represent one of the most common physical causes of degradation for externally exposed *RC* elements. It could occur when the concrete is of insufficient pore size and pore distribution. In combination with critical water saturation (>91%) the freezing of water could lead to concrete deterioration due to the volume expansion. Deterioration symptoms are an ongoing loss of concrete surface, local popouts or micro cracking and loss of concrete strength at later stages. In general concrete with low *w*/*c*-ratio has higher frost resistance than concrete with high w/c-ratio. Proper frost resistance is given if the air content is approximately about 4% in volume and if the air-bubbles are well distributed.
Cracking and spalling of concrete cover, combined with bar oxidation, represent the degradation process affecting most of the elements of existing *RC* bridges, even if they are exposed in a non aggressive environmental condition (Figure 2.2). The alkaline nature and density of concrete represents a chemical and physical barrier against corrosion attacks on reinforcing steel bars. Durability of concrete structures depends on the protection that the surrounding concrete provides to the steel reinforcement against penetration of chlorides, water and oxygen, which are some of the essential ingredients that induce reinforcement

corrosion. In particular, the carbonation process of the concrete surface, when there is a limited concrete cover, paves the way to corrosion, caused by water and oxygen. General corrosion is associated with the formation of iron oxides, commonly referred to as “brown rust”. The volume of these oxides is several times greater than that of the parent steel. The volumetric expansion of a corroded bar generates tensile hoop strains in the surrounding concrete, leading to the development of longitudinal cracking and to the subsequent spalling of the concrete cover.

Many deficiencies exhibited by existing *RC* bridges are the consequence of lack of durability rules in the original design and poor quality control during construction, leading to an early deterioration of structure performance.

Fig.2.2 An overview of possible defects detectable on RC/PRC bridges.

The most common design defects related to the superstructure elements can be outlined as follows:

- *insufficient concrete cover:* this deficiency is widespread among existing *RC-PRC* bridges. The insufficient concrete cover does not offer enough protection against the penetration of carbonation, and corrosion reduces the effective section of reinforcing steel bars;
- *sub-standard concrete quality*: insufficient compaction, poor curing, excessive porosity, use of improper constituents (aggregate, admixtures, water). The frequent adoption in existing bridges of porous concrete, made by using a high water/cement ratio, led to an acceleration of the carbonation phenomenon in the course of time. A related aspect, which can lead to possible corrosion effects in post-tensioned cables, is represented by the *insufficient grouting of tendon ducts*;
- *insufficient standards in reinforcement design*: it is a general design defect, due to insufficient standards related to the adoption of overstrenght factors and detailing rules accounting for dynamic amplification effects, possible increment of variable axle loads, shrinkage and thermal effects. This often results in poor confinement of elements, and inadequate shear reinforcement. It is generally coupled with the next effect;
- *under-dimensioning of secondary elements for effective traffic loads*, in terms of thickness, stiffness, reinforcement. This is generally due to an underestimation of effective axle loads incrementing during the in-service life of the structure. The consequences are shear cracks, bending cracks, large deflections, which most times can be easily detected also by simple visual inspection;
- *weakness of details:* it is strictly interrelated with lack of durability rules in the original design, Structural connections and nodes are frequently the elements most exposed to environmental agents, without any protection, and often represent the starting points of the degradation process. Details like saddles in gerber structures, anchorages of tie-rods in arches, ancillary structures like approaching slabs are often not well defined in reinforcement detailing, with overlapping bars not adequately anchored, while often and approximate solutions have been adopted for casting *in-situ* during construction without ensuring the minimum required cover;

- *inefficient bearings:* in many existing bridges the bearings are inefficient or sometimes completely lacking, with main beams resting directly on pier or abutment tops, without any supporting devices;
- *insufficiently durable expansion joints:* expansion joints are often completely lacking in existing bridges, or worn away due to poor maintenance and dynamic effects related to the passage of vehicles. Expansion joints are exposed to weathering, and water coming through them represent the main source of degradation for the *RC* elements;
- *inadequate waterproofing and drainage system*: inadequate control of drainage is the major cause of deterioration of concrete bridge components where roadway de-icing chemicals are used;
- *lack of seismic design specifications*: earthquake resistant rules for bridge design were only recently adopted by the Italian code. Thus existing bridges exhibit inadequate strength of piers and abutments to resist lateral seismic forces, the deficiencies regarding in particular shear reinforcement, detailing for section ductility, and foundation capacity. Also bearings and supports are generally inadequate for the transmission of inertial loads to the substructure.

In addition to the design defects affecting deck and elevations, it is necessary to consider those related to the foundation systems, like static inadequacy for reduction of bearing capacity and/or increase of loads, differential settlements and/or undermining at foundation base.

2.3 Deterioration processes in masonry/stone bridge typologies

Thousands of old road and railway masonry arch bridges are still in operation in the Italian transportation network. According to a recent survey approximately 40%, of the railway bridges in Europe are masonry arch bridges (SB-ICA 2007), and the same percentage is substantially representative also for Italy. Among existing road bridges the relative percentage is smaller, but still very significant, about 25% with reference to the *I.Br.I.D*. database.

Most of masonry arch bridges are part of the historical heritage of the XIXth century. Many rehabilitation techniques, which are derived from the historical

heritage restoration field and were reserved in the past to monumental buildings, can be effectively used also for these type of structures.

Most of masonry arch bridges being in service since more than 100 years, the appearance of damages is inevitable, partly due to action of nature and aging of the masonry materials in bad maintenance condition, and partly due in increased traffic loads, with the passage of time.

Masonry arch bridges are usually quite robust structural systems, their possible weakness not being usually related to the state of stress under permanent uniform symmetric loads, which is low in respect to material characteristics, but rather to the trigger of antimetric collapse mechanisms, due to vertical (heavy traffic axle loads) or horizontal (seismic) forces.

The main deficiencies in masonry arch bridges can be broadly classified into two categories: foundation damages and superstructure damages.

Among the foundation various defects, local undermining, differential settlements, and masonry dislocations due to loss of mortar joint represent the most common.

The main problem for identifying foundation damages consists in the difficulty in inspecting underground structures. Therefore, the first step to detect the problems of any wrong workings of the foundation system, implies in the observation and analysis of the symptoms, eventually shown by the superstructure, being the consequence of rotations or differential movements at the foundation level. Masonry bridges, due to their high stiffness and their brittle structural behaviour, are generally unable to absorb foundation settlements without structural damage.

As for the superstructure defects, they are more easily detectable by visual inspection (Figures 2.3). The main deficiencies can be related to:

- *degradation of materials*, such as brick deterioration, the loss of mortar joint, the loss of brick units and salt efflorescence in the bricks. This phenomena are often due to inadequate rainwater drainage system, freeze-thaw cycles and penetrating vegetation;
- *arch barrel deformations* with longitudinal or transverse cracking;
- *opening of arch joints*, separation between bricks rings in multi barrel vaults;
- *spandrel wall movements*: sliding, bulging, detachment from the barrel. Spandrel walls have small inertia and are generally weak elements in respect to out-of-plane behaviour (pressures orthogonal to the spandrel

walls are due to the weight of the infill material and traffic loads, as well as to horizontal transverse seismic action);

- *fractures* in the piers and in the wing walls.

Fig.2.3 An overview of possible defects detectable on masonry/stone bridges.

2.4 Deterioration processes in steel bridges

To date steel and composite bridge decks represent a modest percentage of the existing road bridges in Italy, being them extensively used as substitutive of precast *RC* girder decks only since the middle *80's*. Among steel and composite structures, orthotropic steel decks represent even more a reduced number of existing bridges, being generally applied to medium-long spans, while composite decks are adopted in most of cases.

Steel bridges are distinguished by structural lightness. The high strength to weight ratio of steel has numerous advantages, and the reduced self-weight makes them also particularly suitable for seismic areas. On the other hand, the effect of fatigue is particularly relevant for steel decks, since the influence of load cycles on the serviceability limit stress values is very high if compared to the relatively low dead weights.

One of the predominant effects of the degradation process in steel bridges are material corrosion and delamination of principal structural elements (Figure 2.4).

These phenomena particularly appear in structures where the protective layers have been damaged by environmental agents and the protective coating has not been properly maintained. The corrosion phenomenon can be accelerated in existing bridges by several factors like ponding of moisture, presence of cracks, chemical attacks, different metals in contact, presence of cracks, concentration of salts through evaporation, stray electrical currents.
Heavy corroded members have a reduced cross section area, which leads to a reduction of the resistance and stability of the structural element. Corrosive phenomena also influence the mechanical characteristics of the steel material, reducing its design strength.
It is common opinion that a valid alternative to protective coating is represented by corten steel, which exhibits superior corrosion resistance over regular carbon steel as a result of the development of a protective oxide film on the metals surface that slows down further corrosion. However it has been observed that in particular environmental condition also in auto-protective steel (corten) decks, corrosion and delamination of the surface of structural elements can significantly affect the bridge state of condition and residual service life.
During the *90's*, several researches focused on the assessment of existing steel structures, mainly those very much exposed to fatigue loading such as bridges or crane supporting structures (Caramelli et al. 1990; Caramelli and Croce 2000). These studies, as well as lessons learned from the unnecessary demolition of great structures or the poor performance of strengthening measures on some old structures led to a better understanding of the response of existing structures and therefore improved assessment methods.
Orthotropic steel decks, directly subjected to traffic loads in road bridges, are very sensitive to fatigue: in most cases, fatigue defects appear as fatigue cracks, which affect the top plates, longitudinal ribs and cross-beams of the deck (Figure 2.4). They can propagate if exposed to cyclic loading due to traffic loads but also to temperature differences or wind loads (de Jong 2004; de Jong and Boersma 2004). Fatigue fractures are caused by the simultaneous action of cyclic stress, tensile stress, and plastic strain (SB-ICA 2007): cyclic stress initiates a crack and tensile stress propagates it, then the final sudden failure of the remaining cross section occurs by either shear or brittle fracture. The fatigue fracture can be quite easily recognized also by visual inspection because of its typically silky and smooth appearance.
In a steel bridge, after visual inspection of structural elements, to detect spatial distribution of the damage, it is very important to carry out a series of destructive

tests on samples taken from the bridge structural elements, in order to characterize the main material properties and verify the welds. The most important tests used in this kind of analyses are traction tests, X-ray, metallographic tests, electron microscope scanning and Vickers hardness tests. A metallographic test image can confirm the diagnosis if striations are present on the crack surface.

Fig.2.4 An overview of possible defects detectable on steel bridges.

Generally speaking, the poor fatigue performance exhibited by this kind of steel bridges built in the last 30 years is related to insufficient fatigue design (Caramelli et al. 1990) and lack of sensitivity to the problem. The main causes

of fatigue in steel decks are often linked to inappropriate structural details adopted, welding defects included at the time of fabrication or unforeseen stresses and deformations at the joints. Also poor maintenance can play an important role, the dynamic effects of truck-loads being often amplified by the bad condition of the deck bituminous layer.

2.5 Conclusions

Today retrofit and strengthening interventions for existing bridges are made more and more necessary by structural and functional deficiencies, related to natural ageing, degradation processes, poor maintenance, increased traffic loads and upgraded safety standards.
Deterioration processes reduce the strength of structural components and the comfort level to road users. The codes, in the course of bridge service life, have been updated due to changes in the vehicular traffic, thus imposing static retrofit of structures and functional widening of decks. In addition, in Italy, seismic retrofitting of bridges has recently become compulsory for all structures having a strategic function for Civil Protection activities.
The condition assessment of an existing bridge requires a complex comprehensive approach deeply involving both the use of standard procedures, like *in-situ* and laboratory tests and less conventional tools such as structural monitoring and dynamic identification techniques.

3 MANAGEMENT OF BRIDGES' MAINTENANCE AND SEISMIC ASSESSMENT

3.1 Introduction

The most significant investments in economic and technological terms on infrastructural networks are often focused on major structures, such as bridges and viaducts. Generally, an increasing demand to improve the management methods of bridges is becoming evident. Many road and rail managing authorities have made a significant effort to develop Bridge Management Systems (*BMSs*) with the aim of evaluating the condition of each bridge belonging to an asset of managed structures (Zonta et al. 2007); Zanini et al. 2013; Biondini et al. 2014), and thus to provide, useful information when allocating resources and establishing management policies in a bridge network (Carturan et al. 2014). A *BMS* represents a systematic methodology with which a bridge public authority can manage the whole activities related to the maintenance of its bridge structures asset (Hudson et al. 1993) in order to optimize the life-cycle management of each structure and avoid any kind of failure or bridge out of service which can lead to severe indirect losses to infrastructure's users. Several *BMSs* have been developed over years: Thoft-Christensen (1995) proposed one for reliability theory, Markow (1995) suggested one for highways, Kitada et al. (2000) developed one specifically thought for steel bridges. During the last decade, several research projects focused on the themes of the management at network level of existing bridges have been financed by the European Commission and related guidelines have been produced i.e. *BR.I.M.E.* (2001), *COST345* (2004), *SA.MA.R.I.S.* (2005) and *Sustainable Bridges* (2006). In *BMSs* currently available a decision making process is almost dependent on a combination of the quantitative/qualitative information obtained from *in-situ* investigations and visual inspections. The scientific community has been deepened these topics and contributed to the development of many *BMSs* currently in use worldwide. Referring to European experiences, contributions provided by Franchetti et al. (2004), Pellegrino et al. (2004); Zonta et al. (2007); Pellegrino et al. (2011); Hofmann et al. (2012); Kamya (2012); Söderqvist and Veijola (2012); Torkkeli and Lämsä (2012); Yue

et al. (2012); Fruguglietti and Pasqualato (2014), Mendonça and Brito (2014) and Powers and Hinkeesing (2014) can represent the recent state of art on this specific field. Issues related to the seismic assessment of existing bridges have been also considered in this work, since bridges have been proven to be the most vulnerable elements in transportation networks subjected to seismic events. Past experiences have shown how bridges in their life can experience structural problems due to environmental conditions and natural disasters: concrete cover damage that exposes bars to atmosphere, steel corrosion, concrete damage by icing cycles, ageing of structural materials are some causes leading to the degradation of reinforced concrete bridges' mechanical properties, thus amplifying the effects of a quake occurrence and increasing the risk of structural local - or in the worst cases global – collapses (Franchin et al. 2006; Modena et al. 2014; Morbin et al. 2015). The optimal distribution of a limited budget is therefore a challenge connected to prioritization issues in order to maximize the service level of an infrastructural system: in this way, maintenance interventions against natural ageing and seismic retrofit interventions aimed to reduce local/global structural vulnerabilities are intertwined, assuming the role of the two major issues in the rational bridge management process for a public authority or a private company.
Although all these issues concerning both the design of *BMSs* and the seismic assessment of existing bridges have been exhaustively deepened by several authors in literature, few studies have been conducted from the economical point of view, traducing visual inspection and seismic assessment outcomes in economical terms. In this chapter the description of an extensive activity of visual inspections and seismic vulnerability analysis has been performed on 150 road bridges with the aim to provide useful provisional equation for the estimation of maintenance and seismic retrofit costs for reinforced concrete/prestressed reinforced concrete and masonry bridges.

3.2 Procedure for the state of maintenance assessment

The procedure for the state of maintenance assessment of bridges adopted in this work is that described in Pellegrino et al. 2011. In the following, a synthetic description of the method is shown. The system of inspections is the visual

survey method, according to standards of most countries (*BR.I.M.E.* 2001) and by the Italian codes (Italian Ministry of Infrastructures, 2008). Visual inspections can be undertaken on main structural and non-structural elements of a bridge to assess their condition without using special equipment or traffic flow restrictions. The method lead to define a global parameter called *Total Sufficiency Rating* (*TSR*) which represent a comprehensive qualitative indicator of the health state of each bridge structure. The calculation of the *TSR* parameter is performed using a specific algorithm, based on the definition of the *Condition Value* (*CV*) of each element composing a bridge. The *CV* represents a condition related to a precise group of defects of the element for which it is estimated. For every inspectionable element of the bridge it is possible to define a *CV* value from 1 to 5; in case it is not possible to express any evaluation, *CV* is assumed equal to 0. Table 3.1 describes the gravity of the detected defects for each *CV*.

Defects	***CV***
No judgement	0
No meaningful defect	1
Minor defects that do not cause damage	2
Moderate defects that could cause damage	3
Severe defects that cause damage	4
Non-functional or non-existent element	5

Table 3.1 The Condition Value (CV).

Once defined a *CV* for each visible element, specific *Conversion Factor* (*CF*), *Location Factor* (*LF*) and *Weight* (*W*) are considered in order to give a different relative significance to every bridge element that have to be evaluated, in relation to its relative importance in the definition of the *TSR* value. In this work, the datasheets implemented by Pellegrino et al. 2011 for a rapid evaluation of the *CV* of each single bridge element, were improved by defining for each specific *CV* – defined by a series of detectable defects induced by different causes – a specific possible maintenance intervention protocol characterized by different relative cost values. In Table 3.2, an example of updated datasheet related to a reinforced concrete beam is shown. The subsequent step is the definition of the *Element Sufficiency Rating* (*ESR*), i.e. the 'grade of importance' of a single bridge element, as follows:

$$ESR = CF \times LF \times (RT \times TI \times NBI \times AF) \quad (3.1)$$

where *RT* is the *Road Type factor* (Table 3.3), *TI* is the T*raffic Index factor* (Table 3.4), *NBI* is the N*etwork Bridge Importance factor* (Table 3.5) and *AF* is the A*ge Factor* (Table 3.6). These corrective coefficients are conceived for taking into account the road type to which a bridge belongs, the daily traffic volume on the bridge, the importance of the bridge into the network and its ageing.

CV	Visual aspects	Possible causes	Possible maintenance interventions [€/ml]	Cost [€/ml]
0	No judgement	-	-	-
1	No defects	-	No maintenance interventions	0
2	Superficial defects of concrete Superficial removing of previous repair Regular grid of thin cracks (w < 0,3 mm) No deep cracks on the top (w < 0,3 mm) Some exposed bars Moisture traces on the top Any protective elements corroded Accidental superficial damages (only concrete cover involved)	Construction errors Freeze-thaw phenomena, run-off, infiltration of water, overload, river current actions, shrinkage, temperature variations, localized tension on abutments, absence or lack of functionality of supports Insufficient rebars Lack of waterproofing Physical or chemical agents Impact of vehicles, vessels, solid transport (river)	Concrete surface cleaning, to be performed only in the areas speckled by sandblasting and brushing, in order to obtain clean surfaces in such a way as to render them free of foreign elements and eliminate cortically weak areas. Including transport and landfilling waste material. €/ml 50,00 Concrete surfaces shaving, for an average thickness of 3 mm, by spraying or hand mortar, premixed, polymer modified, one-component, thixotropic, equipped with synthetic polyacrylonitrile fibers, resistant to aggressive environment. Including cleaning discovered rebars, support saturation, application in several layers and finishing €/ml 107,50 Provision and application of two-component epoxy that carry out the function of curing the material recovery and primer for any subsequent application of a protective elastic aliphatic polyurethane €/ml 22,50 Provision and application of protective elastic aliphatic polyurethane €/ml 87,50	267
3	Extensive and deep cracks (w > 0,3 mm) Network of horizontal and vertical cracks with branches around the aggregate's particles Concrete discoloration, rust stains Infiltrations of water,	Freeze-thaw phenomena, shrinkage, temperature variations, carbonation, chloride attacks, alkali-aggregate (*AAR*) or alkali-silicate (*ASR*) reaction, overloads, high localized tensions Initial sulphur attack	Cortical demolition of portions of structures to a depth equal to the concrete cover, to be carried by hand or with hammers being careful not to damage the existing reinforcing bars. Including blasting the final plan, vigorous washing with water under pressure and landfilling of waste material €/ml 60,00 Corrosion coating, with organic inhibitor, high thickness suitable for protection of reinforcing bars €/ml 2,00 Restoration of deteriorated concrete structures with a single layer from 1 to 5 cm, with the use of welded mesh for interventions of a thickness greater than 2 cm, by the application of cement mortar premixed with B-component,	

	efflorescence, scaling, traces of salts Non negligible accidental damages	Carbonation, chlorides, problems in the drainage system, poor quality of concrete, deposits of salts Impact of vehicles, vessels, solid transport (river)	expansion contrasted with aging in air, thixotropic, containing synthetic polyacrylonitrile fibers, resistant to aggressive environment. Considering an intervention of 2 cm thickness €/ml 215,00 Provision and application of two-component epoxy that carry out the function of curing the material recovery and primer for any subsequent application of a protective elastic aliphatic polyurethane €/ml 22,50 Provision and application of protective elastic aliphatic polyurethane €/ml 87,50	385
4	Craters, detachments, delamination Exposed corroded bars (loss of section < 20%) Percolation of water, salt deposits, stalactites Accidental significant damages (damaged rebars)	Freeze-thaw phenomena, insufficient rebars, carbonation, problems in the drainage system, chlorides, alkali-aggregate reaction Poor quality of porous concrete Lack of waterproofing, use of chlorides Impact of vehicles, vessels, solid transport (river)	Hydro-demolition and removal of cortical conglomerate of intradox deck or on vertical surfaces of piers and abutments for their rehabilitation, performed with high pressure water jets, including any mechanical brushing or sandblasting of reinforcing bars existing supply water, landfill of waste material. Excluded from price possible installation of scaffolding. €/ml 385,00 Corrosion coating, with organic inhibitor, high thickness suitable for protection of reinforcing bars €/ml 2,00 Provision and installation of welded steel wires of improved adhesion of any size and diameter to be applied on the outside of the reinforcement rods, stripped prior to reinforcement of concrete castings or rehabilitation, including cutting, shaping, the scrap, overlapping and fixing with iron wires ligatures. Excluded from the price any scaffolding. €/ml 15,00 Restoration of deteriorated concrete structures with a single layer from 1 to 5 cm, with the use of welded mesh for interventions of a thickness greater than 2 cm, by the application of cement mortar premixed with B-component, expansion contrasted with aging in air, thixotropic, containing synthetic polyacrylonitrile fibers, resistant to aggressive environment. Considering an intervention of 2 cm thickness €/ml 430,00 Provision and application of two-component epoxy that carry out the function of curing the material recovery and primer for any subsequent application of a protective elastic aliphatic polyurethane €/ml 22,50 Provision and application of protective elastic aliphatic polyurethane €/ml 87,50	940

5	Great detachment of concrete Exposed corroded bars (loss of section > 20%) Great percolation of water, large deposits of salts and stalactites Absolutely significant damages (cut rebars)	Freeze-thaw phenomena, insufficient rebars, carbonation, problems in the drainage system, chlorides, alkali-aggregate reaction Lack of waterproofing, use of chlorides Impact of vehicles, vessels, solid transport (river)	Hydro-demolition and removal of cortical conglomerate of intradox deck or on vertical surfaces of piers and abutments for their rehabilitation, performed with high pressure water jets, including any mechanical brushing or sandblasting of reinforcing bars existing supply water, landfill of waste material. Excluded from price possible installation of scaffolding. €/ml 385,00 Arrangement of reinforcing bars, ended the demolition. Including burdens for cutting, straightening, new folds, repositioning of the bars, ligatures, wire / hooks to tie, spacers, and all possible measures to make existing reinforcing bars eligible for any treatment or concrete cast. Excluded from price possible installation of scaffolding. €/ml 14,00 Provision and installation of welded steel wires of improved adhesion of any size and diameter to be applied on the outside of the reinforcement rods, stripped prior to reinforcement of concrete castings or rehabilitation, including cutting, shaping, the scrap, overlapping and fixing with iron wires ligatures. Excluded from the price any scaffolding. €/ml 15,00 Restoration of concrete (also with increased section) for thicknesses from 6 to 10 cm, by means of application for casting (horizontal structures) or jacketing (vertical structures) of cementitious grout, premixed, two-component, expansion countered, reo-dynamic, provided with synthetic fibers polyacrylonitrile, resistant to aggressive environment. The price includes all burden associated to working, the cleanliness of the existing bars and the mortar surface finishing. €/ml 537,50 Structural retrofit by the use of *FRP* unidirectional carbon fibers with high elastic modulus, impregnated *in-situ* with the polymer matrix. The price includes all burdens related to the operations of setting up of the fibrous reinforcement: edges rounding, surface imperfections grinding and sanding, applying epoxy primer, apply skim coat, epoxy adhesive application, application fibrous reinforcement. €/ml 507,00 Provision and application of two-component epoxy that carry out the function of curing the material recovery and primer for any subsequent application of a protective elastic aliphatic polyurethane €/ml 22,50 Provision and application of protective elastic aliphatic polyurethane €/ml 87,50	1570

Table 3.2 Example of a datasheet for Condition Value (CV) maintenance intervention costs definition of a reinforced concrete beam.

Road	*RT*
Highway	0.80
National road	0.90
Provincial road	0.95
Secondary road	1.00

Table 3.3 Road type (RT) factors.

Traffic [in vehicles per day]	*TI*
High (> 20000 vpd)	0.90
Middle 6000-20000 vpd	0.95
Low (< 6000 vpd)	1.00

Table 3.4 Traffic index (TI).

Situation	*NBI*
1: long deviation on unsuitable alternative road	0.96
2. short deviation on unsuitable alternative road or long deviation on suitable alternative road	0.98
3. short deviation on suitable alternative road	1.00

Table 3.5 Network bridge importance (NBI).

Year of construction	*AF*
Before 1900	0.97
1900-1945	0.98
1946-1970	0.99
1971-present	1.00

Table 3.6 Age factor (AF).

In such way issues concerning the specific element health state and the bridge state implication on the infrastructural system to which it belongs are both considered in the estimate. Four levels of efficiency have been established for the bridge elements, as shown in Table 3.7. Once defined the *ESR* value, the calculation of the *TSR* has been performed with the following equation:

$$TSR = \frac{100 \cdot TSR_{real} + TSR_{\min} \cdot CoF}{100 + CoF} \tag{3.2}$$

where TSR_{real} is calculated as shown in Equation 3.3, TSR_{min} is estimated assuming $CV = 5$ for all the elements that are not evaluated even if present and

CoF is derived with Equation 3.4. Table 3.8 represents the four levels of efficiency established for a whole bridge structure.

$$TSR_{real} = \frac{10 \cdot RF \cdot NBI \cdot AF \cdot \sum_{i=1}^{n} \left(CF_i \cdot W_i \right)}{\sum_{i=1}^{n} W_i} \tag{3.3}$$

$$CoF = \frac{100 \sum_{i=1}^{t} W_i}{\sum_{i=1}^{n} W_i} \tag{3.4}$$

Level of efficiency	Level of urgency for action	***ESR***
1	Maximum urgency for action	1-10
2	Short-term intervention	11-20
3	Medium-term intervention	21-30
4	Long-term intervention	31-100

Table 3.7 Efficiency and urgency levels of intervention for bridge elements.

Level of efficiency	Level of urgency for action	***TSR***
1	Maximum urgency for action	1-30
2	Short-term intervention	31-40
3	Medium-term intervention	41-60
4	Long-term intervention	61-100

Table 3.8 Efficiency and urgency levels of intervention for the whole bridge.

3.3 Procedure for the seismic assessment of masonry/stone bridges

The high stiffness of the resisting structural system of masonry/stone arch structures ensures the substantial absence of relative displacements until the seismic acceleration reaches values able to transform the structure into a mechanism, through non-dissipative plastic hinges leading to the structure collapse. The key parameter for the determination of the structural response is the peak ground acceleration (*PGA*) for the site in which the bridge is placed.

Several studies have underlined how the assessment of masonry/stone arches can be properly conveyed by limit analysis (Heyman 1966; Heyman 1982; Clemente et al. 1995; Clemente 1998) also in compliance with current Italian regulations (Italian Ministry of Infrastructures, 2008). A collapse mechanism must be defined for the implementation of limit analysis of masonry/stone arch bridges; the type of mechanism mainly depends on the geometrical characteristics of the bridge itself.

Various collapse mechanisms can be considered according to the number of spans of the arch bridge and in relation of the slenderness of piers and abutments.

Single-span bridges generally have massive abutments that can be assumed as infinitely rigid constraints. Under these assumptions, the most vulnerable element to seismic action in longitudinal direction appears to be the arch, which can be subjected to antimetric collapse mechanisms through the creation of 4 plastic hinges. In this case the seismic response of the bridge is mostly influenced by the geometric characteristics of the arch presenting a local failure mechanism, in particular by f/L and s/L ratios, where f is the arch rise, L the span length and s the arch thickness. For single span bridge abutments, when the ratio between the abutments height H_a and the abutments base width B_a in longitudinal direction is sufficiently large, the most vulnerable mechanism in longitudinal direction is a global failure mechanism involving both the springers and the arch. In general, the structure is less susceptible to seismic actions in transversal direction but the most vulnerable elements are those referred to the spandrel walls, which can undergo to an out-of-plane collapse. Typically, this kind of mechanism does not affect the global structural safety but can cause instability of the road surface.

In multi-span bridges the seismic vulnerability in longitudinal direction is mainly influenced by pier slenderness H_p/B_p (the ratio between pier height H_p and longitudinal pier base width B_p): for growing values of this ratio a collapse mechanism involving also the piers due to the creation of plastic hinges at their bases can arise (Figure 3.1a). For multi-span bridges with thick piers the most fragile element is represented by the arch: a potential antimetric collapse mechanism can occur in each span, similarly to what happens for single-span bridges. The seismic behaviour in transversal direction is therefore influenced by piers slenderness and bridge (and piers) width. The local collapse mechanism due to spandrel wall overturning, previously described for single-span bridges, remains to be cited for multi-span bridges (Figure 3.1b). Seismic

vulnerability can be more significant in transversal direction than in longitudinal one for multi-span bridges with slender piers: in these cases the assessment could be conducted by means of non-linear static analyses through the implementation of a specific finite element model.

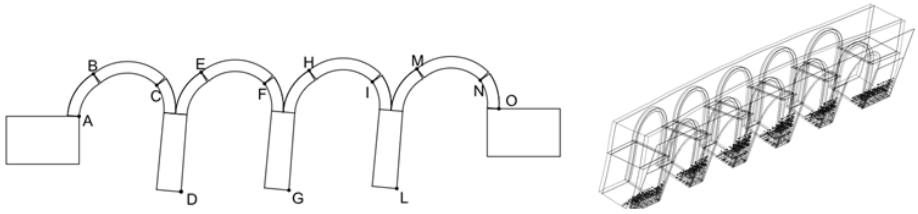

Fig.3.1 Masonry arch multi-span collapse mechanisms for bridges with slender piers in longitudinal (a) and transversal (b) directions.

In the specific case of the masonry/stone bridges' stock analysed in this work, 92% of them belongs to the single-span typology with stiff abutments and multi-span bridges with thick piers, whereas slender multi-span bridges are the 8% of the cases.

For most of the considered structures (92%) the seismic analysis consisted in the evaluation of the seismic capacity of the arch through the study of the main kinematic mechanisms whereas for the remaining cases it was necessary to develop a non-linear static analysis.

A mechanism was assumed *a priori* and the horizontal force enabling that mechanism was calculated determining the related coefficient a_0 through the application of the *Principle of Virtual Works* as:

$$P_v + \alpha_0 P_h = 0 \tag{3.5}$$

where P_v represents the vertical load and P_h are the horizontal forces acting on the structure. The plastic hinges are placed where the pressure line becomes tangent to the arch intrados or extrados. The pressure line can be iteratively calculated assuming a four hinges initial configuration: if this line passes through the hinges and is completely contained in the arch thickness, the assumed hinges' disposition is the correct one; if otherwise the line remains outside the arch thickness the procedure has to be iterated.

This approach has allowed to evaluate the horizontal action that the structures are able to carry during the mechanism evolution (Figure 3.2a). Applying the *Principle of Virtual Works* to a deformed configuration of the same structure, it

can be observed a gradual reduction of the coefficient α until reaching the limit case beyond which the structure collapses due to equilibrium loss. According to the above concepts the capacity curve has been constructed for each analysed bridge, with the following expression:

$$\alpha = \alpha_0 (1 - \frac{d_k}{d_{k0}}) \tag{3.6}$$

where d_{k0} is the maximum displacement of the control point, d_k is the displacement of the control point, function of the α coefficient (Figure 3.2b).

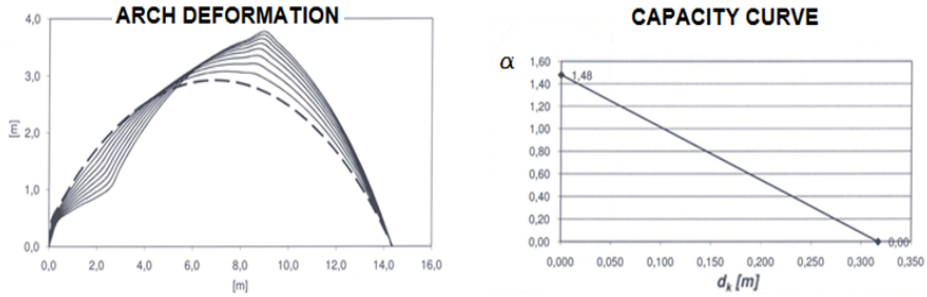

Fig.3.2 Example of arch progressive collapse mechanism (a) and capacity curve (b).

In the overall seismic vulnerability assessment of the bridges, the specific vulnerabilities of the structural elements constituting masonry/stone arch bridges (arch, spandrel wall, piers, abutments, foundations) have been investigated.

The spectral acceleration a^*_0 has been compared with the elastic spectral acceleration $a_g(P_{VR})$ corresponding to T = 0, amplified by the soil factor S. The elastic spectral acceleration is scaled by a structure reduction factor q at the *Ultimate Limit State* (*ULS*):

$$a^*_0 \geq a_g(P_{VR}) \cdot S \tag{3.7}$$

$$a^*_0 \geq \frac{a_g(P_{VR}) \cdot S}{q} \tag{3.8}$$

Furthermore, a comparison between the ultimate displacement d^*_u and the displacement demand obtained from the displacement spectrum S_{De} corresponding to the secant period T_s was made:

$$d_u^* \geq S_{De}(T_s) \quad (3.9)$$

$$T_s = 2\pi\sqrt{\frac{d_s^*}{a_s^*}} \quad (3.10)$$

where d^*_s is the secant displacement (equal to $0{,}4d^*_u$) and a^*_s is the seismic acceleration derived from the capacity curve corresponding to a displacement value equal to d^*_s.

The results obtained above have been expressed by means of safety factors FC_i for each one of them (Eqs. 3.11, 3.12, 3.13), calculated as the ratio between a resistance parameter *R* and a demand parameter *E*.

$$F_{C,1} = \frac{R}{E} = \frac{a_0^*}{a_g(P_{VR}) \cdot S} \quad (3.11)$$

$$F_{C,2} = \frac{R}{E} = \frac{a_0^*}{\frac{a_g(P_{VR}) \cdot S}{q}} \quad (3.12)$$

$$F_{C,3} = \frac{R}{E} = \frac{d_u^*}{S_{De}(T_s)} \quad (3.13)$$

Once verified the arches, the procedure provided, as second step, to the evaluation of the structural capacity of the spandrel walls, i.e. the most vulnerable elements when horizontal forces are acting in transversal direction. The application of the *Principle of Virtual Works* has led to evaluate the horizontal load multiplier coefficient *α* turning the structure into a mechanism. In this case, the mechanism consists in a rotation of the spandrel wall around a cylindrical base hinge. Seismic assessment has been performed considering a rectangular wall with constant thickness *t*, height *Z* and unitary length according to Rota et al. (2005). The *α* coefficient for seismic loads has been calculated by means of the following rotation balance equation:

$$\alpha P \frac{h}{2} + \alpha P_{SOIL} Z_{SOIL} + \alpha N h + S_h \frac{Z}{3} - S_v t - \left(N + P\right)\frac{t}{2} = 0 \quad (3.14)$$

where *P* represents the spandrel wall weight, *S* the lateral ground horizontal action, *N* the vertical force applied at the top of the wall and αP_{SOIL} takes into account the inertia of the filling material adjacent to the spandrel wall. Safety factors FC_i have been calculated also for the spandrel wall.

Lastly, assessment of the abutments has been done. It has been evaluated if the arch collapse mechanism involve or not the abutments. If a mechanism is localized only in the arch (as in almost all of the bridges analysed), a safety factor FC_i as the ratio between the resisting bending moment M_{Rd} of the abutments and the relative demand bending moment M_{Sd} was evaluated. If abutments are involved in the collapse mechanism a limit analysis for evaluating the global collapse mechanism and the relative coefficient multiplier α_0 has been performed. The safety factor FC_i against sliding of the foundation has been calculated as the ratio between the frictional resistance F_{Rd} and the base shear force F_{Sd}. The safety factors obtained for the abutments and foundations (Eqs. 3.15, 3.16) have then been used for estimating the resisting peak ground acceleration $PGA_{RES,i}$ (Eq. 3.17) as a function of the demand peak ground acceleration $PGA_{SOLL,i}$:

$$F_{C,ABUTMENTS} = \frac{R}{E} = \frac{M_{Rd}}{M_{Sd}} \quad (3.15) \qquad F_{C,FOUNDATION} = \frac{R}{E} = \frac{F_{Rd}}{F_{Sd}} \quad (3.16)$$

$$PGA_{RES} = F_{C,i} \cdot PGA_{SOLL} \quad (3.17)$$

Finally, the remaining 8% of slender multi-span masonry/stone bridges have been studied with specific *3D* models and a macro-modelling approach. *MidasFEA* code (MidasFEA, 2009) was used and masonry/stone was modelled as homogeneous continuum, with eight- and six-node elements. The numerical models have been characterized by material and geometrical non-linearity. The *Total Strain Crack Model* implemented in *MidasFEA* was used as constitutive law for masonry. Specific checks/verifications on the reliability of the elements and constitutive laws used in the models are included in the documentation available in *MidasFEA* (2009) user manual.

3.4 Procedure for the seismic assessment of reinforced concrete bridges

The significant number of *RC-PRC* bridges analysed in this work has justified the creation of a specific seismic assessment procedure. The major seismic vulnerabilities have been attributed to the vertical elements such as piers and

abutments. The structural capacity of the abutments has been assessed in terms of resistance with the aim of checking that they remain elastic up to *ULS*. A specific finite element model has been realized for each abutment and a static analysis has been developed. The abutments have been modelled by means of *Strand7 v.2.4* code (*Strand7* v.2.4 2010), discretizing the structures with bi-dimensional plate elements and subsequently performing linear static analyses. Hence adopted finite element models are rather simple and currently used in the common practice. Specific checks/verifications on the reliability of the elements and analyses used in the models are included in the documentation available in *Strand7 v.2.4* (2010) user manual.

These analyses have been performed to obtain the entity of the acting forces in the abutments in terms of bending at the wall base, bending moment at the top of the wall, shear failure at wall bottom and shear failure on the lateral walls (Figure 3.3).

A safety factor FC_i has been calculated by dividing the bending moment/shear resisting forces by the relative bending moment/shear acting forces obtained:

$$F_{C,i} = \frac{R}{E} = \frac{M_{Rd}}{M_{Sd}} \qquad (3.18)$$

$$F_{C,i} = \frac{R}{E} = \frac{F_{Rd}}{F_{Sd}} \qquad (3.19)$$

$$PGA_{RES} = F_{C,i} \cdot PGA_{SOLL} \qquad (3.20)$$

Regarding the piers, once defined the materials' main mechanical characteristics and the localization of the reinforcing steel bars, the moment-curvature diagram of the element section has been found, calculating yielding Φ_y and ultimate Φ_u curvature and their corresponding bending moment values.

Moment-curvature diagram has been calculated in both principal directions for each pier due to the different longitudinal and transversal structural response. Once defined the length of the plastic hinge L_{pl}, rotation and their relative displacement capacity values have been evaluated for different limit states, considering the top of the pier as control point.

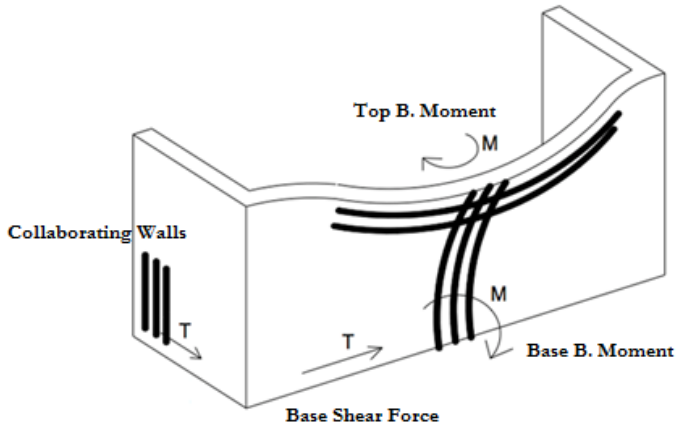

Fig.3.3 Assessment of the reinforced concrete bridge abutments.

The obtained displacement capacity value S_{Rd} has then been compared with the displacement demand S_{Sd}, calculated from the displacement elastic spectrum for each limit state considered and computing the safety factor values (Eq. 3.21). The obtained results have been converted in terms of resisting accelerations, according to Eq. (3.22):

$$F_{C,i} = \frac{S_{Rd}^{SL_i}}{S_{Sd}^{SL_i}} \quad (3.21)$$

$$PGA_{RES}^{SL_i} = F_{C,i} \cdot PGA_{SOLL}^{SL_i} \quad (3.22)$$

The acting shear F_{Sd} at the pier bottom has been compared with the corresponding resisting shear T_{Rd}.

The failure mechanisms described above have been considered because they are representative of the main potential seismic vulnerabilities for the structural typologies included in the reinforced concrete bridges' stock of this work. Other potential vulnerabilities for reinforced concrete bridges have been considered but any potential significant issue has not been observed. In particular, a comparison between deck displacement demand and available bearing length has been performed and bearing loss and potential pounding effects between adjacent simply supported spans have been checked without showing any problems.

For each masonry/reinforced concrete bridge, the minimum safety factor value $FC_{i.min}$ (between those calculated) has been assumed as representative of the main seismic vulnerability indicator for each structure, and considered in the subsequent analyses.

3.5 The Vicenza's road network case study

The procedures described in the previous sections were applied to evaluate the maintenance condition state and the fast seismic vulnerability assessment of 150 bridges managed by Vi.abilità S.p.A., the road agency of the Vicenza province, North-Eastern Italy. Figure 3.4 shows the main preliminary information on the stock of analysed bridges: it can be observed how the 54% of them is single-span bridge type, while the remaining 46% is multi-span type. The prevalence of structural material is the prestressed reinforced concrete/reinforced concrete typology (75%), whereas the remaining part is composed by masonry bridges (21%) and steel bridges (4%). According to *OPCM 3362/04* (2004), 90% is located in Seismic Zone 3, whereas 3% belongs in Seismic Zone 2 and the remaining 7% is situated in Seismic Zone 4.

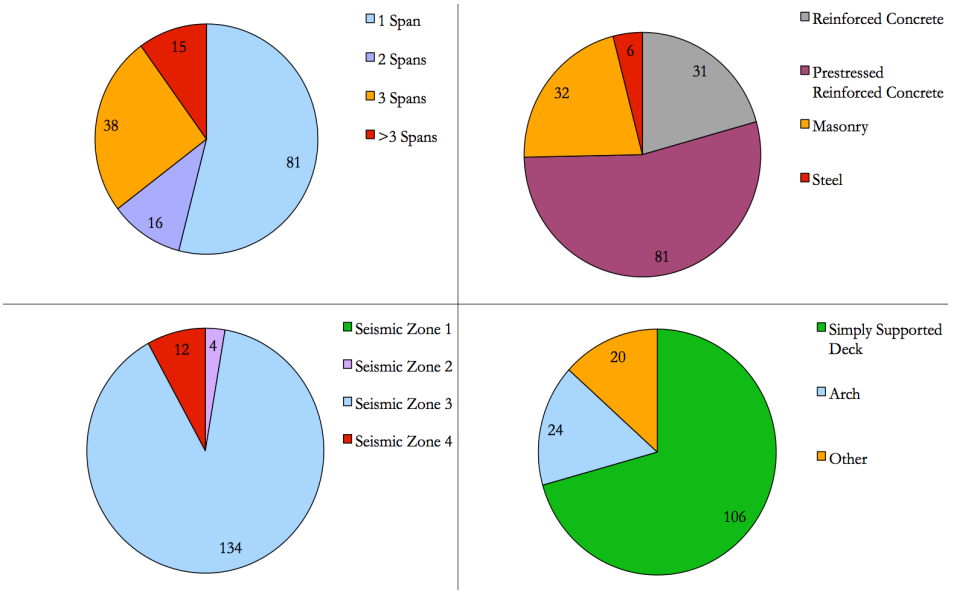

Fig.3.4 Main preliminary information of the 150 Vi.abilità S.p.A. bridges.

The majority of them is characterized by a simply supported structural scheme (71%), while arched bridges are the 16% and other structural schemes are represented by the remaining 13%. In Figure 3.5 a global view of the distribution of the 150 analysed bridges is given.

For each bridge the *TSR* index was evaluated according to the methodology described in Pellegrino et al. 2011 previously summarized in Section 3.2 and the seismic vulnerability assessment was performed following the simplified

procedures explained above in Sections 3.3 and 3.4. Total maintenance cost was calculated for each bridge as the sum of the single element maintenance costs, derived by the product of unitary maintenance element costs reported in the datasheets (see Table 3.2) for the related bridge elements' main geometrical characteristics (ml, m^2, etc.). Finally, the unitary maintenance cost in [€/m^2], referred to 1m^2 of bridge deck was calculated as follows:

$$\text{Unitary maintenance cost} = \frac{\text{Total maintenance cost}}{\text{Deck area}} \tag{3.23}$$

In such way, each bridge is characterized by a couple of values: the *TSR* value, representing its state of maintenance on the basis of the qualitative information collected during the visual inspection and the unitary maintenance cost, i.e. the amount of resources needed to bring back 1m^2 deck to a condition state equal to that of a new bridge, by removing the whole local and diffused defects found on the existing deteriorated structure.

Figure 3.6 shows, as example, the *TSR* and unitary maintenance cost calculation for the Brenta's bridge. The Brenta's bridge (Figure 3.6a) is located in the Bassano del Grappa Municipality, on the SP 248 provincial road. The bridge has 12 simply supported spans composed each one by 5 prestressed reinforced concrete beams with span lengths of 31,6m-33,1m, beam height of 2,3m and width of 0,5m, supporting a concrete slab of 0,35m thickness. Framed reinforced concrete piers have a maximum height of 7m and are composed by 3 columns with a circular section of 1,2m diameter and a transverse beam 1,4m high. Bridge abutments have a height of 5m and a thickness of 1,5m. Collaborating walls have a length of 5m and a thickness of 1m. In Figures 3.6b and 3.6c transversal and longitudinal sections of the Brenta's bridge are shown. On the basis of the main geometrical characteristics and the outcomes of the visual inspection, *TSR* value and unitary maintenance cost have been calculated as shown in Figure 3.6d.

With regard to the seismic assessment, the procedures explained above in Sections 3.3-3.4 were applied for each bridge structure. Seismic analysis was performed according to the typology of structure and specific safety factors FC_i were calculated, identifying the worst one $FC_{i,min}$ which represent the main critical issue of a specific bridge structure.

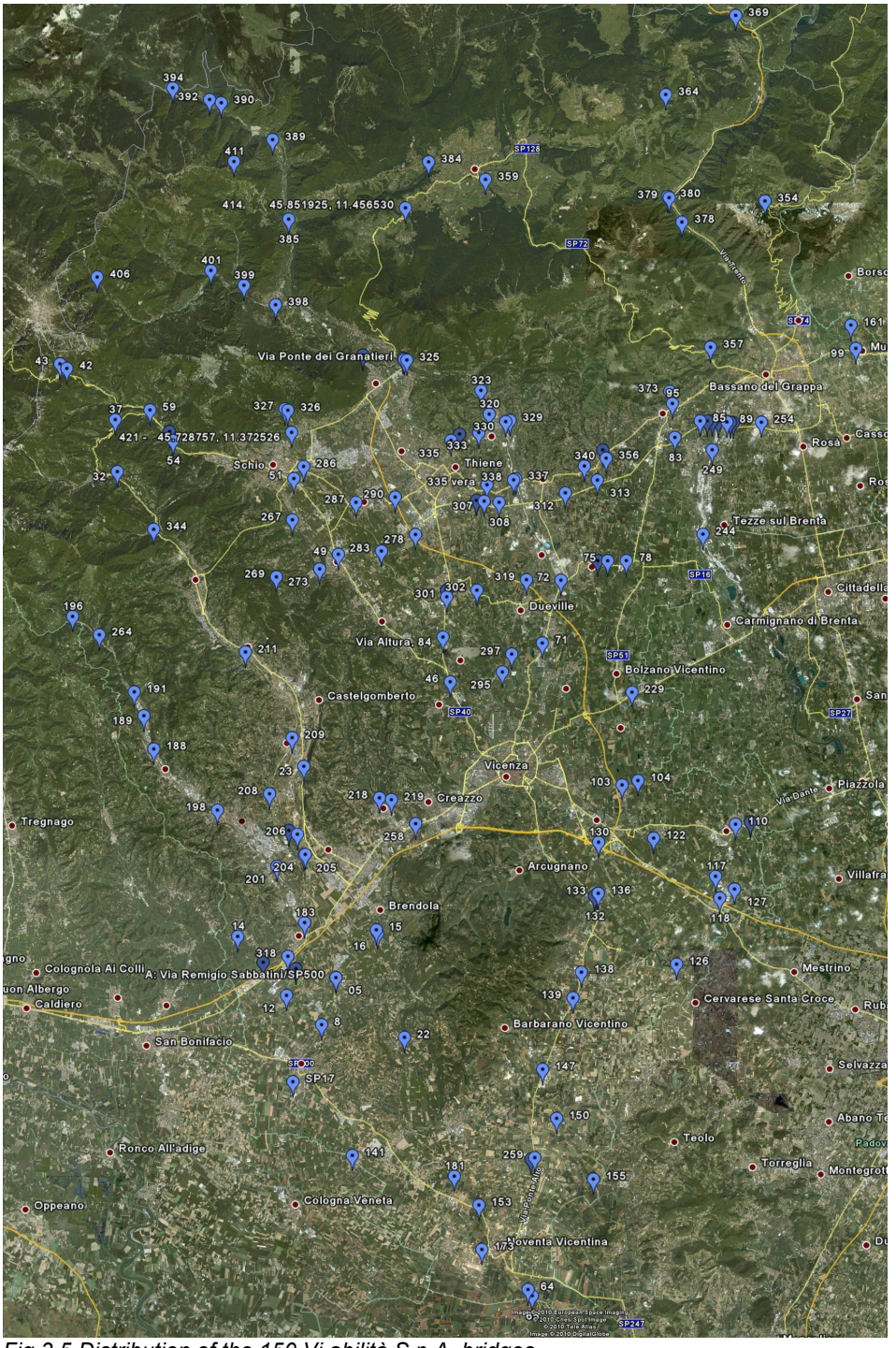

Fig.3.5 Distribution of the 150 Vi.abilità S.p.A. bridges.

(a)

(b)

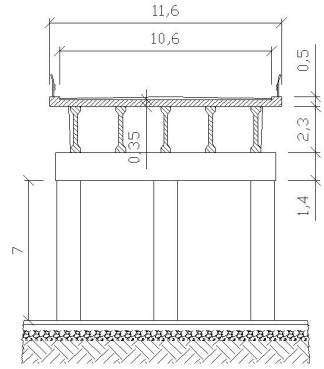

(c)

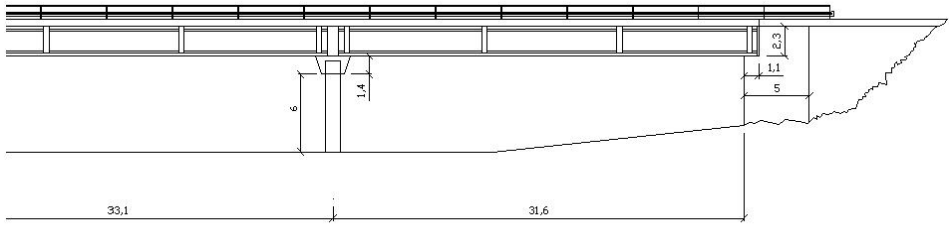

(d)

Bridge ID:	88	Brenta's bridge

Code	Elements	CV	CF	LF	Wel.evaluated	Wel.present	RT	TI	RF	NBI	AF	ESR	Element Maintenance Cost [€]	
A2	Longitudinal elements	3	4	5	10	10	0,95	0,90	0,86	0,98	1,00	17	0,00	
A1	Pier	3	4	5	10	10	0,95	0,90	0,86	0,98	1,00	17	320.279,96	
A1	Transversal elements	3	4	6	9	9	0,95	0,90	0,86	0,98	1,00	20	0,00	
B1	Deck	3	4	6	9	9	0,95	0,90	0,86	0,98	1,00	20	429.835,68	
	Support equipment	0	0	6		9	0,95	0,90	0,86	0,98	1,00	0	0,00	(*)
	Seismic devices			6			0,95	0,90	0,86	0,98	1,00		0,00	
	Abutment	0	0	7		8	0,95	0,90	0,86	0,98	1,00	0	0,00	(*)
	Embankment			7			0,95	0,90	0,86	0,98	1,00		0,00	
	Walls			7			0,95	0,90	0,86	0,98	1,00		0,00	
	Aboutment Foundations	0	0	8		7	0,95	0,90	0,86	0,98	1,00	0	0,00	(*)
	Pier Foundations	0	0	8		7	0,95	0,90	0,86	0,98	1,00	0	0,00	(*)
A1	Waterproofing	2	7	9	6	6	0,95	0,90	0,86	0,98	1,00	53	0,00	
A1	Pavement	3	4	9	6	6	0,95	0,90	0,86	0,98	1,00	30	35.517,42	
A1	Guard-rail	3	4	9	6	6	0,95	0,90	0,86	0,98	1,00	30	139.152,60	
C1	Joint	2	7	9	6	6	0,95	0,90	0,86	0,98	1,00	53	0,00	
	Sidewalk			10			0,95	0,90	0,86	0,98	1,00		0,00	
	Parapets			10			0,95	0,90	0,86	0,98	1,00		0,00	
A1	Water selling	1	10	10	5	5	0,95	0,90	0,86	0,98	1,00	84	0,00	
A1	Accessories	3	4	10	5	5	0,95	0,90	0,86	0,98	1,00	34	886,95	

Σel.evaluated	10		
Σel.present	14		
ΣWevaluated	72		
ΣWel.present	103		
CoF	70	>	70
TSRreal	41		
TSRminimum	35		
TSR	39		

Σ Single elements costs [€]	925.672,61
Construction site installation cost (3%) [€]	27.770,18
Total maintenance costs [€]	**953.442,79**
Deck area [m²]	**4.572,72**
Unitary maintenance costs [€/m²]	**208,51**

(*) The element was not evaluated

Fig.3.6 Brenta's bridge: general view (a), transversal section (b), longitudinal section (c), TSR calculation (d).

According to *OPCM 3362/04* (2004), a unitary seismic retrofit intervention cost in [€/m^2] has been defined for each bridge in relation to the $FC_{i,min}$ value, following the subsequent equations:

Unitary seismic retrofit cost = 450 if $FC_{i,min} \leq 0,2$ (3.24)

$$\text{Unitary seismic retrofit cost} = \frac{380\text{-}400 \cdot \text{FC}_{\text{i,min}}}{3} \quad \text{if } 0{,}2 < FC_{i,min} < 0{,}8 \qquad (3.25)$$

$$\text{Unitary seismic retrofit cost} = 0 \quad \text{if } FC_{i,min} \geq 0{,}8 \qquad (3.26)$$

It can be noticed how for bridges with $FC_{i,min}$ values between 0,8 and 1, the unitary seismic retrofit cost is equal to zero although the seismic assessment outcomes present criticalities: this issue is due to the assumption of simplified seismic analysis methods. In fact, in most cases, performing seismic analyses of higher complexity allow to better estimate the capacity of these structures leading to move the $FC_{i,min}$ to values higher than 1.
Table 3.9 shows, as example, the outcomes obtained from the application of the simplified seismic assessment procedure described in Pellegrino et al. 2014. Seismic assessment outcomes highlight how the Brenta's bridge is characterized by criticalities for abutments' top bending moment and piers' shear and longitudinal/transversal base bending moment due to lack of adequate longitudinal rebars and stirrups.

Limit State	FC_i	**Description**
Functionality	0,107	Pier base transversal bending moment
Damage	0,556	Pier base longitudinal bending moment
Life	0,164	Pier base transversal shear
Collapse	0,550	Abutment top bending moment
$FC_{i,min}$	**0,107**	

Table 3.9 Seismic assessment of the Brenta's bridge.

Summarizing, each bridge is characterized by 4 parameters:

- a *TSR* value, representing the qualitative outcome of the visual inspection of the state of maintenance of the whole structure;
- a unitary maintenance cost in [€/m^2], which represents the normalized cost referred to 1m^2 deck for the execution of maintenance works with the aim of remove the whole local and diffused defects found on the existing deteriorated structure;

- a $FC_{i,min}$ value, that describes the main criticality detected in the fast seismic assessment of a bridge, according to the procedures described in Sections 3.3-3.4;
- a unitary seismic retrofit cost, given by *OPCM 3362/04* (2004), in [€/m^2], which represents the normalized cost referred to 1m^2 deck for the execution of structural seismic retrofit interventions aimed to increase the resistance against horizontal actions of the elements in which criticatilies were detected.

Considering, as simplifying assumption, the complete independence between maintenance and seismic retrofit costs in accordance with their definitions given above, a unitary total cost can be expressed for each bridge as follows:

Unitary total cost = Unitary maintenance cost + Unitary seismic retrofit cost (3.27)

3.6 Results

The five indicators presented in the last part of Section 3.5 have been calculated for the whole bridges belonging to the stock of analysed Vi.abilità S.p.A. structures. For the subsequent statistical and cost analysis, as it was not always possible to have an exhaustive evaluation of the structures, 140 of the initial 150 bridges, have been considered in the following discussion.

Figure 3.7 shows the subdivision of the *TSR* values estimated for each of the 140 bridges in the urgency levels, according to the classification shown in Table 3.8. It can be observed how over 60% of the bridges need a medium-term maintenance intervention whereas a 10% a short-term one. Only one of them is in a condition of a maximum urgency while the remaining 27% will need a maintenance intervention in a long-term. A preliminary relationship between maintenance costs and maintenance urgency levels can be derived as shown in Figure 3.8.

Bridges with urgency level #1 are characterized by a mean value of unitary maintenance costs is equal to 715€/m^2, for urgency level #2 the mean value decreases to 560€/m^2, for urgency level #3 the mean value is equal to 250€/m^2 and lastly, for urgency level #4 the mean value can be assessed as 50€/m^2. For

the same 140 bridges, the fast seismic assessment has then been performed and a $FC_{i,min}$ value has been evaluated for each structure.

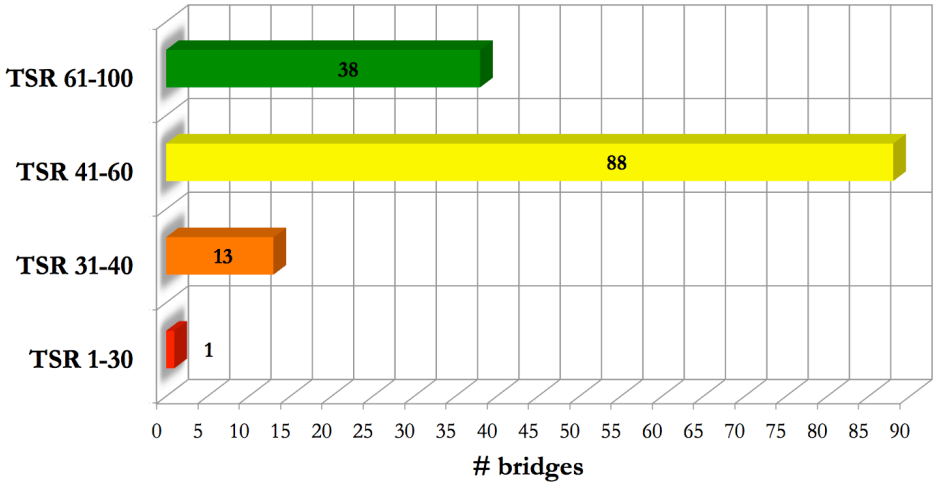

Fig.3.7 Subdivision of the estimated TSR values in urgency bands (see Table 3.8).

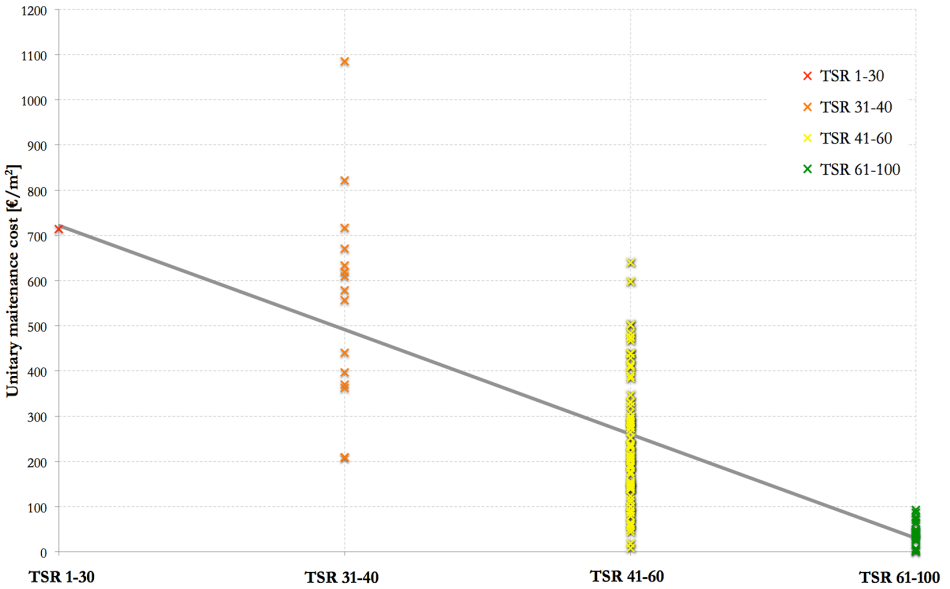

Fig.3.8 Mean unitary maintenance cost for the different urgency levels shown in Table 3.8.

Figure 3.9 represents the seismic assessment outcomes, highlighting for the 50% of considered structures satisfactory seismic verifications, whereas the

remaining 50% of unsatisfied outcomes is characterized by a normal distribution of $FC_{i,min}$ value, with mean value equal to 0,5.

The results obtained from the state of maintenance and seismic assessment have then been used to verify the sussistence of any relationships between costs (expressed in terms of unitary maintenance costs, unitary seismic retrofit costs and unitary total costs) and the outcomes of the visual inspections (*TSR* values) and the seismic assessment analysis ($FC_{i,min}$ values).

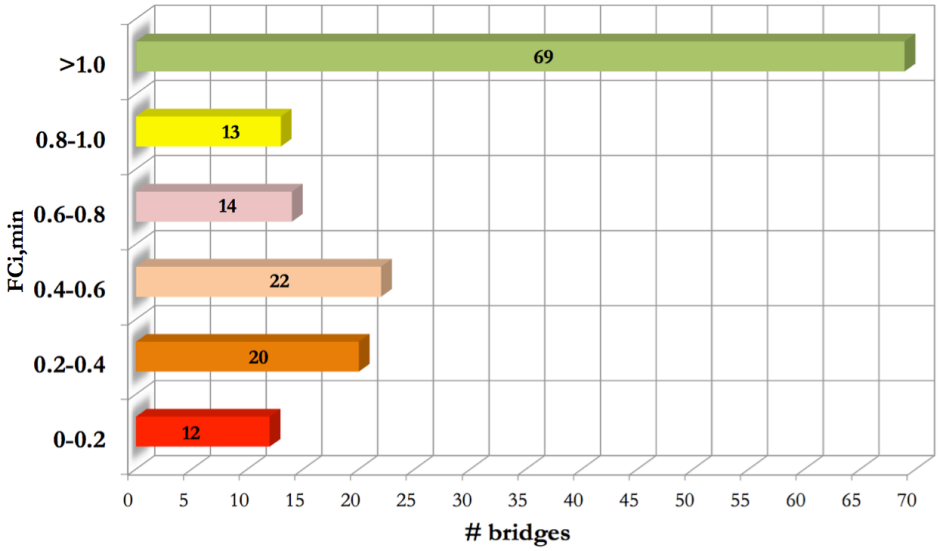

Fig.3.9 Representation of the seismic assessment outcomes for the 140 considered bridges.

The 140 bridges (81 with *CoF* ≥70 and the remaining 59 with *CoF* <70) were grouped in relation to their specific construction material (reinforced concrete/ prestressed reinforced concrete, masonry and steel) in:

- 104 reinforced concrete/prestressed reinforced concrete bridges, 54 with *CoF* ≥70 and the remaining 50 with *CoF* <70;
- 30 masonry bridges, 27 with *CoF* ≥70 and the remaining 3 with *CoF* <70;
- 6 steel bridges, each one with *CoF* <70.

Unitary maintenance costs have been plotted vs. *TSR* value, fitting the data with specific relationships for the whole data (Figure 3.10) and singularly for reinforced concrete/prestressed reinforced concrete bridges (Figure 3.11) and masonry bridges (Figure 3.12). Data referred to steel bridges (Figure 3.13) are insufficient for the calibration of a specific relationship. Bridges characterized by *CoF* ≥70 have been underlined in the graphs.

The relationship between unitary maintenance costs and *TSR* value is decreasing exponential. Mean regression equations (black line) and mean ± sigma equations (gray lines) have been estimated for the whole cases.

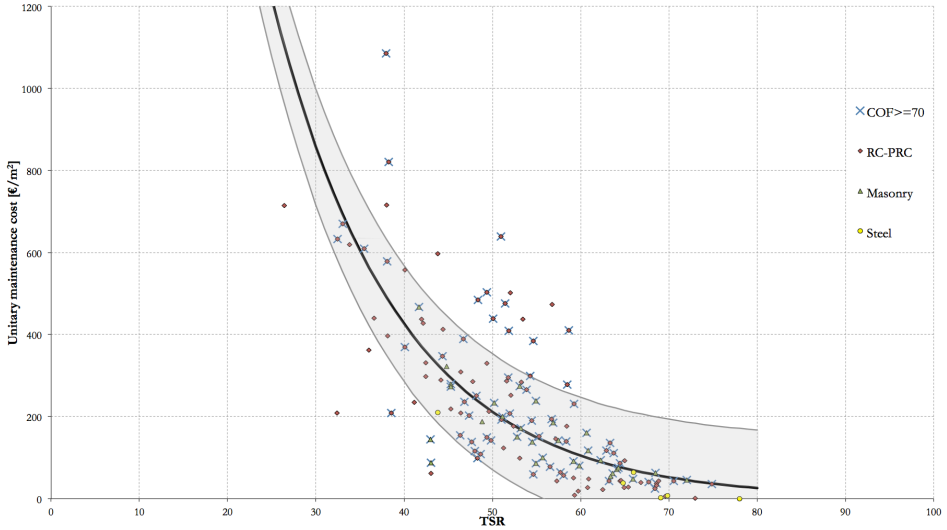

Fig.3.10 Unitary maintenance costs vs. TSR value for the whole 140 analysed bridges.

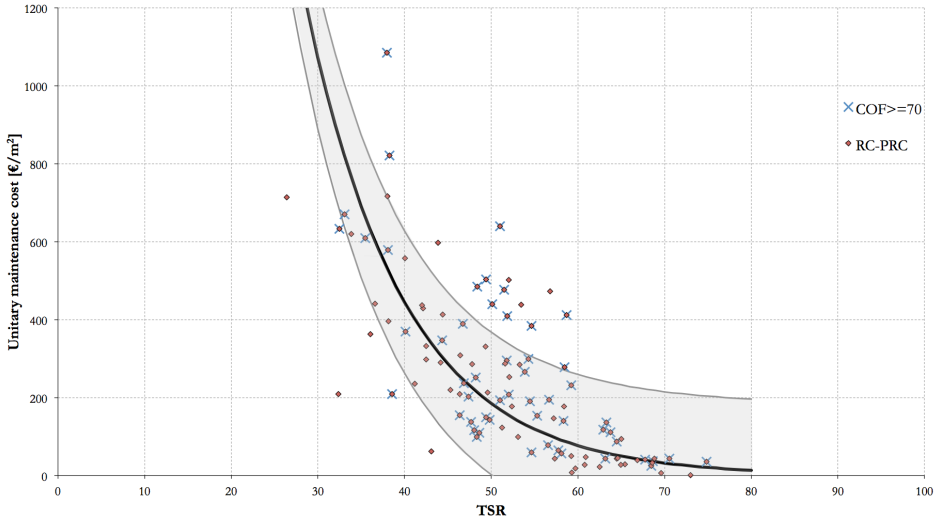

Fig.3.11 Unitary maintenance costs vs. TSR value for the 104 analysed reinforced concrete bridges.

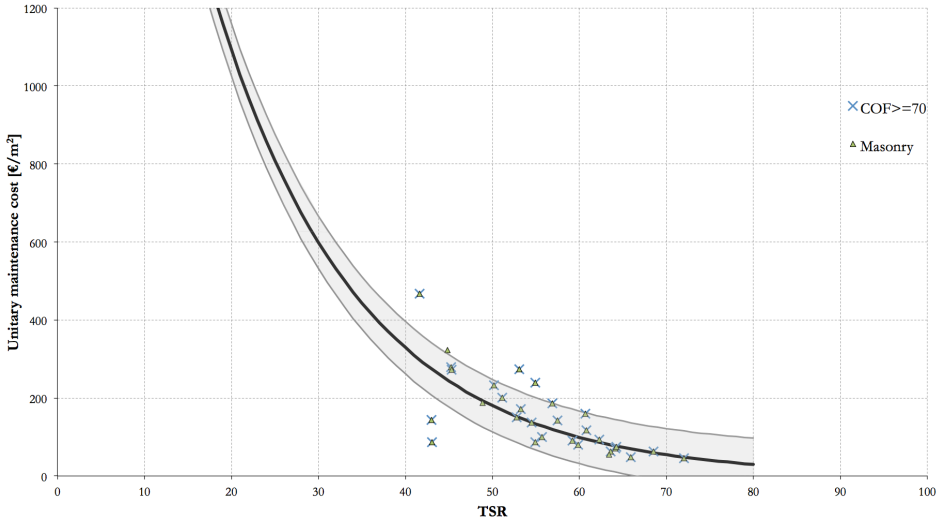

Fig.3.12 Unitary maintenance costs vs. TSR value for the 30 analysed masonry bridges.

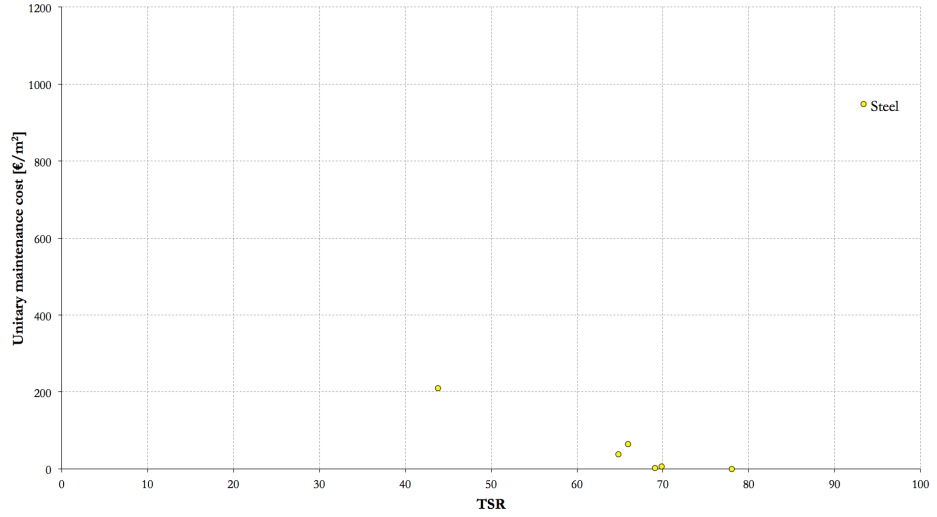

Fig.3.13 Unitary maintenance costs vs. TSR value for the 6 analysed steel bridges.

Figure 3.14 shows the unitary seismic retrofit costs calculated for the 140 analysed bridges according to *OPCM 3362/04* (2004). No correlation has been found between unitary seismic retrofit costs and *TSR* value (Figure 3.15), since the maintenance state of the bridges does not affect outcomes provided by the application of the proposed seismic assessment procedures.

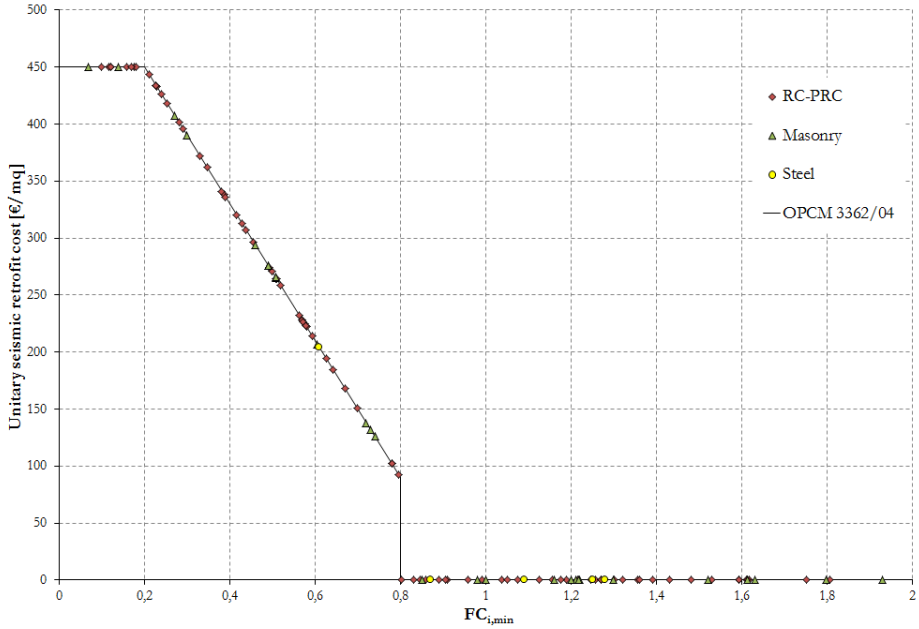

Fig.3.14 Unitary seismic retrofit costs vs. $FC_{i,min}$ value for the whole 140 analysed bridges.

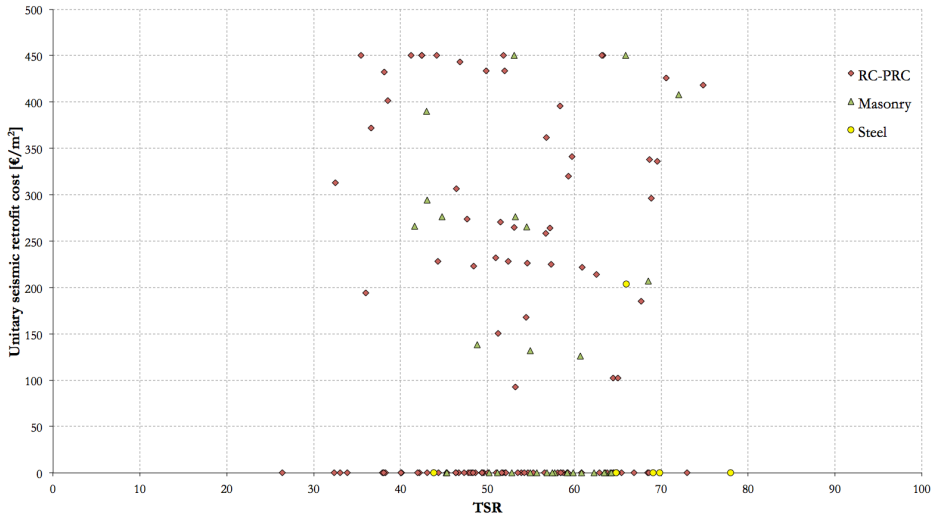

Fig.3.15 Unitary seismic retrofit costs vs. TSR value for the whole 140 analysed bridges.

Unitary total costs (i.e. the sum of unitary maintenance costs and unitary seismic retrofit costs) have been estimated for the whole analysed bridges (Figure 3.16) and then plotted vs. $FC_{i,min}$ and *TSR* values to evidence possible

relationships between these parameters. Figures 3.17-3.20 illustrates the whole 140 unitary total costs assessed vs. $FC_{i,min}$ values, and the relative reinforced concrete/prestressed reinforced concrete (Figure 3.18), masonry (Figure 3.19) and steel (Figure 3.20) subclasses.

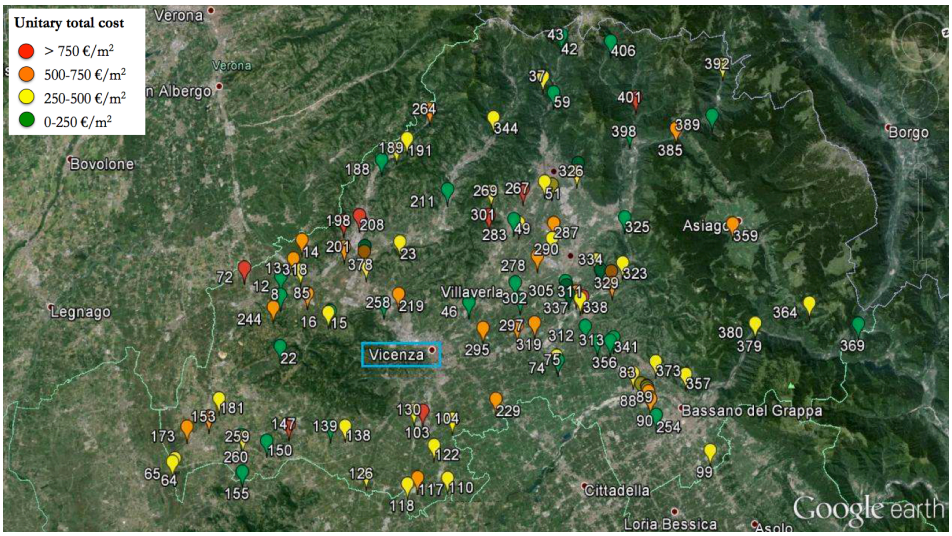

Fig.3.16 Unitary total costs for the whole 140 analysed bridges.

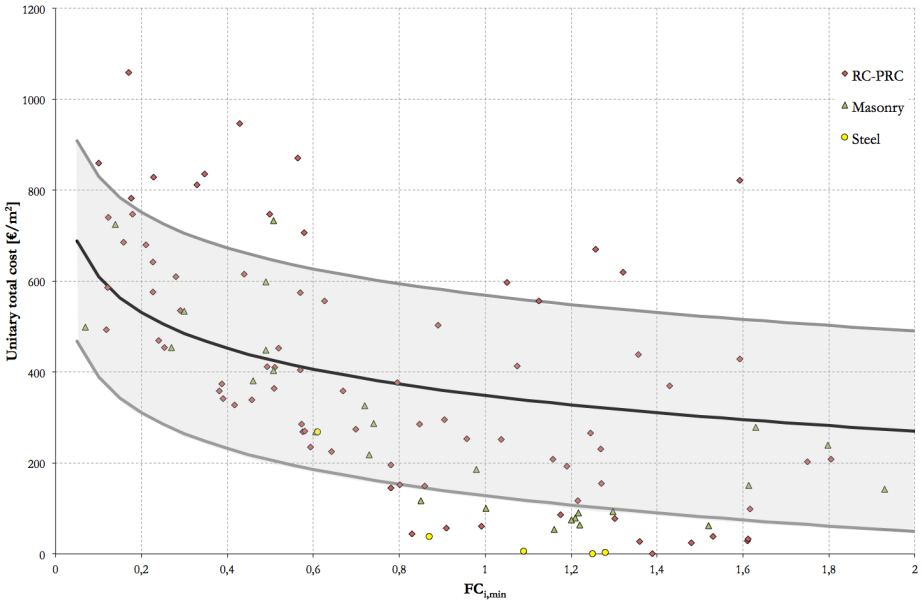

Fig.3.17 Unitary total costs vs. $FC_{i,min}$ value for the whole 140 analysed bridges.

Mean regression equations (black line) and mean ± sigma equations (gray lines) have been estimated for the whole cases.

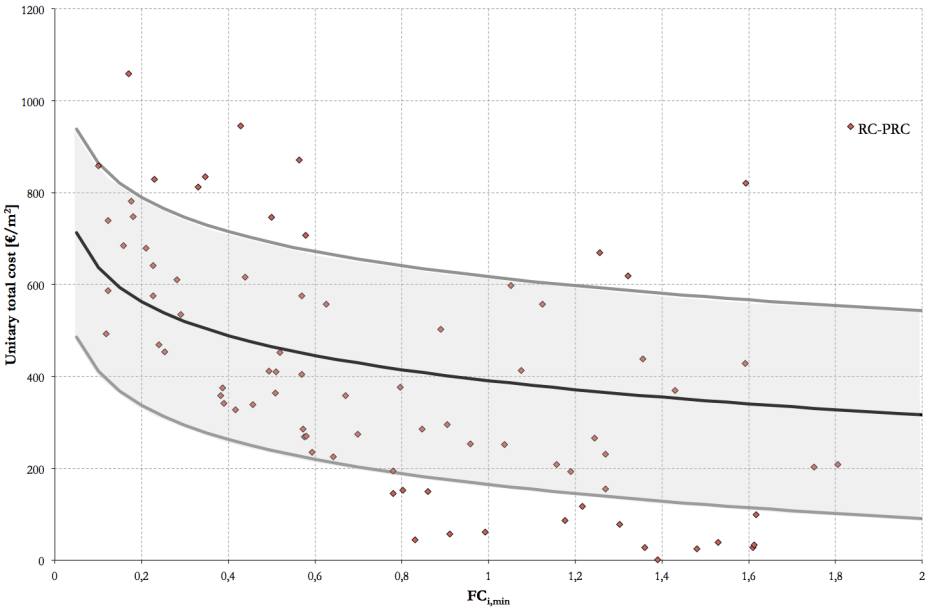

Fig.3.18 Unitary total costs vs. $FC_{i,min}$ value for the 104 analysed reinforced concrete bridges.

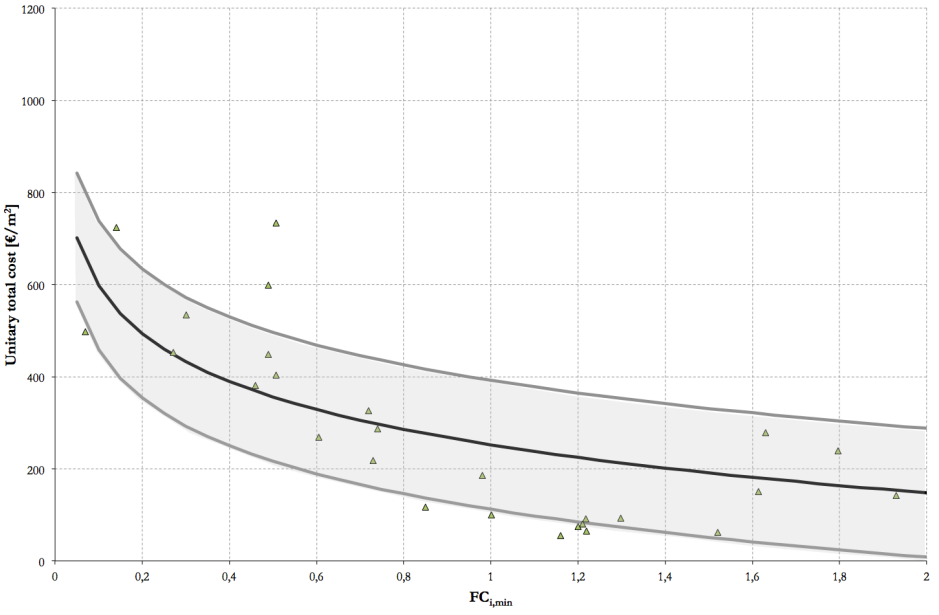

Fig.3.19 Unitary total costs vs. $FC_{i,min}$ value for the 30 analysed masonry bridges.

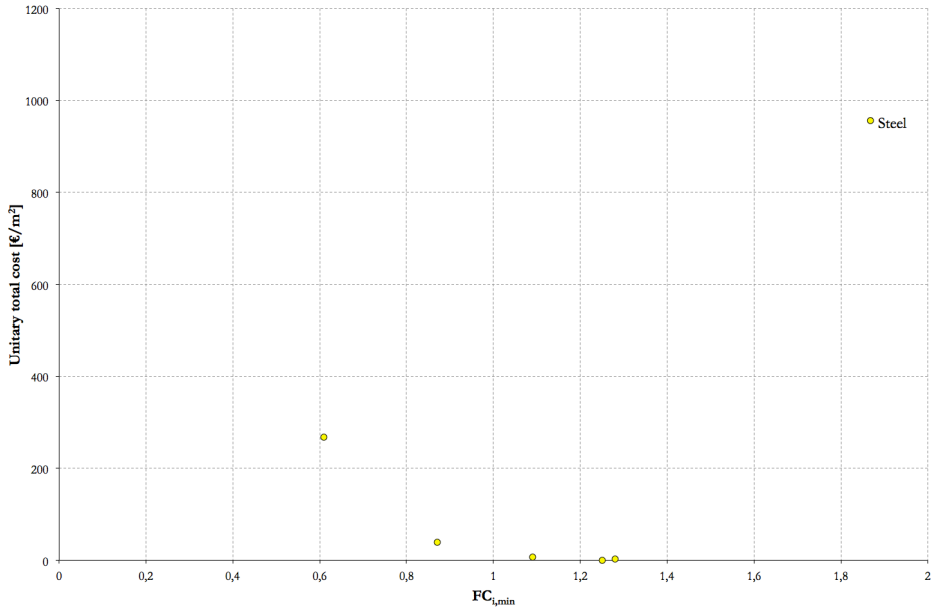

Fig.3.20 Unitary total costs vs. $FC_{i,min}$ value for the 6 analysed steel bridges.

Finally, Figures 3.21-3.24 illustrates the unitary total costs assessed vs. *TSR* values, and the relative reinforced concrete/prestressed reinforced concrete (Figure 3.22), masonry (Figure 3.23) and steel (Figure 3.24) subclasses.

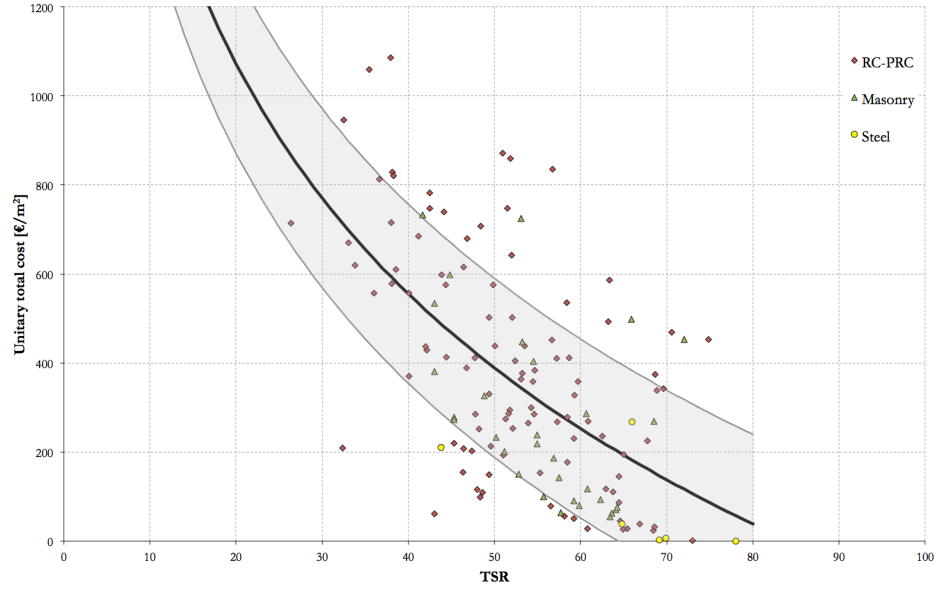

Fig.3.21 Unitary total costs vs. TSR value for the whole 140 analysed bridges.

Mean regression equations (black line) and mean ± sigma equations (gray lines) have been estimated for the whole cases.

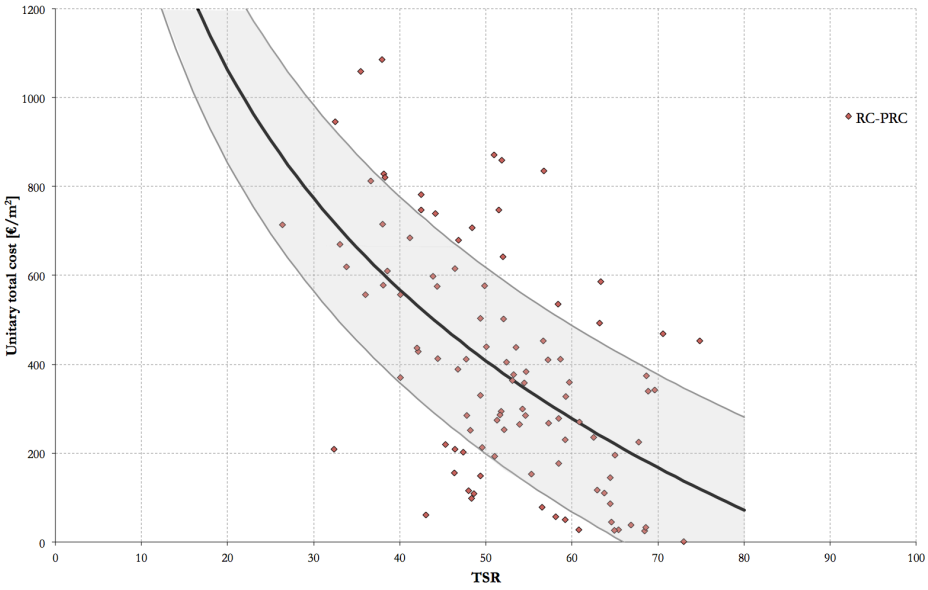

Fig.3.22 Unitary total costs vs. TSR value for the 104 analysed reinforced concrete bridges.

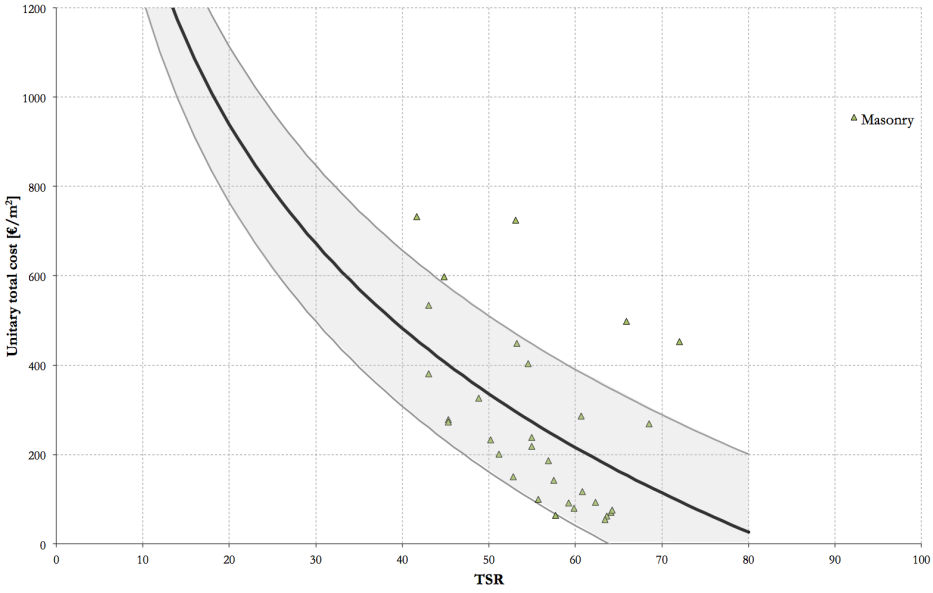

Fig.3.23 Unitary total costs vs. TSR value for the 30 analysed masonry bridges.

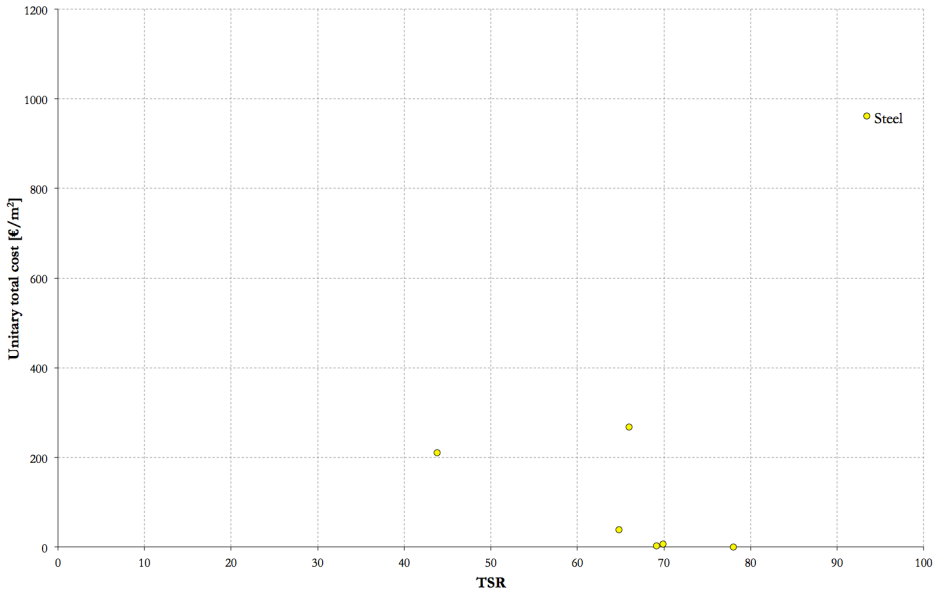

Fig.3.24 Unitary total costs vs. TSR value for the 6 analysed steel bridges.

3.7 Discussion of the results

A statistical analysis has been performed on the data collected from the visual inspections and the seismic assessment outcomes with the aim of estimate a set of regression equations useful for the cost analysis of bridge stocks to be managed.

Formulations have been developed to predict unitary maintenance cost (*UMC*) and unitary total cost (*UTC*) for the whole bridge typologies and specifically for reinforced concrete/prestressed reinforced concrete (*RC-PRC*) and masonry bridges. The lack of data related to steel bridges have not allowed to formulate any provisional relationship between the investigated parameters.

The proposed equations are reported in Table 3.10: decreasing exponential equations for unitary maintenance cost provisions and decreasing logarithmic ones for unitary total cost formulations.

For each provisional equation root mean squared error and R^2 indicator have been calculated for evaluating the accuracy of the provisions: from the analysis

of the results, provisions on masonry bridges seems to be affected by lower variability notwithstanding the lower number of analysed bridges.

Unitary Cost	Typology	Equation	sigma	R^2
Unitary Maintenance Cost	All	$\mathrm{UMC} = 7013{,}2 \cdot e^{-0{,}07 \cdot \mathrm{TSR}}$	141,6	0,5904
	RC – PRC	$\mathrm{UMC} = 15033 \cdot e^{-0{,}088 \cdot \mathrm{TSR}}$	182,8	0,5773
	Masonry	$\mathrm{UMC} = 3624{,}7 \cdot e^{-0{,}06 \cdot \mathrm{TSR}}$	67,2	0,6238
Unitary Total Cost	All	$\mathrm{UTC} = -113{,}3 \cdot \ln(\mathrm{FC}_{\mathrm{i,min}}) + 348{,}54$	220,4	0,2312
	RC – PRC	$\mathrm{UTC} = -107{,}2 \cdot \ln(\mathrm{FC}_{\mathrm{i,min}}) + 390{,}88$	226,1	0,2258
	Masonry	$\mathrm{UTC} = -150{,}2 \cdot \ln(\mathrm{FC}_{\mathrm{i,min}}) + 252{,}11$	139,9	0,4762
	All	$\mathrm{UTC} = -746{,}1 \cdot \ln(\mathrm{TSR}) + 3307{,}5$	201	0,3604
	RC – PRC	$\mathrm{UTC} = -715{,}3 \cdot \ln(\mathrm{TSR}) + 3206{,}5$	209,4	0,3362
	Masonry	$\mathrm{UTC} = -658{,}5 \cdot \ln(\mathrm{TSR}) + 2911{,}7$	174,6	0,2406

Table 3.10 Unitary maintenance cost and unitary total cost provisional equations.

Comparisons between provisional equations have then been performed: Figure 3.25 shows, as example, the comparison between *UMCs* provided for *RC-PRC* and masonry bridges, showing how for *TSR* values lower than 50, masonry *UMCs* are significantly lower than the *RC-PRC* ones. Cost curves were plotted considering the following boundary conditions:

- *UMCs* and *UTCs* were estimated considering a maximum value of 1200€/m^2, since for higher cost values bridge demolition and reconstruction is the best choice;
- *UMCs* and *UTCs* were estimated up to a maximum *TSR* value equal to 80, since is meaningless and economically unseemly to estimate them for bridges characterized by the presence of minimal defects.

UMCs and *UTCs* have been also compared for *RC-PRC* bridges (Figure 3.26) and masonry ones (Figure 3.27): it can be observed how *UTCs* are characterized by higher variability in their predictions than *UMCs*.

A comparison was also performed between *RC-PRC* and masonry *UTCs* (Figure 3.28), showing how the offset between the two provisional formulations is quite significant (about of 60€/m^2).

Finally, a *3D* interpolating surface has been derived for the representation of *UTCs* contemporarily vs. *TSR* and $FC_{i,min}$ values (Figure 3.29). Black dots represent some of the analysed bridges characterized by estimated *UTC* values higher that those predicted by the interpolating surface.

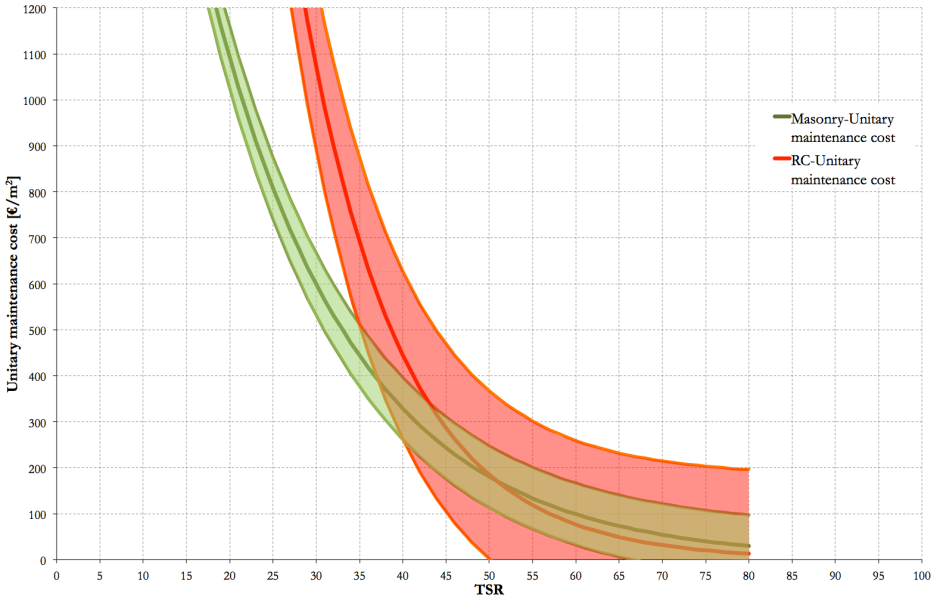

Fig.3.25 Comparison between RC-PRC and masonry unitary maintenance cost provisional equations.

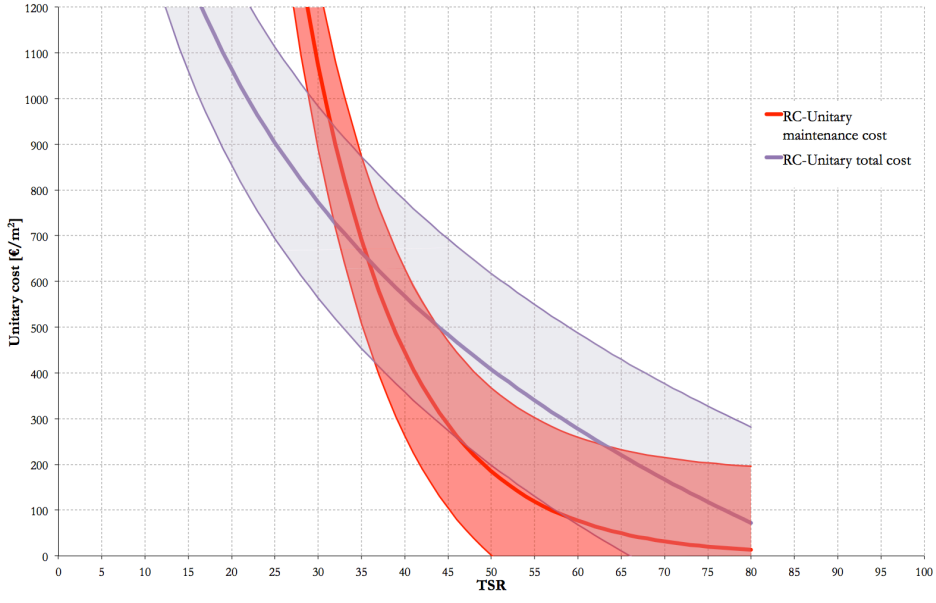

Fig.3.26 Comparison between unitary maintenance cost and unitary total cost provisional equations for RC-PRC bridges.

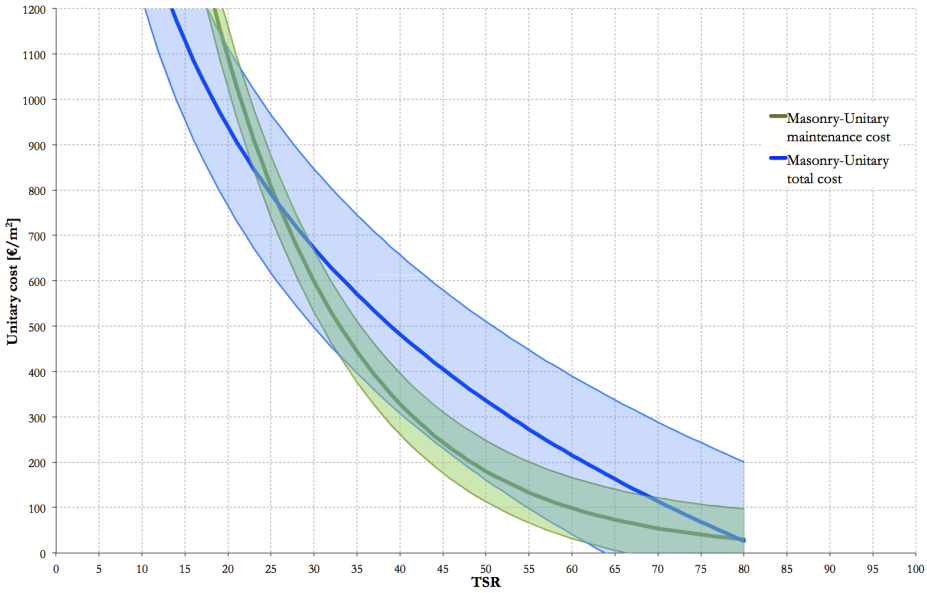

Fig.3.27 Comparison between unitary maintenance cost and unitary total cost provisional equations for masonry bridges.

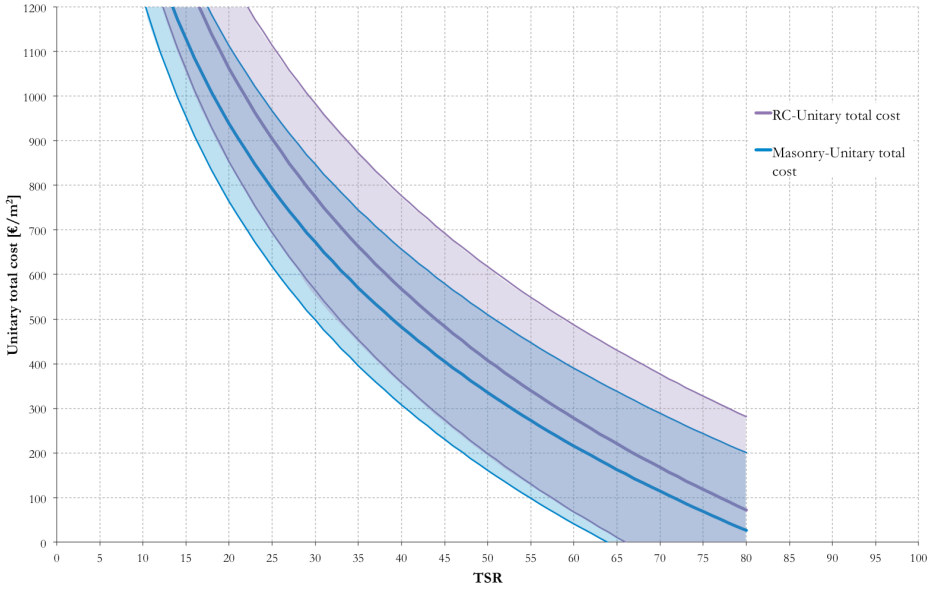

Fig.3.28 Comparison between RC-PRC and masonry unitary total cost provisional equations.

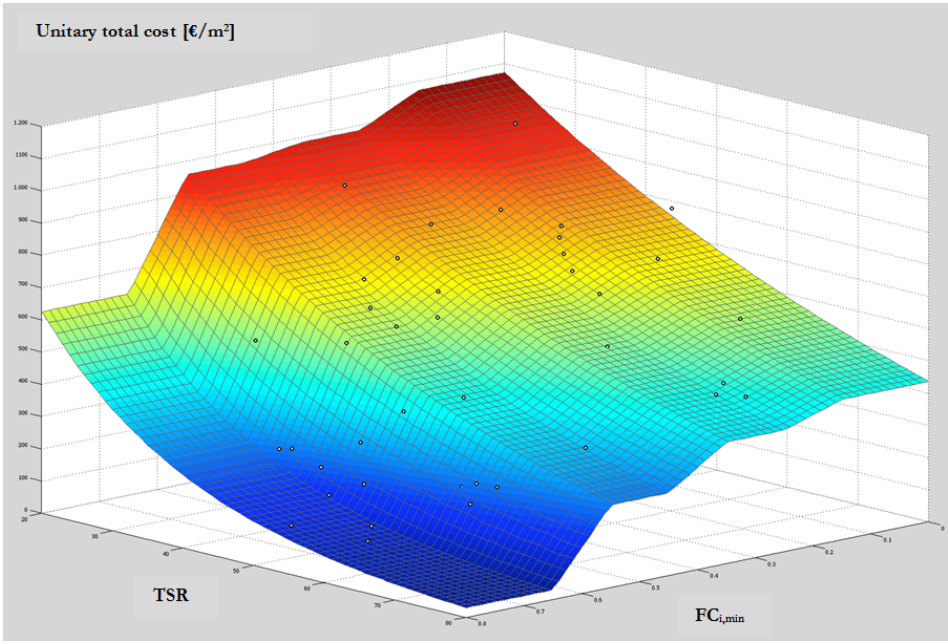

Fig.3.29 Comparison between unitary maintenance cost and unitary total cost provisional equations for masonry bridges.

On the basis of the results obtained from the proposed provisional equations, some considerations can be done:

- regarding unitary maintenance costs, the scatter of the data derived by the *in-situ* visual inspections is partially due to the subjectivity of the inspector: this issue was previously taken into account aiming to minimize it with the calibration of clear structural elements' defect datasheets, but due to the nature of this type of control, the subjective component will never be completely eliminated;
- regarding the dispersion of the data attributable to the cost component related to unitary seismic retrofit costs, it should be observed that similar bridges located in different areas (more or less seismically active) are characterized by different costs: for reducing this variability in case of similar structures it could be possible to assess *UTCs* considering them subjected to the same seismic action. This control was performed on the analysed bridges, highlighting insignificant differences: this is mainly due to the low seismic action differential in the analysed area, thus reflecting in slight variations in the seismic assessment outcomes;
- *UTCs* predictive equations proposed in Table 3.10 should be further optimized, avoiding redundancies in the cost estimation (i.e. taking into

account, as example, that for *RC-PRC* bridges some possible interventions like pier jacketing can be seen both as maintenance and seismic retrofit interventions);

The proposed formulations and more generally the whole methodology allow to quickly manage the maintenance and seismic retrofit of existing bridges, aiming to define a rank in relative terms between assets of bridges belonging to a public authority/private company, with a preliminary estimation of unitary maintenance costs, unitary seismic retrofit costs and unitary total costs for each structure. Once identified bridges most in need of structural interventions, more detailed structural analyses will be later carried out.

3.8 Conclusions

In this work the proposal of an integrated procedure for the evaluation of the maintenance condition state and the seismic vulnerability assessment of existing road bridges was applied to a stock of 150 bridges in the Vicenza province, North-Eastern Italy. Visual inspections were carried out to evaluate a *Total Sufficiency Rating* (*TSR*) and simplified seismic assessment was performed for each bridge, in accordance with Pellegrino et al. (2011) and Pellegrino et al. (2014). For each bridge five parameters were assessed:

- a *TSR* value, representing the qualitative outcome of the visual inspection of the state of maintenance of the whole structure (see Section 3.2);
- a unitary maintenance cost in [€/m^2], which represents the normalized cost referred to 1m^2 deck for the execution of maintenance works with the aim of remove the whole local and diffused defects found on the existing deteriorated structure;
- a $FC_{i,min}$ value, that describes the main criticality detected in the fast seismic assessment of the main structural elements composing each bridge (see Sections 3.3-3.4);
- a unitary seismic retrofit cost, given by *OPCM 3362/04*, in [€/m^2], which represents the normalized cost referred to 1m^2 deck for the execution of structural seismic retrofit interventions aimed to increase the resistance

against horizontal actions of the elements in which criticatilies were detected;

- a unitary total cost in [€/m^2], i.e. the sum of the unitary maintenance cost and the unitary seismic retrofit cost.

The outcomes have been used as input data for a subsequent statistical analysis to derive provisional unitary maintenance, unitary seismic retrofit and unitary total cost equations. A good correlation was found between *TSR* values and unitary maintenance costs, while unitary total costs were characterized by an increased scatter.

The proposed formulations allow public authorities/private managing companies to estimate useful economic indicators for the evaluation of the amount of resources needed for bridge restoration interventions.

4 LIFE-CYCLE OF BRIDGES SUBJECTED TO DETERIORATION

4.1 Introduction

The most significant investments in economic and technological terms on infrastructural networks are often focused on major structures, such as bridges and viaducts (Pellegrino et al. 2014). In this field, the remaining service-life of a bridge structure is the specific time interval in which it can be considered viable from vehicular traffic at the same time ensuring an adequate safety level. In such way, the age of a bridge is not the unequivocal indicator of its efficiency, since in case of a proper maintenance no significant criticalities should be detected over years: this is the case of many ancient historical bridges, in some cases, still yet functional. Bridge regular maintenance and continuous monitoring of the potential ageing effects is therefore a prerequisite for extending the remaining service-life of a structure (Modena et al. 2014).

The United States has always payed attention to the management of the maintenance of its infrastructural network; according to the Federal Highway Administration (*FWHA*), about a third of the more than 570000 bridges belonging to the American main road network is in a state of severe deterioration and needs important maintenance or safety measures to an estimated total amount of 70 billions dollars. During the past decade, the *FHWA* has developed a software called *Pontis*® (currently used in about 40 States), essentially based on the criterion of minimizing the bridges' life-cycle costs. In particular, for each bridge a cost-benefit analysis is performed, where the latter are computed in relation of the differential between the actual maintenance intervention execution and its potential postponement of one annuality.

Several *BMSs* have been subsequently developed over years: Thoft-Christensen (1995) proposed one for reliability theory, Markow (1995) suggested one for highways, Kitada et al. (2000) developed one specifically thought for steel bridges. During the last decade, several research projects focused on the themes of the management at network level of existing bridges have been financed by the European Commission and related guidelines have been produced i.e. *BR.I.M.E.* (2001), *COST345* (2004), *SA.MA.R.I.S.* (2005)

and *Sustainable Bridges* (2006). In *BMSs* currently available a decision making process is almost dependent on a combination of the quantitative/qualitative information obtained from *in-situ* investigations and visual inspections. The scientific community has been deepened these topics and contributed to the development of many *Bridge Management Systems* currently in use worldwide. Referring to European experiences as described in Chapter 3, contributions provided by Franchetti et al. (2004), Pellegrino et al. (2004); Zonta et al. (2007); Pellegrino et al. (2011); Hofmann et al. (2012); Kamya (2012); Söderqvist and Veijola (2012); Torkkeli and Lämsä (2012); Yue et al. (2012); Fruguglietti and Pasqualato (2014), Mendonça and Brito (2014) and Powers and Hinkeesing (2014) can represent the recent state of art on this specific field.

In Italy, any national project is currently in use for the management of the bridge maintenance interventions. The regulatory framework appears undeveloped, in particular if compared to that of other European or American countries. In this context, a *Decree of the President of the Bolzano Province* n°41 (2011) was recently issued in the Autonomous Province of Bolzano (Northern Italy) in which a clear and comprehensive procedure for the different kinds of established in-field surveys was proven, defining the related roles, skills and responsibilities of the whole employees involved in these operations. Owing to the lack of legislation in this specific field, many questions are still left to the discretion of the private companies/public authorities that, for different reasons, are not always able to ensure the compliance of adequate safety and maintenance standards. Moreover, following the issuance of the *Legislative Decree* n°112 (1998), the Central Italian Government moved to regions and local authorities the maintenance management of roads and bridges, emphasizing in some cases interferences and ambiguities in the attribution of duties and responsibilities. Finally, none of these regulations describes a standardized visual inspection execution protocol to which refer for reducing variability in judgments; an adequate Bridge Management System should be developed for systematically organize all the activities connected with the maintenance of infrastructural networks.

Many literature studies have been focused on the numerical modelling of deterioration phenomena commonly affecting civil structures trying to analytically estimate the time-evolution of the ageing of existing structures (Rodriguez et al. 1997; Vidal et al. 2004; Zhang et al. 2009; Saydam et al. 2013; Zanini et al. 2013; Biondini et al. 2014). Despite this, significant troubles in numerically reproducing the real phenomena - in particular in case of effects

concurrence – have been noted, mainly due to the high uncertainty with characterized the predictions if compared with real situations. Furthermore, the execution of numerical simulations of such complexity can be considered impracticable to be performed for hundreds of bridges. The most commonly worldwide used method to detect deterioration conditions of bridge structures with the aim to rationally plan their maintenance over years is based on the visual inspection technique. Generally, different types of controls are performed:

- *superficial inspections*, performed every year by unskilled personnel, with the aim to visually detect the more noticeable defects;
- *general inspections*, carried out at time intervals ranging from 2 to 5 years, visually performed by engineers or technicians with the formulation of a final report;
- *major inspections*, performed at time intervals ranging from 5 to 10 years by qualified personnel with the execution of *in-situ* test for a careful investigation of the main criticalities and mechanical properties of the aging materials composing each bridge structure;
- *in-depth inspections*: special visual inspection to be performed following hazardous events like floods, earthquakes,etc. with the aim of notice the maior criticalities which have to be subsequently detailed with specific *in-situ* investigations.

The outcome of these inspections consists in a series of judgements, used to define maintenance plans and assign higher intervention priorities for bridges more exposed to ageing. The use of the visual inspection technique has clear advantages both from the operational (no traffic interferences, short time duration) and economical point of view; on the contrary it has the drawbacks to be subjected to some fluctuation of results (due to the subjectivity of their ratings), to not allow to detect any latent pathology (e.g., initial stages of the corrosion process) and to not clearly observe defects placed in not easily inspectable parts of the structures without the use of special equipment. For these reasons it is necessary to use statistical techniques for data processing to rationally better control the variance in the judgments (Hasan et al. 2014; Ferreira et al. 2014).
In this regard, this chapter is focused on the development of a statistically-based algorithm allowing to predict bridges' remaining service-life on the basis of the outcomes deriving from the execution of the visual inspection surveys. In

particular, through the application of the Bayesian theory on the visual inspection report data performed on different bridge structural typologies, element deterioration curves have been constructed with the aim of represent the dynamics of the damage progression in the various structural elements. A procedure for the service-life curves construction has been proposed and validated on two bridge stocks defining new relative deterioration indexes useful for the management of numerous structures subjected to environmental ageing.

4.2 The proposed procedure

The proposed procedure is based on the visual inspection outcomes provided for each structural element for which a specific judgement is given. The characteristic element of the proposed application is the definition of specific element deterioration curves for each bridge structural and non-structural component that could be affected by degradation during the bridge service-life. The element deterioration curves are obtained through statistical visual inspection data processing and the use of Bayesan theory: in such way these curves are each time updated with bayesian logic once new visual inspection data – and the related time intervals between the new and the previous ones - are available, with the aim to refine the quality of the deterioration forecast. The deterioration estimation could be the more significant the more amount of data will be available, in particular referring to specific homogeneous bridge categories defined in relation to bridges' construction period, structural scheme, climatic zone, etc…

The procedure is organized in 6 steps as shown in Figure 4.1. Specifically, the inspector has to fill the visual inspection form in relation to the specific bridge characteristics: the visual inspection allows to define a global efficiency indicator of the maintenance state of the bridge at the time of the inspection (*Total Sufficiency Rating*, *TSR,* as previously described) and can be used for the Bayesian updating of the element deterioration curves. The subsequent step consists in the generation of potential bridge deterioration scenarios, aimed to estimate a projection of the *TSR* value over years, assessing the time intervals needed for observe the bridge structure in particular efficiency levels, on the basis of the element deterioration curves previously described. In such way, it is

possible to fit these provisions and calculate a mean remaining service-life of each analysed bridge.

Lastly, once defined *Road Type* (*RT*) and *Network Bridge Importance* (*NBI*) coefficients, used for weighting bridges' relative importance in the context of an infrastructural network management, specific *TSR* values and *Deterioration Progression Indexes* (*DPI*) can be evaluated to represent what might be the global deterioration state of a bridge in a hypothetical future year in which the road agency expects to perform a maintenance intervention. In the following a more detailed description of each step is provided.

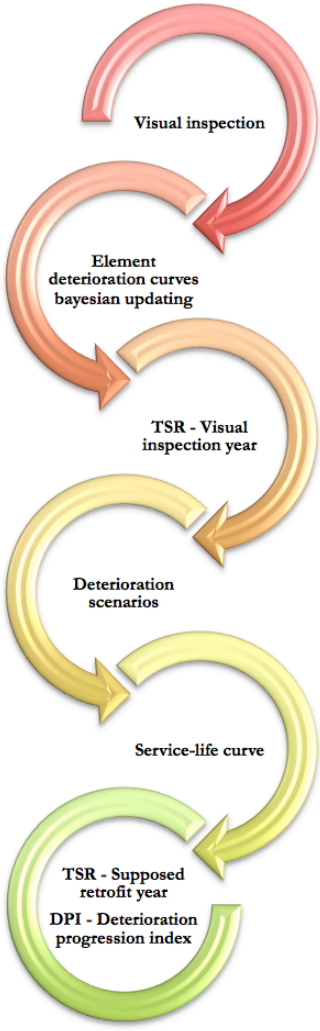

Fig.4.1 The proposed framework for the bridge deterioration time evolution assessment.

4.2.1 Visual inspection

The visual inspection is performed by a technician that has to detect, element by element, any defect or visible deterioration phenomenon and has to fill a visual inspection form in which assigning a *Condition Value* (*CV*) ranging from 1 to 5 for each bridge component. In the case of not easily inspectable elements, a *CV* = 0 is assigned. If a specific element is not present on a bridge structure, no judgement is given.
The definition of the *CVs* has been revised for the structural elements with respect to the previous version described in Pellegrino et al. 2011 by adding a series of "*defect tables*" in which the whole potential detectable deterioration phenomena are described and characterized with:

- a specific weight (*G*), defined according the damage potential severity;
- an extension coefficient (k_1) equal to 20% – 50% – 100%;
- an intensity coefficient (k_2) equal to 20% – 50% – 100%.

For each of them a *Defect Index* (*DI*) taking into account all the above factors is calculated as:

$$DI = G \times k_1 \times k_2 \tag{4.1}$$

In Figure 4.2 a defect table for concrete beams is shown as example. Once defined the sum of the *DIs* for each element, the related *CV* is estimated with a linear relationship:

$$\mathrm{CV} = 1 + \frac{4}{\sum \mathrm{G}} \sum \mathrm{DI} \tag{4.2}$$

where $\Sigma DI = 0$ corresponds to a $CV = 1$ and the maximum value of ΣDI lead to a $CV = 5$. The $\sum G$ value is equal to the total weight of the possible defect combinations potentially detectable during a visual inspection on a specific structural element.
This value has to be evaluated by formulating possible hypotheses of defects coexistence also in relation to their nature (defects with durability or structural implications). Multiple tests have been performed on different elements leading to the estimation of a mean value of $\sum G = 14$. Non-structural and secondary

elements have been indeed evaluated with unitary *CVs*, without using an analytical approach like the previously described one.

1 - LONGITUDINAL ELEMENTS					
DEFECT	DEFECT PRESENCE	G	DEFECT EXTENT	DEFECT INTENSITY	DI
Active moisture spots	TRUE	1,00	1 1	1 1	1,00
Passive moisture spots	TRUE	4,00	1 1	0 0	0,00
Washed/deteriorated concrete	TRUE	2,00	1 1	1 1	2,00
Concrete crawlspaces	TRUE	2,00	1 1	0,5 0,5	1,00
Concrete cover detachment	FALSE	2,00	1 1	1 1	0,00
Oxidized bars	FALSE	5,00	1 1	1 1	0,00
Uncovered/oxidized stirrups	TRUE	3,00	0,2 0,2	1 1	0,60
Cobweb cracks	TRUE	1,00	1 1	0 0	0,00
Transversal cracks	FALSE	5,00	0,2 0,2	0,5 0,5	0,00
Diagonal cracks	FALSE	5,00	0,5 0,5	1 1	0,00
Anchorages capillar cracks	FALSE	1,00	0,5 0,5	0 0	0,00
Unsealed anchorages	FALSE	2,00	0,5 0,5	0 0	0,00
Anchorages swabs detachment	TRUE	1,00	0,5 0,5	1 1	0,50
Lesions of beam core along prestressing cables	TRUE	2,00	0,5 0,5	0,2 0,2	0,20
Lesions at the bottom of the prestressing bulb	FALSE	2,00	0,5 0,5	0,5 0,5	0,00
Uncovered sleeves	TRUE	2,00	0,5 0,5	0 0	0,00
Beam/transverse detachment	TRUE	3,00	0,2 0,2	0,2 0,2	0,12
Deteriorated casting resumptions	FALSE	1,00	1 1	0 0	0,00
Prestressing cables area reduction	FALSE	5,00	1 1	0,2 0,2	0,00
Internal moisture	FALSE	2,00	0,2 0,2	0 0	0,00
Oxidized/uncovered bars at the beam ends	FALSE	2,00	1 1	0,2 0,2	0,00
Damages caused by bearings	FALSE	4,00	0,2 0,2	0,5 0,5	0,00
Vehicular collision damage	FALSE	4,00	0,2 0,2	0,2 0,2	0,00
					5,42

CV	1,6

Fig.4.2 Defect table for a reinforced concrete/prestressed reinforced concrete beam.

4.2.2 Element deterioration curves bayesian updating

In the evaluation of a parameter on the basis of data collected in different time instants, in which the previous information is refined via the detection of new data on the same parameter, the Bayesian approach proves to be a suitable methodology for the information variability control. In this context, the concept of probability is interpreted as the confidence degree in the occurrence of a certain event and it is related to its knowledge, or on the converse to its unknowing. The main advantage offered by this approach is the possibility to make probabilistic statements about any event, regardless to the condition of having a perfectly symmetric problem or the possibility or not to replicate again a test many times.

A fundamental statistical bayesian inference case is the observation of a result of *n* random variables normally and independently distributed:

$$X_1,\ldots,X_n \sim N(\mu;\ \sigma^2) \qquad (4.3)$$

Knowing σ^2 the aim is to make inference on the θ parameter. Considering the likelihood L_θ (x_1, x_2, … x_n), function of the θ parameter and the x_1, x_2, … x_n data, the application of the Bayes theory lead to the definition of the *a posteriori* probability density function:

$$f_{post}(\vartheta) = \frac{L_{\vartheta(x_1,x_2,\dots x_n)}\,\pi(\vartheta)}{\int L_{\varphi(x_1,x_2,\dots x_n)}\,\pi(\varphi)\,d\varphi} \tag{4.4}$$

where the normal probability density function is:

$$f(x_i|\vartheta) = \frac{1}{\sqrt{2\pi\sigma^2}}\, e^{\frac{-(x-\mu)^2}{(2\sigma^2)}} \tag{4.5}$$

Because of the independency of the considered variables, it is possible to define the joint probability density function as the product of the singular densities:

$$L_{\vartheta(x_1,x_2,\dots x_n)} = \frac{1}{\sqrt{2\pi\sigma^2}}\, e^{\frac{-(x_1-\mu)^2}{(2\sigma^2)}} \cdot \frac{1}{\sqrt{2\pi\sigma^2}}\, e^{\frac{-(x_2-\mu)^2}{(2\sigma^2)}} \cdots \frac{1}{\sqrt{2\pi\sigma^2}}\, e^{\frac{-(x_n-\mu)^2}{(2\sigma^2)}} \tag{4.6}$$

and simplifying obtaining:

$$L_{\mu(x_1,x_2,\dots x_n)} = C(x_1,\dots,x_n)\exp^{\left\{-\frac{(\bar{x}-\mu)^2}{2\sigma^2}\right\}} \tag{4.7}$$

where:

$$C(x_1,x_2,\dots x_n) = \frac{1}{(2\pi\sigma^2)^{n/2}}\exp^{\left\{-\frac{\sum_{i=1}^{n}(x_i-\bar{x})^2}{2\sigma^2}\right\}} \tag{4.8}$$

The exact expression of $C(x_1, x_2, \dots x_n)$ is not function of the μ parameter that has to be estimated. Replacing (4.7) in (4.4), and using μ instead of θ for the evaluation of the f_{post} and v instead of ϕ as integration variable, the following equation can be derived:

$$f_{post}(\mu) = \frac{C(x_1,\dots,x_n)\exp^{-n\left\{\frac{(\bar{x}-\mu)^2}{2\sigma^2}\right\}}\pi(\mu)}{\int C(x_1,\dots,x_n)\exp^{-n\left\{\frac{(\bar{x}-\upsilon)^2}{2\sigma^2}\right\}}\pi(\upsilon)\,d\upsilon} = \frac{\exp^{-n\left\{\frac{(\bar{x}-\mu)^2}{2\sigma^2}\right\}}\pi(\mu)}{\int \exp^{-n\left\{\frac{(\bar{x}-\upsilon)^2}{2\sigma^2}\right\}}\pi(\upsilon)\,d\upsilon} \tag{4.9}$$

where it can be observed how $C(x_1, x_2, \dots x_n)$ is irrelevant. Once an *a priori* probability density function $\pi(\mu)$ has been choosen, depending on the degree of knowledge of the investigated variable, the integral in Equation 4.9 can be

defined. The solution to assume a normal *a priori* probability density function allow to derive a normal *a posteriori pdf* too, therefore enabling to immediately iterate the procedure once new data are acquired. Considering the following function:

$$\pi(\mu) = \frac{1}{\sqrt{2\pi{\tau_0}^2}} e^{\frac{-(\mu-\mu_0)^2}{(2{\tau_0}^2)}} \tag{4.10}$$

the *a priori* normal *pdf* is characterized by a mean value μ and variance ${\tau_0}^2$, so therefore μ_0 is considered the most likely μ value, whereas ${\tau_0}^2$ represents the level of uncertainty with respect to it. Substituting $\pi(\mu)$ in Equation 4.9, the f_{post} expression can be derived:

$$f_{post}(\mu) = \frac{1}{\sqrt{2\pi{\tau_p}^2}} e^{\frac{-(\mu-\mu_p)^2}{(2{\tau_p}^2)}} \tag{4.11}$$

In such way also the *a posteriori pdf* is normal with expected mean value μ_p and variance ${\tau_p}^2$ calculated as follows:

$$\mu_p = \frac{\frac{1}{\tau_0^2}\mu_0 + \frac{n}{\sigma^2}\bar{x}}{\frac{1}{\tau_0^2} + \frac{n}{\sigma^2}} \qquad {\tau_p}^2 = \frac{1}{\frac{1}{\tau_0^2} + \frac{n}{\sigma^2}} \tag{4.12}$$

In particular, in this study, the Bayesian updating has been coincieved for the prediction of the number of annualities needed from a generic bridge component for moving from a specific *CV* to the next worsen one, thus formulating a deterioration provision based on a set of previously available data and progressively updated with new information collected during the visual surveys.

4.2.3 Total Sufficieny Rating (TSR) assessment

The procedure for the evaluation of the bridge maintenance state through the calculation of the *Total Sufficiency Rating* (*TSR*) has been lightly updated on the basis of the proposal described in Pellegrino et al. 2011. A brief overview of the procedure and the main changes introduced with this work is herein described.

First of all, given the nature of the visual inspection technique, the elements hardly visible – like abutments and piers foundations or waterproofing– have been deleted, since in this context any judgement is meaningless.
After the definition of the *CVs* for the structural/non-structural elements of the bridge with the methodology described in §4.2.1, the *Condition Factor* (*CF*) for each of them has been estimated, as shown in Table 4.1. The relationship between *CV* and *CF* has been revised with respect to the previous version proposed in Pellegrino et al. 2011. For non-integer values of *CV*, linear interpolation is allowed for the calculation of the related *CF*.

CV	0	1	2	3	4	5
CF	0	100	70	50	25	1

Table 4.1 Proposed relation between Condition Value and Condition Factor.

The elimination of same unvisible elements has lead to the revision of the *Location Factor* (*LF*) and the related element *Weights* (*W*) to be considered in the *TSR* calculation, as shown in Table 4.2. No changes in the values of the different *Road network Type* (*RT*), *Traffic Index* (*TI*), *Network Bridge Importance* (*NBI*) and *Age Factor* (*AF*) coefficients have been made.
For each bridge component an *Element Sufficiency Rating* (*ESR*) ranging from 1 to 100 can be calculated as described in Pellegrino et al. 2011. Once defined the whole *ESR* values, the *TSR* value can be assessed with the following revised procedure:

- estimation of the TSR_{REAL} value, as follows:

$$\mathrm{TSR_{REAL}} = (\mathrm{RF\ x\ NBI\ x\ AF}) \left(\frac{\sum_{i=1}^{t} \mathrm{CF_i\ W_i}}{\sum_{i=1}^{n} \mathrm{W_i}} \right) \tag{4.13}$$

- elements which could not be inspected are considered with a *CV* equal to 3, avoiding unnecessary penalties. The revised procedure lead to the calculation of the TSR_{NV} of the *n-t* non-valuable elements (in substitution of the previous TSR_{min}), as follows:

- $$\mathrm{TSR_{NV}} = (\mathrm{RF\ x\ NBI\ x\ AF}) \left(\frac{\sum_{i=1}^{n-t} \mathrm{CF_i\ W_i}}{\sum_{i=1}^{n} \mathrm{W_i}} \right) \tag{4.14}$$

- the final formulation for the *TSR* evaluation is expressed as:

$$TSR = \frac{[TSR_{REAL} \sum_{i=1}^{t} W_i + TSR_{NV} (\sum_{i=1}^{n} W_i - \sum_{i=1}^{t} W_i)]}{\sum_{i=1}^{n} W_i} \quad (4.15)$$

In any case, if the sum of the weights of the evaluated elements is lower than the 70% of the total sum of weights, the *TSR* evaluation must not be performed due to the scarsity of available information. Every bridge, in such way, belongs to a different urgency level class in relation to its *TSR* value: in this work the urgency classes have been revised as shown in Table 4.3. Figure 4.3 shows the graphical user interface for the *TSR* value assessment.

Bridge element	***LF***	***W***
Longitudinal elements, arches, pillars, piers	5	12
Transversal elements, slabs, support equipments, seismic devices	6	10
Abutments, approach embankment, walls	7	8
Joints, water selling	9	6
Pavements, slab curb, guard-rail, sidewalks, utilities, lighting	10	4

Table 4.2 Proposed Location Factor (LF) and related Weights (W) values.

Urgency intervention level	***TSR***
Maximum intervention urgency	1 – 25
Short-term intervention urgency	26 – 50
Mid-term intervention urgency	51 – 70
Long-term intervention urgency	71 – 100

Table 4.3 Proposed efficiency and urgency levels of intervention for the whole bridge.

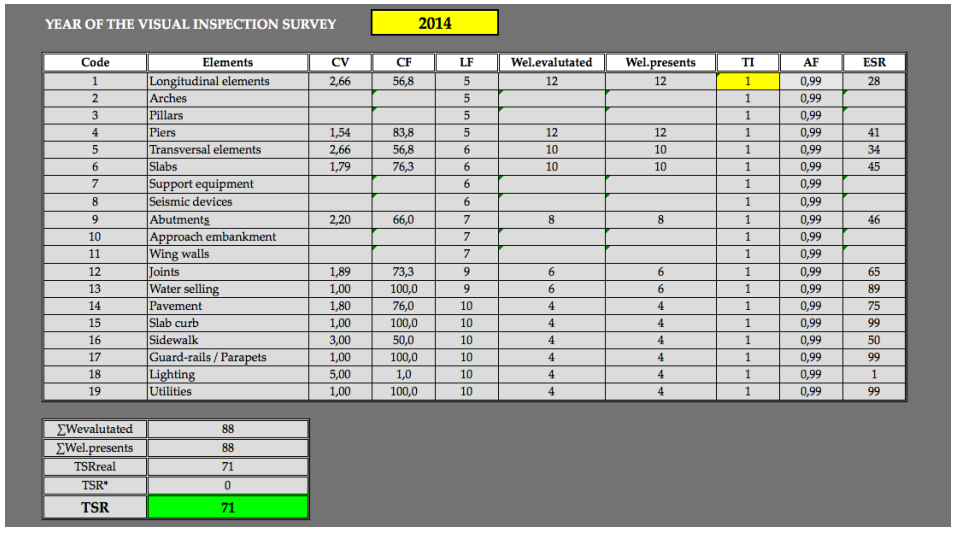

YEAR OF THE VISUAL INSPECTION SURVEY: 2014

Code	Elements	CV	CF	LF	Wel.evalutated	Wel.presents	TI	AF	ESR
1	Longitudinal elements	2,66	56,8	5	12	12	1	0,99	28
2	Arches			5			1	0,99	
3	Pillars			5			1	0,99	
4	Piers	1,54	83,8	5	12	12	1	0,99	41
5	Transversal elements	2,66	56,8	6	10	10	1	0,99	34
6	Slabs	1,79	76,3	6	10	10	1	0,99	45
7	Support equipment			6			1	0,99	
8	Seismic devices			6			1	0,99	
9	Abutments	2,20	66,0	7	8	8	1	0,99	46
10	Approach embankment			7			1	0,99	
11	Wing walls			7			1	0,99	
12	Joints	1,89	73,3	9	6	6	1	0,99	65
13	Water selling	1,00	100,0	9	6	6	1	0,99	89
14	Pavement	1,80	76,0	10	4	4	1	0,99	75
15	Slab curb	1,00	100,0	10	4	4	1	0,99	99
16	Sidewalk	3,00	50,0	10	4	4	1	0,99	50
17	Guard-rails / Parapets	1,00	100,0	10	4	4	1	0,99	99
18	Lighting	5,00	1,0	10	4	4	1	0,99	1
19	Utilities	1,00	100,0	10	4	4	1	0,99	99

∑Wevalutated	88
∑Wel.presents	88
TSRreal	71
TSR*	0
TSR	**71**

Fig.4.3 Proposed algorithm for the assessment of the Total Sufficiency Rating (TSR).

4.2.4 Deterioration scenarios

The revised procedure for the *TSR* assessment is subsequently coupled with the element deterioration curves to generate specific deterioration scenarios for the simulation of the progressive deterioration of the bridge health state, synthetically described by the *TSR* index.

First, deterioration scenarios are computed for the visual inspection year and for the year in which a hypotetic maintenance intervention could be performed. On the basis of these scenarios, through an iterative algorithm, other four different deterioration scenarios – one for each urgency intervention level described in Table 4.3 – are computed, estimating also their related annualities. Figure 4.4 shows the 6 deterioration scenarios estimated for a generic bridge.

In particular, starting from the *CVs* of the elements evaluated during the visual inspection, an iterative increase/decrease of their values with a ΔCV = 0,2 is performed, deriving a new *TSR* value. The process ends when the *TSR* value falls into the desidered urgency intervention level. Regarding the definition of the specific annuality related to each *TSR* value, an arithmetic mean is performed between the predicted ages of only the structural elements: this solution can be refined considering also specific weights for each component involved in the annuality calculation.

Fig.4.4 Example of deterioration scenarios processing.

4.2.5 Service-life curve construction

On the basis of the deterioration scenarios previously obtained, the related *TSR*-annuality data are interpolated to define a mean service-life curve of the bridge, which visualize the degerative performances of the structure in terms of *TSR* value over years.

The remaining service-life period can be defined as the residual time interval in which a bridge structure ensures an adequate functionality and at once safety level. It is assumed in fact that for *TSR* values lower than 20, a bridge structure can no longer be considered safe for the traffic flow transitability: in this situation the service-life curve slope significantly grows due to the increased exposition to further failures. It can be also observed how performing maintenance interventions in conditions of advanced degradation situations is not the optimal solution under an economical point of view, since the highest marginal utilities can be reached in case of mid-term urgency intervention states.

The service-life curve of a bridge structure can therefore be fitted by a parabolic equation like:

$$TSR\,(t) = at^2 + bt + c \qquad (4.16)$$

where t is the annuality expressed in years and a, b, c are coefficients to be calibrated each time in relation to the data derived from the deterioration scenarios. Figure 4.5 shows an example of the bridge service-life curve estimation for a generic bridge.

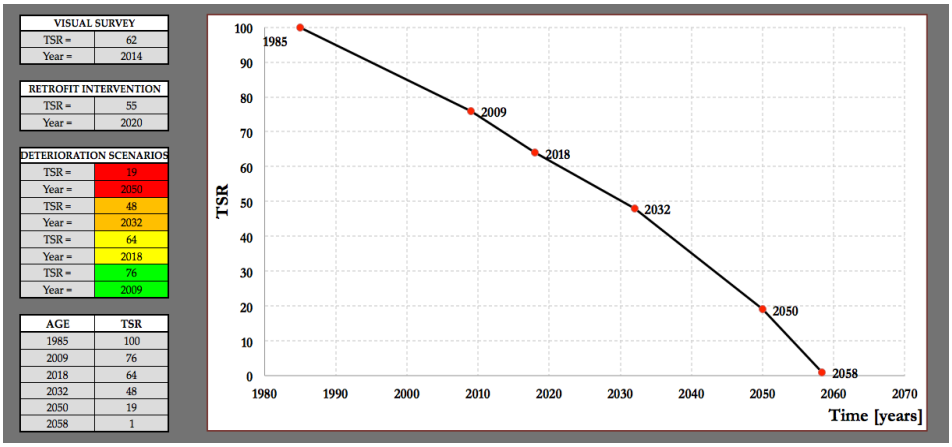

Fig.4.5 Example of the bridge service-life curve estimation.

4.2.6 TSR and Deterioration Progression index (DPI) assessment

Finally, once the service-life curve of a bridge has been defined, *TSR* and the *Deterioration Progression Index* (*DPI*) can be estimated for the annuality in which a potential intervention is planned, previously defining *NBI* and *RT* coefficients (which can vary over time and so have to be specified in relation to the specific investigated annuality).
The *DPI* is calculated dependently on the specific urgency intervention class to which the structure will belong in the hypothetical intervention year as the ratio between the *TSR* values is such urgency intervention class and their related annualities, expressed in years:

$$DPI = \Delta TSR / \Delta t \tag{4.17}$$

The *DPI* value will be greater for bridges characterized by lower *TSR* values, since deterioration speed will be more significant for more degradated structure. In the context of the management of clusters of bridges, once defined the hypothetical intervention annualities, *DPIs* can be used for highlight relative deterioration speeds and guide owners in the selection of the best intervention plan policy to be followed in the allocation of economical resources.

4.3 Case study

The proposed procedure has then been applied to a specific case study to evaluate the effectiveness of its provisional capacity. The bridges under analysis are the A27 highway overpasses located between the tollbooths of Venice North and Vittorio Veneto: in this highway section about thirty of this bridge type are characterized by homogeneous structural typology, materials, construction year and limate zone. The high homogeneity level makes them suitable to be statistically treated as a homogeneous data sample. Twelve of them have been subsequently considered since the remaining had already experienced previous maintenance interventions.
The structural scheme of the analysed bridges consists in three simply-supported spans for a total length of 61,5m, the external ones realized with

reinforced concrete beams with span length equal to 12m, whereas the central one characterized by two steel beams and a reinforced concrete slab with a span length of 37,5m. Spans are sustained with two reinforced concrete framed piers with squared columns of 0,9m and an eccentric transverse beam of 1,2m high. Figure 4.6 shows some detailed views of the structural typology under investigation. Reinforced concrete abutments, joints, approach embankments and pavements are also present whereas no seismic devices have been detected. Finally, non-structural components like water sellings, sidewalks, slab curbs, guard-rails and lighthings have been identified.

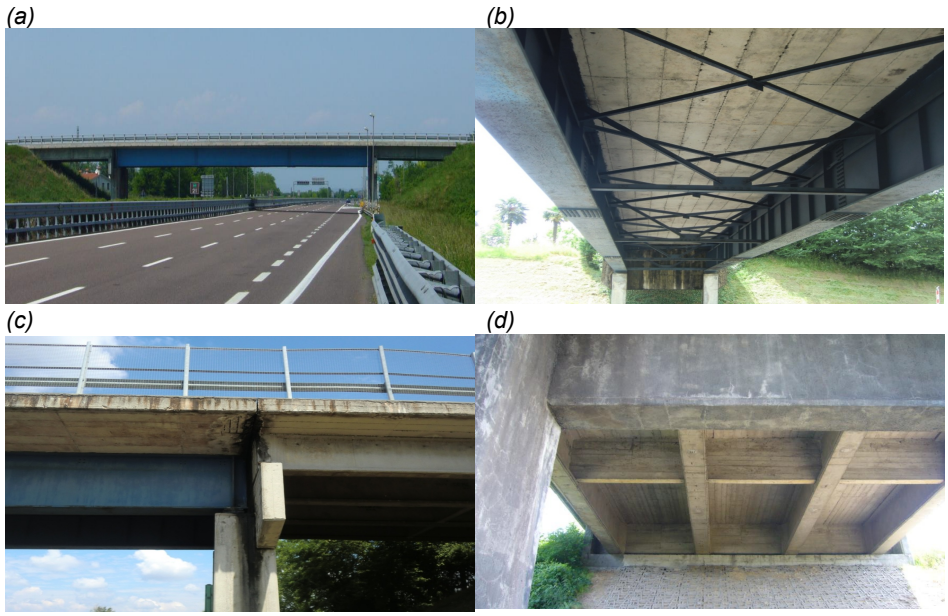

Fig.4.6 General view (a), main steel span (b), lateral reinforced concrete spans (c) and detail of the beams bearing (d) of the analysed A27 highway bridges.

A significant degradation has been detected on the various structural/non-structural elements during the visual inspection to each bridge. In the following, a brief description of the deterioration phenomena observed is reported:

- *reinforced concrete piers*: in most cases a rainwater washout has been detected due to inadequate water selling systems. A significant number of exposed steel rebars has been observed due to construction errors and in many cases concrete cover detachment, particularly in correspondence of the transverse reinforced concrete beam, as shown in Figure 4.7;

- *steel beams*: oxidation phenomena have been observed, often in the extradoxal flanges and protective varnish exfoliations have been observed (Figure 4.8) but without reaching significant corrosion levels;
- *reinforced concrete slab*: many moisture spots have been found in different parts of the deck slabs probably due to the loss of functionality of the waterproofing (Figure 4.8). No significant cracks have been observed and no rebars corrosion phenomena has been noted;
- *support equipments, joints*: in many cases the first ones have not been clearly visible, so no judgment has been given; regarding joints, significant damages have been detected with the observation in some cases of significant cracks between the adiacent decks (Figure 4.9);

Fig.4.7 Piers (a, b) and transverse reinforced concrete beams (c, d) deterioration state detected on the analysed bridges.

- *pavements, water sellings:* pavements have been characterized by good conditions, only occasionally cracked if excluded the areas in correspondence to the joints; regarding water selling systems, in most cases no drains have been found and in general the lack of care to this specific non-structural component has lead to develop significant

(a) (b)

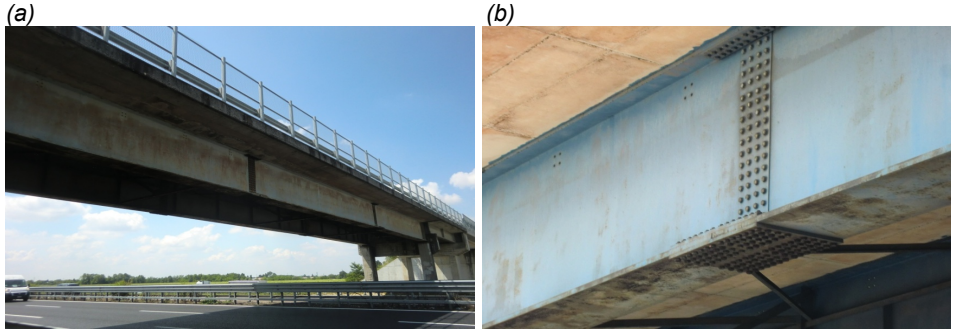

(c) (d)

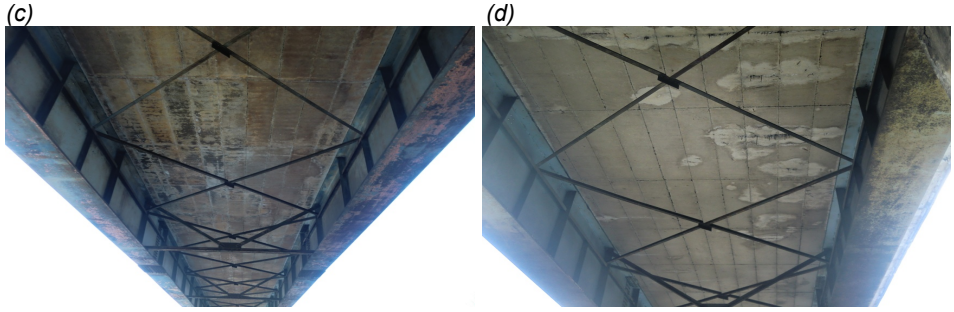

Fig.4.8 Steel beams (a, b) and reinforced concrete slabs (c, d) deterioration state detected on the analysed bridges.

(a) (b)

(c) (d)

Fig.4.9 Equipment supports (a, b) and joints (c, d) deterioration state detected on the analysed bridges.

degradation states for other most important structural elements (Figure 4.10). In some structures no water selling systems have been detected; in other ones the installation of such systems has taken place at different times with respect to the age of bridge construction;

- *slab curbs, sidewalks*: the first ones have been often characterized by serious deterioration situations as also the sidewalks too, sometimes showing the underneath corroded steel rebars (Figure 4.11);
- *guard-rails, lighting*: although present in each analysed bridge, guard-rails are not conform with respect to the current regulations; regarding lighting, some punctual defects have been noted and in few cases no lighting has been found.

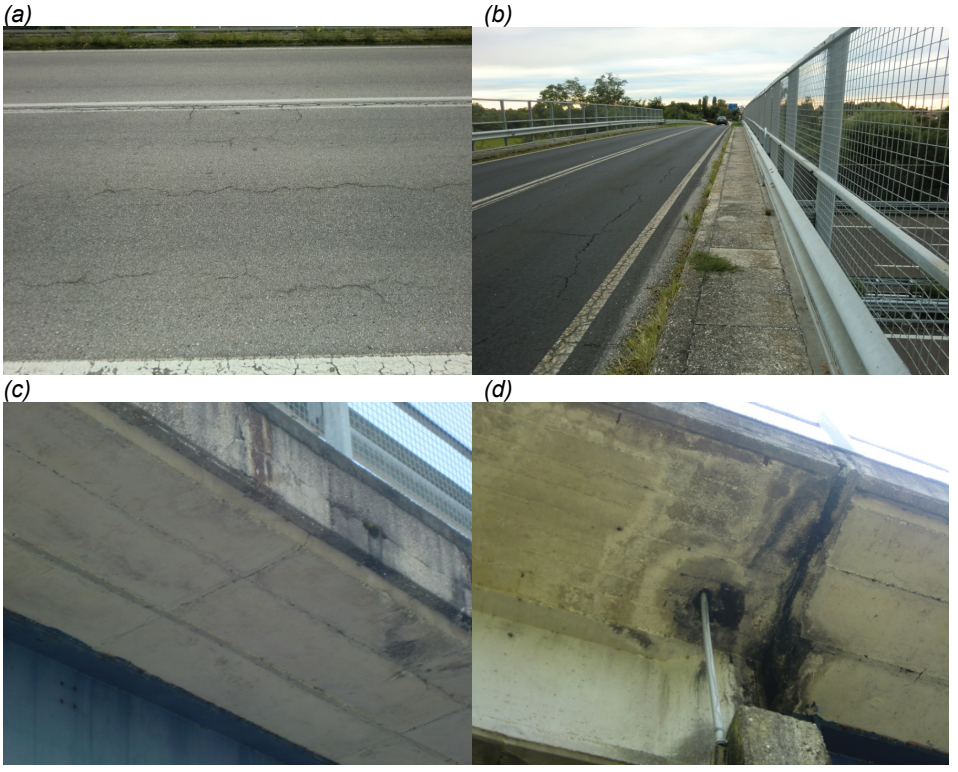

Fig.4.10 Pavements (a, b) and water disposals systems (c, d) deterioration state detected on the analysed bridges.

The information collected during the visual inspection allowed to fill the visual inspection forms and to assess a specific *CV* for each bridge component: with these data it is first possible to update the element deterioration curves via

Bayesian techniques and at the same time estimate the *TSR* value at the time of the visual inspection for the analysed bridge.

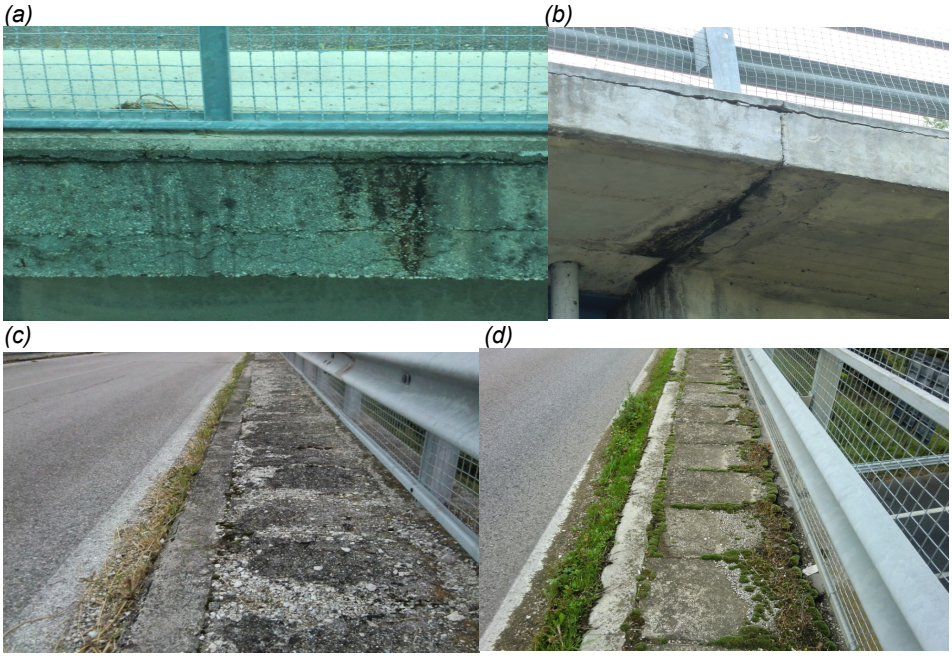

Fig.4.11 Slab curbs (a, b) and sidewalks (c, d) deterioration state detected on the analysed bridges.

Regarding the Bayesian updating of the element deterioration curves, known for each brigde component the *CVs* visual inspection outcomes of a pair of subsequent inspections and the relative time interval *Δt* between them, it is possible to define by extrapolation the $\Delta t[CV_i - CV_{i+1}]$ needed to increase of a unitary value a certain integer *CV* to the next integer one with the following:

$$\Delta t|\mathrm{CV(i)} - \mathrm{CV(i+1)}| = \frac{\Delta t}{12\Delta \mathrm{CV}} \tag{4.18}$$

where *Δt* is expressed in months whereas $\Delta t[CV_i - CV_{i+1}]$ is expressed in annualities. The higher number of available data and the more significant may be the provisional capacity of the element deterioration curves. In the following, an application is shown as example to better explain the elment deterioration curves Bayesian updating technique: the definition of the number of annualities needed fot moving from *CV* = 1 to *CV* = 2 for a reinforced concrete slab on the basis of 5 pairs of visual inspections collected on 5 different bridges belonging

to a stock of about fourty bridges located in the Rovereto Municipality, in the Autonumous Province of Trento, Northern Italy. In Table 4.4 the main data used for the following analysis are provided.

Bridge #	*CV* 1st inspection	*CV* 2nd inspection	*ΔCV*	*Δt* [months]	*Δt*[CV_i - CV_{i+1}] [years]
1	1,13	1,79	0,66	79	10,0
2	1,63	2,45	0,82	46	4,7
3	1,45	1,85	0,40	46	9,6
4	1,75	3,01	1,26	79	5,2
5	1,00	1,24	0,24	46	16,0

Table 4.4 Visual inspection data of reinforced concrete slabs for the evaluation of Δt[CV1 – CV2].

Let θ (number of annualities needed from moving to *CV* = 1 to *CV* = 2) the parameter to be assessed. Considering θ as a random variable normally distributed and assuming -due to the lack of previous data- an *a priori* θ distribution characterized by a mean value μ_0 = 15 years and a variance τ_0 = 15 years, the hypotheses system is defined as follows:

H_0: $\theta = \theta_0 = 15$
H_1: $\theta = \theta_1 \neq 15$ (4.19)

assuming a significant uncertainty level to the *a priori* information. The new data collected and shown in Table 4.4 are characterized by a mean value $\bar{x}$ = 16,02 years and a variance σ = 9 years. With these new data it is possible to update the θ distribution by calculating the *a posteriori* mean value μ_p and variance τ_p as follows:

$$\mu_p = \frac{\frac{1}{\tau_0^2}\mu_0 + \frac{n}{\sigma^2}\bar{x}}{\frac{1}{\tau_0^2} + \frac{n}{\sigma^2}} = 15,98 \qquad \tau_p^2 = \frac{1}{\frac{1}{\tau_0^2} + \frac{n}{\sigma^2}} = 2,94 \tag{4.20}$$

Figure 4.12 gives a graphical representation of the likelihood function and the *a priori* and *a posteriori* probability density functions of the θ number of annualities needed from moving to *CV* = 1 to *CV* = 2. It can be observed how both the *a priori* and the information derived from the sample of new data have a significant impact in the definition of the *a posteriori* probability density function.

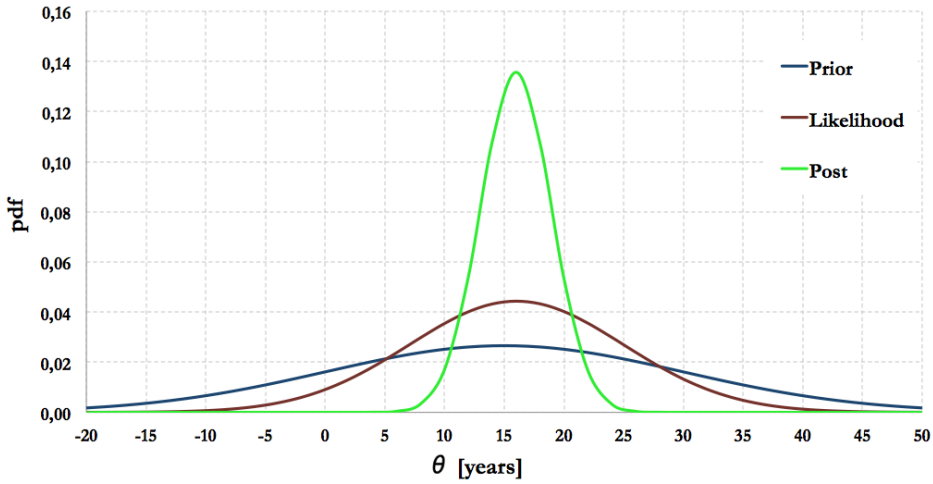

Fig.4.12 A priori, a posteriori pdfs and likelihood function of the θ parameter.

Repeating this calculation for the remaining *CV* intervals (*CV2→CV3*, *CV3→CV4* and *CV4→CV5*) and defining for each of them a 90% confidence interval for the evaluation of the *a posteriori* mean value of the number of annualities needed for moving to *CV* = *i* to *CV* = *i+1*, it is possible to describe the *CV* deterioration time evolution over years for the reinforced concrete slab element. Table 4.5 reports the analysis outcomes for the reinforced concrete slab element.

$\lvert CV_i\text{-}CV_{i+1}\rvert$	$\Delta t\lvert CV_i\text{-}CV_{i+1}\rvert$ *lower bound* [years]	$\Delta t\lvert CV_i\text{-}CV_{i+1}\rvert$ *mean value* m_p [years]	$\Delta t\lvert CV_i\text{-}CV_{i+1}\rvert$ *upper bound* [years]	$\Delta t\lvert CV_i\text{-}CV_{i+1}\rvert$ *cumulative standard deviation* [years]
1 → 2	13,9	16,0	18,1	4,2
2 → 3	24,4	30,4	36,4	11,9
3 → 4	29,3	36,7	44,1	14,8
4 → 5	34,0	41,0	49,0	15,0

Table 4.5 Main parameters of the reinforced concrete slab deterioration curves.

The last column of Table 4.5 shows the cumulative standard deviation, i.e. the comprehensive variability including the uncertainty values calculated in the precedening *CVs* intervals. Finally, Figure 4.13 represents the element deterioration curves for the main structural components present in the bridge type under analysis, i.e. piers, beams and slabs obtained by the above procedure.

It can be observed how these element deterioration trends have to be considered coming from a bridge stock characterized by homogeneities in the climatic zone and used materials, but with different structural schemes and construction ages. In such way the variability expressed by the cumulative standard deviation of each element deterioration curve represent this specific item. The procedure has been finally reiterated by updating element deterioration curves with the new set of *CVs* data specifically collected during two successive visual inspections perfomed on the analysed overpasses and shown in Table 4.6.

Bridge	**#1**	**#2**	**#3**	**#4**	**#5**	**#6**	**#7**	**#8**	**#9**	**#10**	**#11**	**#12**
Element	***CV***	***CV***	***CV***	***CV***	***CV***	***CV***	***CV***	***CV***	***CV***	***CV***	***CV***	***CV***
Longitudinal elements	2,84	2,97	2,31	2,84	2,84	2,84	2,84	2,97	3,49	2,31	2,84	2,82
Arches	-	-	-	-	-	-	-	-	-	-	-	-
Pillars	-	-	-	-	-	-	-	-	-	-	-	-
Piers	3,05	2,47	2,50	2,71	2,95	2,14	2,89	2,95	3,26	2,47	3,08	2,77
Transversal elements	2,40	2,24	2,55	2,55	2,86	2,33	2,38	2,33	2,55	2,63	2,94	2,52
Slabs	1,93	2,09	1,99	2,16	1,99	2,26	2,26	1,91	2,42	1,92	1,98	2,08
Support equipments	0	0	0	0	0	0	0	0	0	0	0	0
Seismic devices	-	-	-	-	-	-	-	-	-	-	-	-
Abutment	-	-	-	-	-	-	-	-	-	-	-	-
Approach embankment	1,0	2,0	2,0	2,0	2,0	1,0	1,5	1,0	1,5	2,0	1,0	2,0
Walls	-	-	-	-	-	-	-	-	-	-	-	-
Joints	4,0	1,0	3,0	3,0	3,0	4,0	3,0	4,0	5,0	4,0	5,0	4,0
Water selling	5,0	1,0	5,0	1,0	5,0	5,0	5,0	5,0	5,0	5,0	5,0	4,0
Pavement	2,0	1,0	2,0	2,0	2,0	2,0	2,0	2,0	2,0	2,0	2,0	2,0
Slab curb	4,0	4,0	4,0	4,0	4,0	4,0	4,0	2,0	4,0	4,0	4,0	4,0
Sidewalk	4,0	3,0	1,0	4,0	5,0	5,0	4,0	4,0	5,0	5,0	5,0	4,0
Guard-rail Parapets	1,0	1,0	1,0	1,0	1,0	1,0	1,0	1,0	1,0	1,0	1,0	1,0
Lighting	1,0	5,0	5,0	5,0	5,0	5,0	5,0	1,0	1,0	5,0	5,0	4,0
Utilities	-	-	-	-	-	-	-	-	-	-	-	-

Table 4.6 CVs assessed during the second visual inspections to the analysed bridge overpasses.

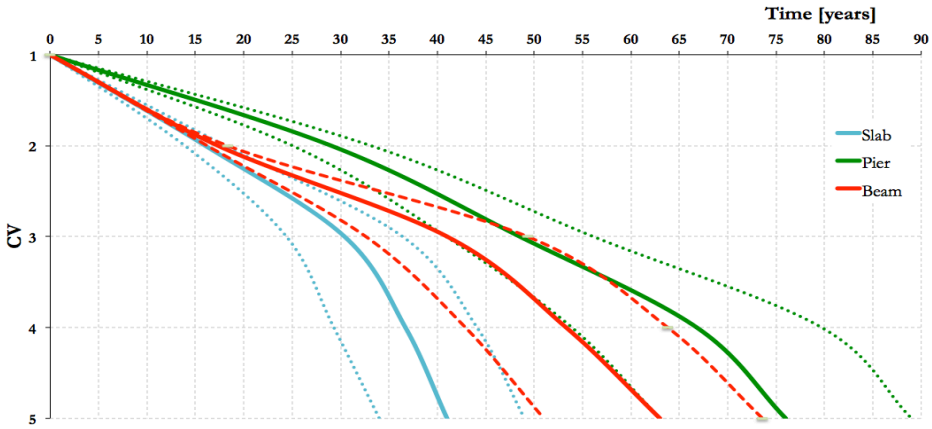

Fig.4.13 Piers, beams and slabs mean, upper and lower bounds element deterioration curves.

For each of the 12 analysed highway overpasses the relative specific *TSR* value has been assessed (see Table 4.7), considering for each of them the coefficients *TI* = 1 and *AF* = 0,99. The *TSR* average value for the analysed overpasses for the visual inspection annuality (2014) is equal to *TSR* = 43,4 years.

Once defined the element deterioration curves, deterioration scenarios have been calculated for each bridge considering 2020 as the year of the retrofit intervention. The outcomes of the deterioration scenarios simulation have been used, previously defining the coefficients *RT* = 0,80 and *NBI* = 0,98, for the construction of the service-life curves of each of the analysed bridges, as shown in Figure 4.14.

The service-life curves will allow A27 owners to better plan the maintenance interventions to be put in place for ensuring an adequate serviceability and safety level.

Finally, *DPIs* have been calculated for the whole bridges according to §4.2.6 and reported in Table 4.7: this index has to be considered in relative terms when comparing many bridges needing retrofit interventions, with the aim to identify those will be subjected to faster aggravations of the *TSR* values.

Bridge	**#1**	**#2**	**#3**	**#4**	**#5**	**#6**	**#7**	**#8**	**#9**	**#10**	**#11**	**#12**
TSR	41,8	53,6	44,1	49,7	37,8	45,1	41,2	41,9	40,8	43,3	36,8	44,2
IPD	1,35	1,23	1,26	1,23	1,22	1,21	1,28	1,33	1,27	1,18	1,14	1,23

Table 4.7 TSR and DPI values assessed for the the analysed A27 highway overpasses.

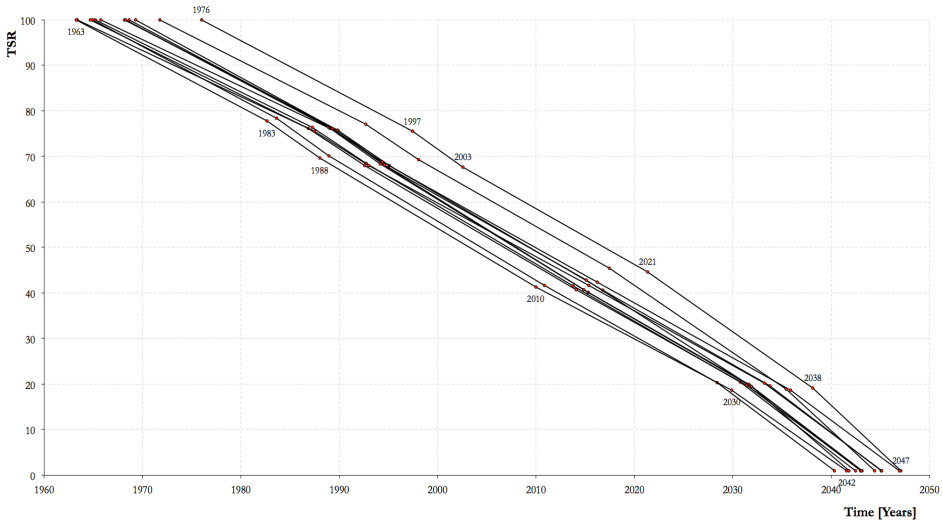

Fig.4.14 The service-life curves for the analysed A27 highway overpasses.

4.4 Discussion of the results

The service-life curves obtained for the A27 highway overpasses have then been critically evaluated: since the period of construction of the bridges is known, corresponding about with the year of the highway opening (1972), the validation of the proposed procedure can be achieved by observing how the estimated age in which those structures were characterized by *TSR* values approximately equal to 100 is roughly coincident with the first *70s'*.

The age of each bridge structure has been assessed as the arithmetic mean value of the age values of only their structural components: in such way a compensation effect between the different age values can be reached in the estimate of the each structure age value.

It can also be noticed how a careful classification of different bridges in similar categories, and the availability a statistically consistent number of data referred to past visual inspections should allow to obtain even more realistic representations of the natural ageing of the bridge components. In such way these efforts would enable an easier and more economical management of existing bridges. Conversely, the more heterogeneity will be present in the data to be statistically treated, the more cumulative standard deviation will be

observed in the element deterioration curves, thus negatively reflecting in the provisional accuracy of the proposed procedure. This issue can be clearly observed if a comparison between service-life curves of a homougeneous and an heterogeneous bridge samples is made. For this reason, service life-curves for a group of 20 heterogeneous bridges belonging to the road network of the Rovereto Municipality (same climatic zone, materials but different construction ages and structural typologies) have been also calculated and represented in Figure 4.15 according to the proposed procedure described above and have then been compared with the A27 overpasses' ones (same climatic zone, materials, construction age and structural typology).

TSR values and *DPIs* have been evaluated for the Rovereto Municipality sample and shown in Table 4.8. The *TSR* average value for for the visual inspection annuality (2014) is equal to *TSR* = 49,5 years and the *DPI* average value is equal to *DPI* = 1,42.

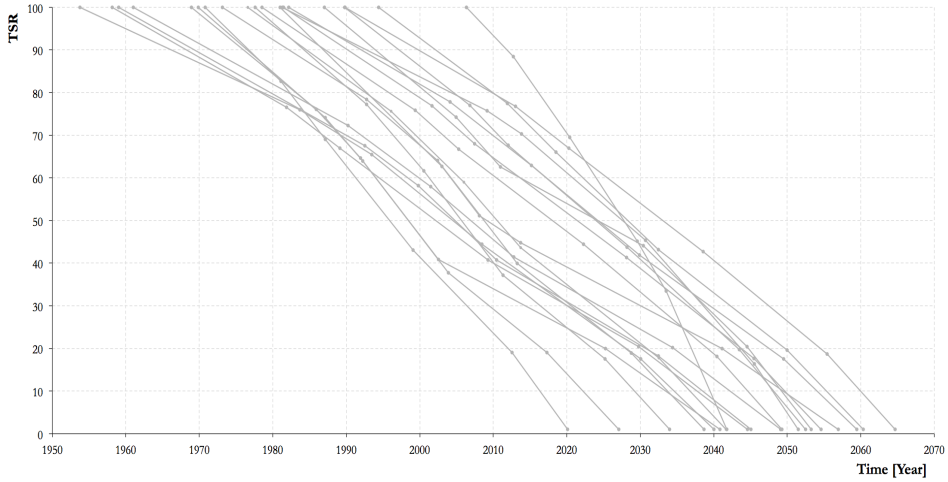

Fig.4.15 The service-life curves for the 20 considered Rovereto Municipality bridges.

Bridge	**#1**	**#2**	**#3**	**#4**	**#5**	**#6**	**#7**	**#8**	**#9**	**#10**
TSR	55,3	59,6	39,0	43,1	37,5	64,7	37,1	36,0	75,4	73,8
IPD	1,31	1,29	1,36	1,99	1,24	1,44	1,02	0,99	1,34	1,72
Bridge	**#11**	**#12**	**#13**	**#14**	**#15**	**#16**	**#17**	**#18**	**#19**	**#20**
TSR	70,1	64,8	15,6	33,4	59,7	30,4	23,7	44,5	40,2	86,6
IPD	1,48	1,48	2,38	1,41	0,96	0,92	1,39	1,13	0,98	2,66

Table 4.8 TSR and DPI assessed for the 20 considered Rovereto Municipality bridges.

The outcomes underline how the service-life curves obtained for the A27 overpasses homogeneous sample are characterized by a lower variability than those obtained for the Rovereto Municipality sample, since the heterogeneity of the latter ones is higher.

Figure 4.16 shows how the time interval measures can represent in such a way the dispersion in the capacity prediction of the proposed procedure: Table 4.9 reports these time intervals for different *TSR* values corresponding to the boundaries between the urgency levels adopted in this work (see Table 4.3). The results highlight how for the A27 sample the mean time interval can be estimated in about 12 years: this evaluation can be considered representative of the natural variability attributable to the deterioration phenomena, leading to quite different deterioration patterns on analogous structures placed in the same climatic zone.

Another interesting evaluation can be made by the calculation of the mean values and the related standard deviations of the number of annualities in which the structure is characterized by the same urgency level, according to Table 4.3. Table 4.10 shows these information highlighing how the heterogeneous Rovereto Municipality sample is characterized as expected by lower standard deviation values if compared to the A27 stock.

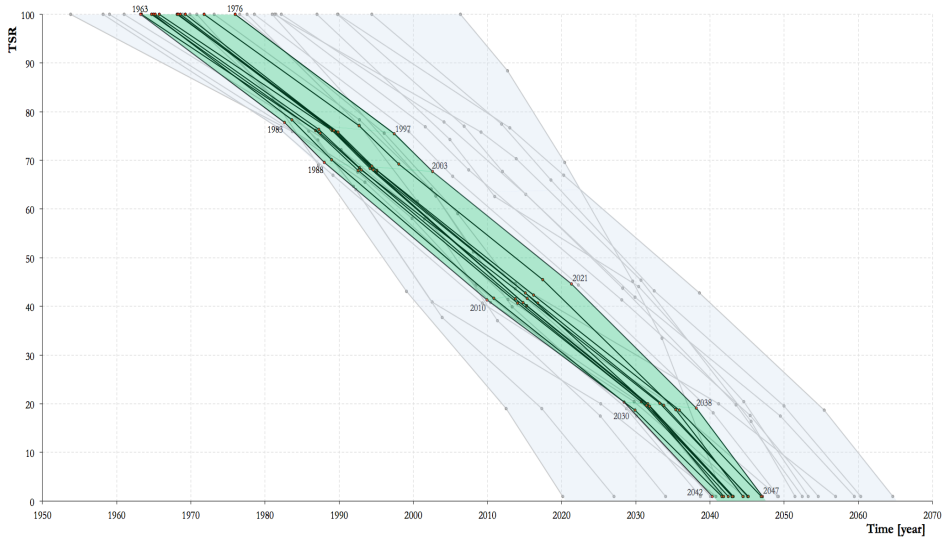

Fig.4.16 Comparison between the service-life curves for the A27 highway overpasses and the 20 considered Rovereto Municapility bridges.

TSR	A27 [years]	Rovereto Municipality [years]
100	12	40
70	13	33
50	13	37
25	10	42
1	11	45

Table 4.9 Comparison between the A27 and Rovereto Municipality time interval values calculated for significant TSR values.

TSR	A27		Rovereto Municipality	
	Mean [years]	St. Dev. [years]	Mean [years]	St. Dev. [years]
100 - 70	29,11	1,63	24,06	5,76
70 - 50	15,62	0,66	12,41	2,80
50 - 25	19,08	1,61	17,68	3,95
25 - 1	14,87	1,51	14,88	3,85

Table 4.10 Mean and standard deviation values of the number of annualities for each urgency level calculated for the A27 and Rovereto Municipality stocks.

Finally, once defined the service-life curves of each bridge, it should be possible to define future bridges' remaining service-life scenarios able to support owners in the planning of the maintenance resources. Figures 4.17 and 4.18 shows, as example, the remaining service-life scenarios respectively for the A27 overpasses and the Rovereto Municipality bridges for four different future annualities (2014, 2020, 2030 and 2040) with the aim to represent the actual (2014), a short-term (2020), a mid-term (2030) and a long-term (2040) degradation scenarios that will be reached in case of no maintenance interventions. The remaining service-life scenarios describe the degradation of each structure in terms of *TSR* values and are represented in Figures 4.17 and 4.18 with different colours in relation to their specific urgency classes (green for long-term urgency intervention, yellow for mid-term urgency intervention, orange for short-term urgency intervention and red for maximum urgency intervention). Bridges with black dots are characterized by few data availability, so in such cases, no previsions have been performed.

Figure 4.17 highlighs how already from the analysis of the actual scenario a significant general degradation state has been detected in the majority of the A27 overpasses; the general condition considerably worsens in the 2030 scenario with an increasing number of structures needing a maximum urgency maintenance intervention. For this reason, it can be noted how the 2030 can be

considered as the maximum temporal horizon in which perform a general maintenance intervention program for extend the remaining service-life of the A27 overpasses.

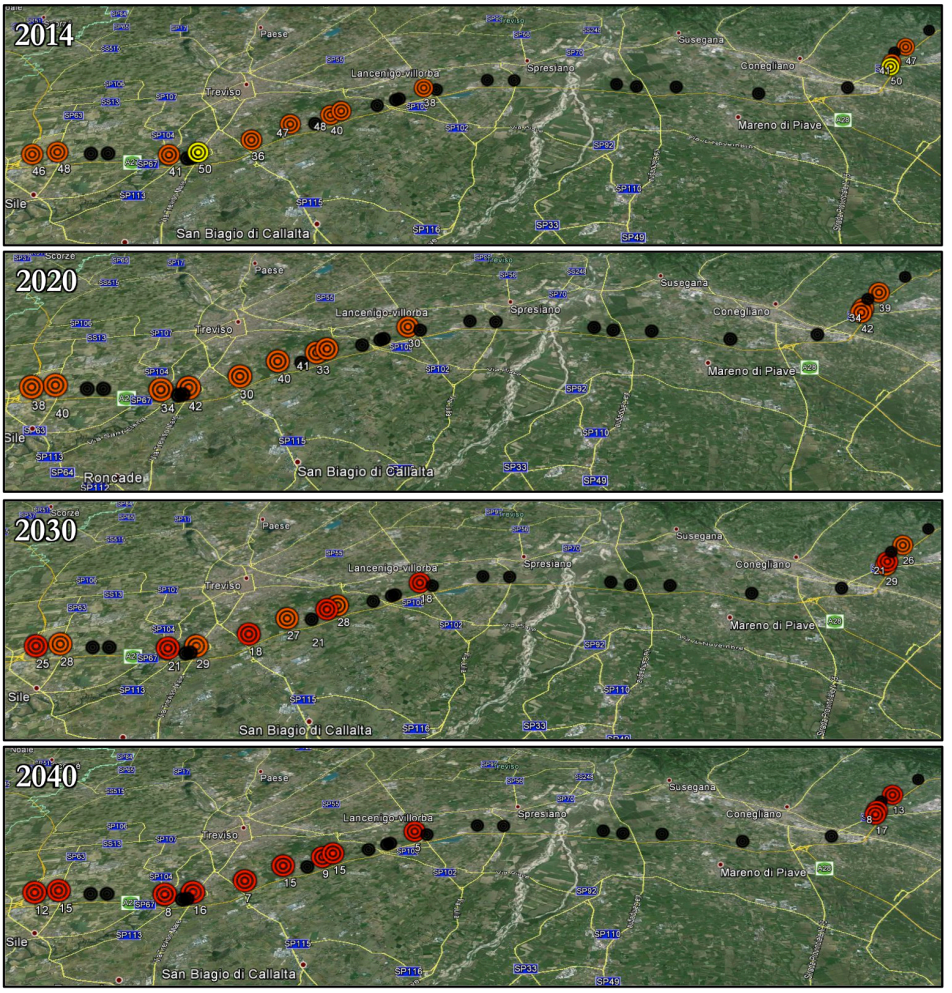

Fig.4.17 Remaining service-life scenarios for the analysed A27 overpasses.

Figure 4.18 shows the outcomes for the heterogeneous sample of the Rovereto Municipality bridges: in this case due to the main differences regarding structural typologies and construction ages (varying from 1955 to 2007), various degradation conditions can be observed from the analysis of the actual scenario, moving from structures belonging to the long-term urgency intervention class to the maximum urgency levels. Such context, the most

common for a public agency/private owner, in which different structures have to be maintened, the importance of a correct management is crucial for optimize the economical resources allocated for retrofit interventions.

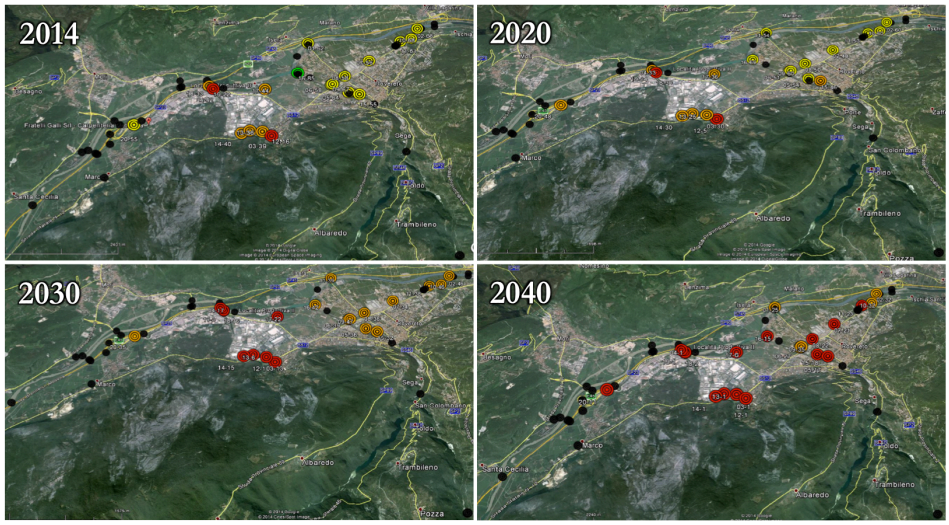

Fig.4.18 Remaining service-life scenarios for the analysed Rovereto Municipality bridges.

4.5 Conclusions

In this work a statistically-based algorithm for the prediction of bridges' remaining service-life on the basis of the outcomes deriving from the execution of the visual inspection surveys has been illustrated. Through the application of the Bayesian theory on the visual inspection report data performed on different bridge structural typologies, element deterioration curves have been constructed with the aim of represent the dynamics of the damage progression in the various structural elements. A procedure for the service-life curves construction has been proposed and validated on two bridge stocks characterized by different heterogeneity levels, highlighting the goodness of the model provisional capacity, in spite of the relatively limited availability of visual inspection data. *DPIs* have been subsequently calculated for each bridge. Finally remaining service-life scenarios have been proven and critically discussed.

The analyses outcomes confirm the good provisional capacity of the proposed methodology, evidencing how dispersion in the prediction are mainly imputable to the heterogeneity of the degradation phenomena, even thought a part thereof could be reduced with a consistent numerousness of visual inspection data.
Concluding, the proposed procedure seems to be an useful instrument allowing public authorities/private managing companies to estimate useful economic indicators for the evaluation of the amount of resources needed for bridge restoration interventions.

5 THE ROLE OF INSPECTIONS IN IMPROVING SEISMIC ASSESSMENT OF EXISTING BRIDGES

5.1 Introduction

In transportation networks, bridges are willingly considered among the most vulnerable elements, also for having a strategic role in terms of civil protection aims and first aid in emergency states and immediate post-earthquake rescue operations. These infrastructures, mostly built or reconstructed after World War II (Pellegrino et al. 2011) have a significant age and have been designed without considering seismic criteria. The development of new or improved seismic regulations in the last years has led to pay greater attention to seismic design issues, foreshadowing urgent need of seismic assessment of such existing structures for road and railway managing authorities. In light of these reasons, managing authorities are nowadays interested in increasing the knowledge level of their structures' condition with the aim of using such data for a proper seismic assessment of the bridges (Biondini et al. 2013, Zanini et al. 2013) and the network in which they are included (Carturan et al. 2013a,b).

In most of the *BMSs* currently in use worldwide, *in-situ* and laboratory investigations are not typically foreseen and rationally planned, because of the huge amount of structures to manage. Referring to European experiences, *in-situ* material characterization aimed to a proper seismic assessment of large stocks of bridges is often not planned in countries with negligible seismic hazard (Kamya 2012; Torkkeli and Lämsä 2012; Söderqvist and Veijola 2012; Hofmann et al. 2012). Increasing attention is instead spent in areas with more significant seismic activity where, however, the experiences in *Bridge Management Systems* related to large stocks of bridges (Zonta et al. 2007; Yue et al. 2012) typically provide the execution of limited visual *in-situ* inspections finalized to update the condition state of the bridges without quantitative assessment of the mechanical characteristics of the basic materials.

In this respect, this chapter shows the main results related to an agreement between the Department of Civil, Environmental and Architecture Engineering of the University of Padova and the Veneto's (North Eastern Italy) regional roadway managing authority, Veneto Strade S.p.A. aimed at the seismic

assessment of a representative stock of existing bridges located in the main roadway lines in the Veneto region.

Firstly, a preliminary seismic analysis of 335 existing bridges was carried out. In most cases, the main mechanical characteristics of bridge elements were unknown and hence some assumptions about significant properties of the basic materials were done on the basis of the original design documents, guidelines on assessing existing structures and construction practice at the time of the structures' edification.

This work mainly focuses on the process of updating preliminary seismic analyses for a cluster of 71 bridges taken as representative group of the initial 335 bridges. A series of *in-situ* and laboratory investigations and geometrical surveys have been developed on these 71 bridges with the aim of defining main physical and mechanical characteristics of the materials constituting bridge structural elements. Figure 5.1 shows the geographical distribution of the above 71 bridges representing the most common bridge typologies in the Veneto's regional roadway network.

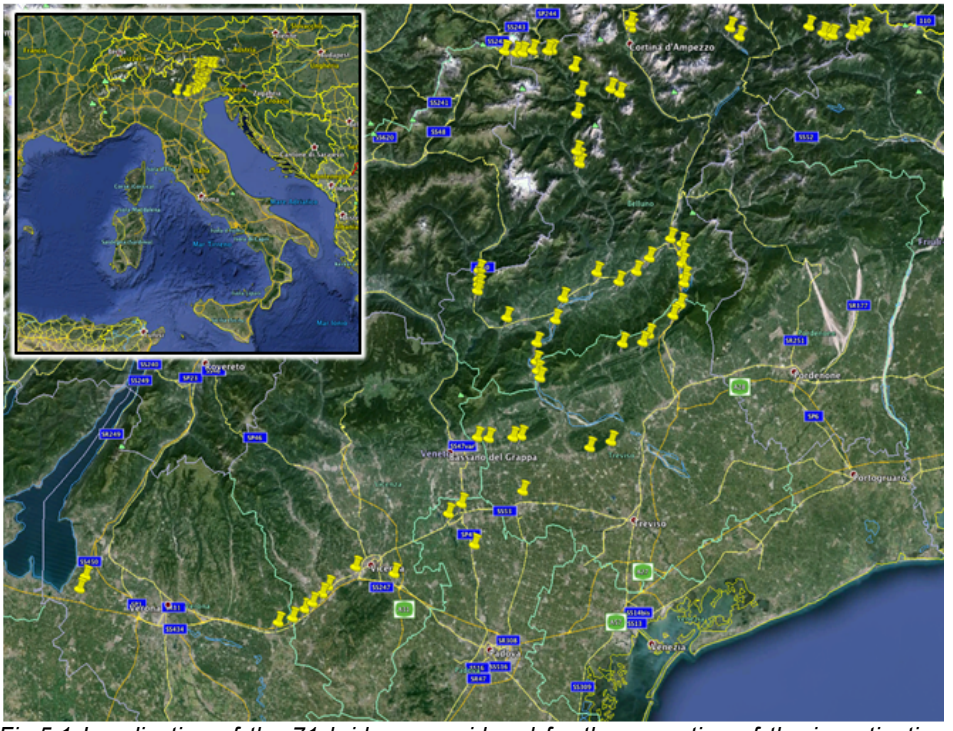

Fig.5.1 Localization of the 71 bridges considered for the execution of the investigation campaign in the Veneto roadway network.

The considered bridges belong to the most common structural typologies as shown in Tables 5.1, 5.2, 5.3 for reinforced concrete structures and in Table 5.4 for masonry/stone bridges. Comparing the results of the seismic assessment derived from the preliminary and the updated analysis could give an unique opportunity for obtaining some insights on appropriate and rational planning of inspections on existing bridges and reliability of basic assumptions for their seismic assessment in actual situations.

The main aim of this chapter is to demonstrate and quantify that the use of properly planned *in-situ* and laboratory investigations on representative bridge structural elements may represent an useful instrument for the execution of careful seismic vulnerability assessment of large stock of bridges and allow avoiding too conservative or unconservative assumptions.

Simply supported decks	Continuous decks	Arched decks
38	6	3

Table 5.1 Structural typologies for the reinforced concrete bridges.

Single Span	2 Spans	3 Spans	4 Spans	5 Spans	> 5 Spans
19	6	10	2	2	8
Average Span Length = 16,65 m					

Table 5.2 Number of spans for the reinforced concrete bridges.

Column Piers	Framed Piers	Wall Piers
5	8	15

Table 5.3 Pier typologies for the reinforced concrete bridges.

MASONRY/STONE BRIDGES NUMBER OF SPANS			MATERIAL	
Single Span	2 Spans	3 Spans	Masonry	Stone
17	4	3	6	18
Average Span Length Value = 9,95 m				

Table 5.4 Number of spans and deck material for the masonry/stone bridges.

5.2 Typical *in-situ* and laboratory tests

The investigation campaign had as main objective the knowledge of the principal geometrical, physical and mechanical properties of the basic materials constituting the 71 examined bridges. According to the data of the above campaign it will be possible to build a structural finite element models as close as possible to the real characteristics of the considered structures. A preliminary investigation plan was carried out, subdividing the 71 bridges in two main categories depending on the construction material: masonry/stone bridges and reinforced concrete bridges (including also pre-stressed concrete bridges). The subdivision by construction material has eased to organize the sequence of *in-situ* tests to be carried out for each category for properly planning the logistic and operative aspects for the execution of such surveys. The investigation campaign has been made performing destructive methods taking into account that any restriction e.g. due to specific architectural value emerged and according to the better accuracy of destructive methods for the characterization of the main mechanical parameters.

With regard to masonry/stone bridges, the investigation consisted in the extraction of masonry/stone samples (Figure 5.2) at the abutments and arches' position to be subsequently tested in laboratory, measurement of the stress state *in-situ* through the use of flat-jacks (Figure 5.3) and *in-situ* evaluation of the capacity through the use of a system of double jacks.

Fig.5.2 Masonry sample taken out from bridge n° 14 and Application of flat jacks for the in-situ stress state estimation in the abutment of bridge n°39.

Table 5.5 summarizes all investigations conducted on 24 masonry/stone bridges: for each structure "X" means that the test has been effectively carried

out whereas “O” means that the test has not been carried out due to execution difficulties or inaccessibility of the site.

MASONRY/STONE BRIDGES’ *IN-SITU* TESTS				
X = the test was carried out		**O = the test was not carried out**		
Bridge n°	**Abutment pull out samples**	**Arch pull out samples**	**Single flat jack**	**Double flat jacks**
2	X	X	X	X
4	X	X	X	X
6	X	O	X	X
9	X	X	O	O
14	X	X	X	X
15	X	X	X	X
21	X	O	X	X
22	O	X	X	X
25	O	O	X	X
26	X	X	X	X
27	O	O	X	X
30	X	X	X	X
31	X	X	X	X
32	X	O	X	X
33	O	O	X	X
39	X	X	X	X
40	X	X	X	X
52	O	X	O	O
54	X	X	O	O
55	X	X	X	X
56	X	X	X	X
61	X	O	X	X
64	O	X	X	X
66	X	O	X	X

Table 5.5 In-situ investigations carried out on masonry/stone bridges stock.

Regarding reinforced concrete bridges, the investigation campaign has been characterized by the execution of pachometer tests in each structure for the geometrical identification of the reinforcing bars location in piers and abutments

(Figure 5.4). Once defined the bars' location, the extraction of rebar samples has been performed to test them in laboratory and evaluate the main steel mechanical characteristics (Figure 5.5).

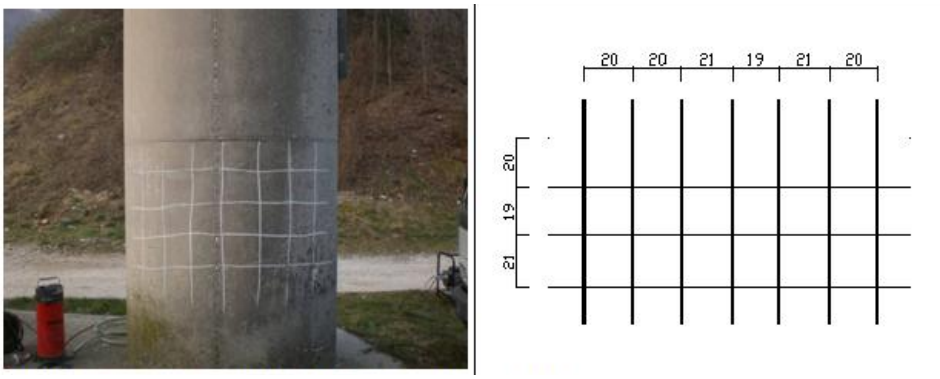

Fig.5.3 Pachometer test execution on the pier of bridge n°1.

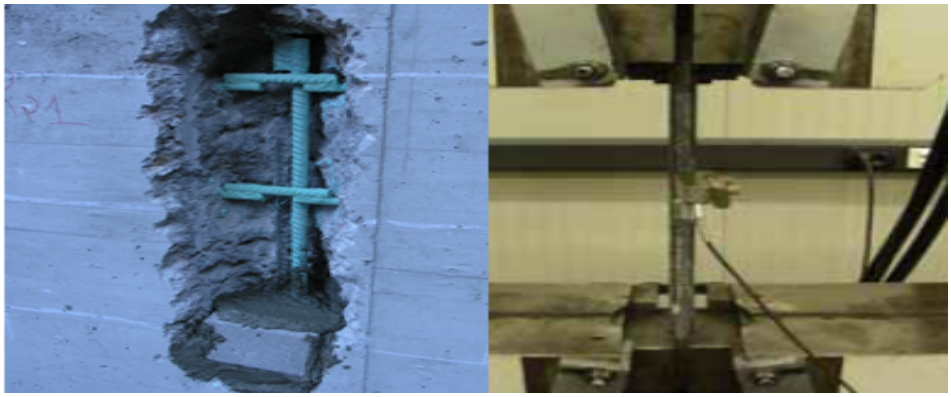

Fig.5.4 Extraction of steel bars' samples and following laboratory tensile test execution for the pier of the bridge n°1.

Finally, a series of concrete samples were taken from abutments and piers (Figure 5.6) with the subsequent estimation of the reinforced concrete mechanical characteristics with laboratory tests (Figure 5.7). Table 5.6 summarizes the tests carried out on reinforced concrete bridges.

Referring to the surrounding soils characterization and their influence on the seismic behaviour of the bridges, specific geological analyses were not developed but soil classification (based on shear wave velocity parameter) provided by the Italian Code (Italian Ministry of Infrastructures, 2008) is considered. The characteristics of the soil are related to the amplification factor taken into account in the definition of the seismic demand.

Fig.5.5 Extraction of concrete samples from the abutment of bridge n°3.

Fig.5.6 Laboratory compressive strength tests on the concrete samples taken from the abutment of bridge n°3.

REINFORCED CONCRETE BRIDGES' *IN-SITU* TESTS						
X = the test was carried out			**O = the test was not carried out**			
Bridge n°	**Pachometer**		**Pull out concrete samples**		**Extraction steel samples**	
	Abutment	**Pier**	**Abutment**	**Pier**	**Abutment**	**Pier**
1	O	X	O	X	O	X
3	X	X	X	X	X	X
8	X	X	X	X	O	X
10	X	X	X	X	X	X
11	X	X	X	X	X	X
12	X	X	X	X	O	X

13	X	O	X	O	X	O
16	X	O	X	O	X	O
17	X	X	X	X	X	X
18	X	O	X	O	X	O
19	X	X	X	X	X	X
20	X	O	X	O	X	O
23	X	X	X	X	X	X
24	X	X	X	X	O	X
28	X	X	X	X	X	X
29	X	O	X	O	X	O
34	X	X	X	X	X	X
35	X	O	X	O	X	O
36	X	O	X	O	X	O
37	X	O	X	O	X	O
42	X	X	X	X	X	X
43	X	O	X	O	X	O
44	X	X	X	X	X	X
45	X	X	X	X	X	X
46	X	O	X	O	X	O
48	X	O	X	O	X	O
49	X	O	X	O	X	O
50	X	O	X	O	X	O
51	X	X	X	X	X	X
53	X	O	X	O	X	O
57	X	O	X	O	X	O
58	X	X	X	X	X	X
62	X	X	X	X	O	O
63	X	X	X	X	O	O
67	O	X	X	X	O	X
68	X	X	X	X	X	X
69	X	X	X	X	X	X
70	O	X	O	X	O	X
71	X	X	X	X	X	X

Table 5.6 In-situ investigations carried out on reinforced concrete bridges stock.

5.3 Results

The seismic assessment of the 71 analysed bridges has been conducted following the procedures previously described in Sections 3.3 and 3.4. In the following the outcomes of these analyses have been critically illustrated.

5.3.1 Mechanical characteristics of the basic materials

In-situ and laboratory investigations have led to the evaluation of the main materials' mechanical characteristics and have allowed the comparison between the values supposed during the first part of the study and those detected during the investigation campaign, obtaining information about the accuracy of the preliminary assumed hypotheses.
In most of the cases the values collected with the investigation campaign were greater than those preliminary estimated whereas only a small sample of bridges was characterized by values from the investigation lower than the assumed ones. Figure 5.7 shows in abscissa firstly assumed values and in ordinate *in-situ* measured values of the concrete compressive and steel yielding strengths, expressed in MPa.
Figure 5.8 represents the variation of the probability density functions (*pdf*) describing assumed and measured compressive concrete strengths (Fig. 5.8a) and assumed and measured tensile steel yielding strength values (Fig. 5.8b). Table 5.7 shows the average values and the relative standard deviations of the materials' mechanical properties. Regarding concrete, the average value of the measured compressive strength is higher than that assumed. Instead, the average value of the measured steel yielding strength is greater than that assumed.
Regarding masonry/stone bridges, although the procedure is substantially based on limit analysis and bridges' geometrical configuration, similar comparisons have been made since the values of the materials' mechanical characteristics derived from *in-situ* investigation campaigns could be useful for the construction of appropriate finite element models of the bridges. Masonry/stone compressive strength and elastic modulus have therefore been firstly assumed equal for all the analysed bridges according to the suggestions of the Italian regulations about the estimation of mechanical parameters of

masonry/stone structures. After *in-situ* measurements of those parameters, the results have been compared with the assumed ones, highlighting how the effective material resistances were often greater than those preliminarily assumed (Figure 5.9).

MATERIALS	Average Value [MPa]		Standard Deviation [MPa]	
	Assumed Value	Measured Value	Assumed Value	Measured Value
Abutments - Concrete compressive strength	29,42	35,9	4,91	14,84
Abutments – Steel tensile yielding stress	426,13	418,97	21,2	30,31
Piers – Concrete compressive strength	31,3	46,35	4,83	17,05
Piers – Steel tensile yielding stress	421,65	405,55	27,85	44,4
Masonry/Stone - Compressive Strength	4,2	4,25	-	0,72
Masonry/Stone - Elastic Modulus	6000	9989,13	-	6529,4

Table 5.7 Average and standard deviation values for concrete, steel and masonry/stone main materials mechanical parameters.

Average and standard deviation values of the main materials' properties have been evaluated also for masonry/stone bridges' stock, listed in Table 5.7 and shown in Figure 5.10.

The results have highlighted higher compressive strength values in the second analysis than those preliminarily assumed. In particular, the average elastic modulus is around 10000 MPa (even if the highest one, related to a stone bridge, was about 26000 MPa). It has to be highlighted that the stock is mostly composed by stone bridges (Table 5.4) typically having higher elastic moduli than masonry ones. Measured quantities have been compared with the assumed ones, evaluating their ratios for each structure and thus evidencing the situations in which *in-situ* investigations show conservative (ratio lower than 1), correct/neutral (equal to 1) or unconservative (higher than 1) assumptions.

(a)

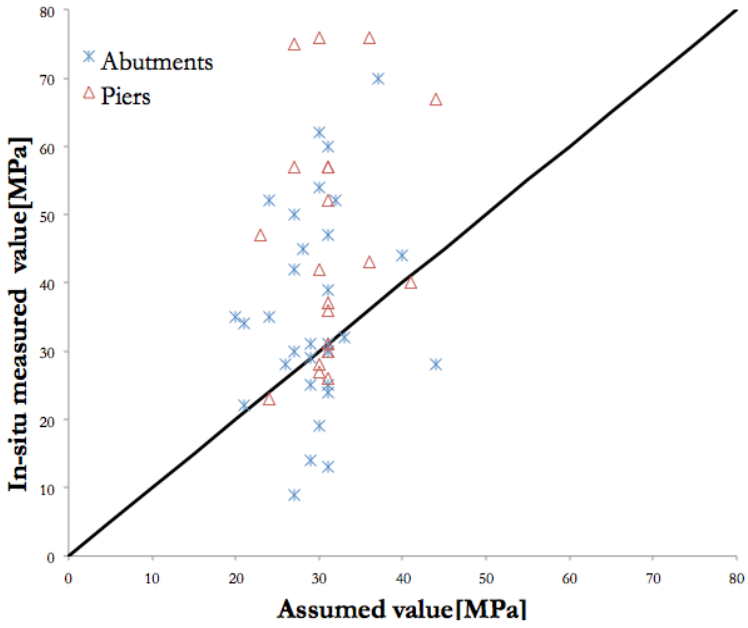

(b)

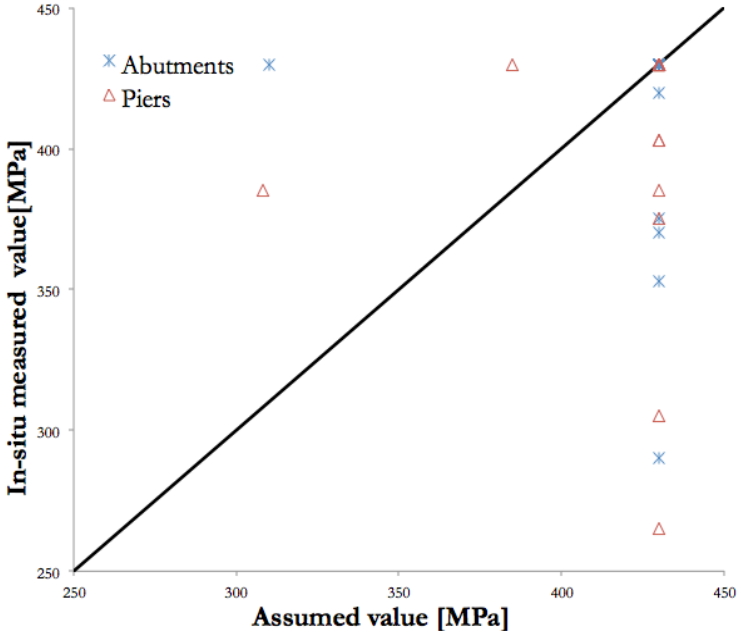

Fig.5.7 Mechanical characteristics for the considered reinforced concrete bridges: concrete compressive strength (a) and steel yielding stress (b).

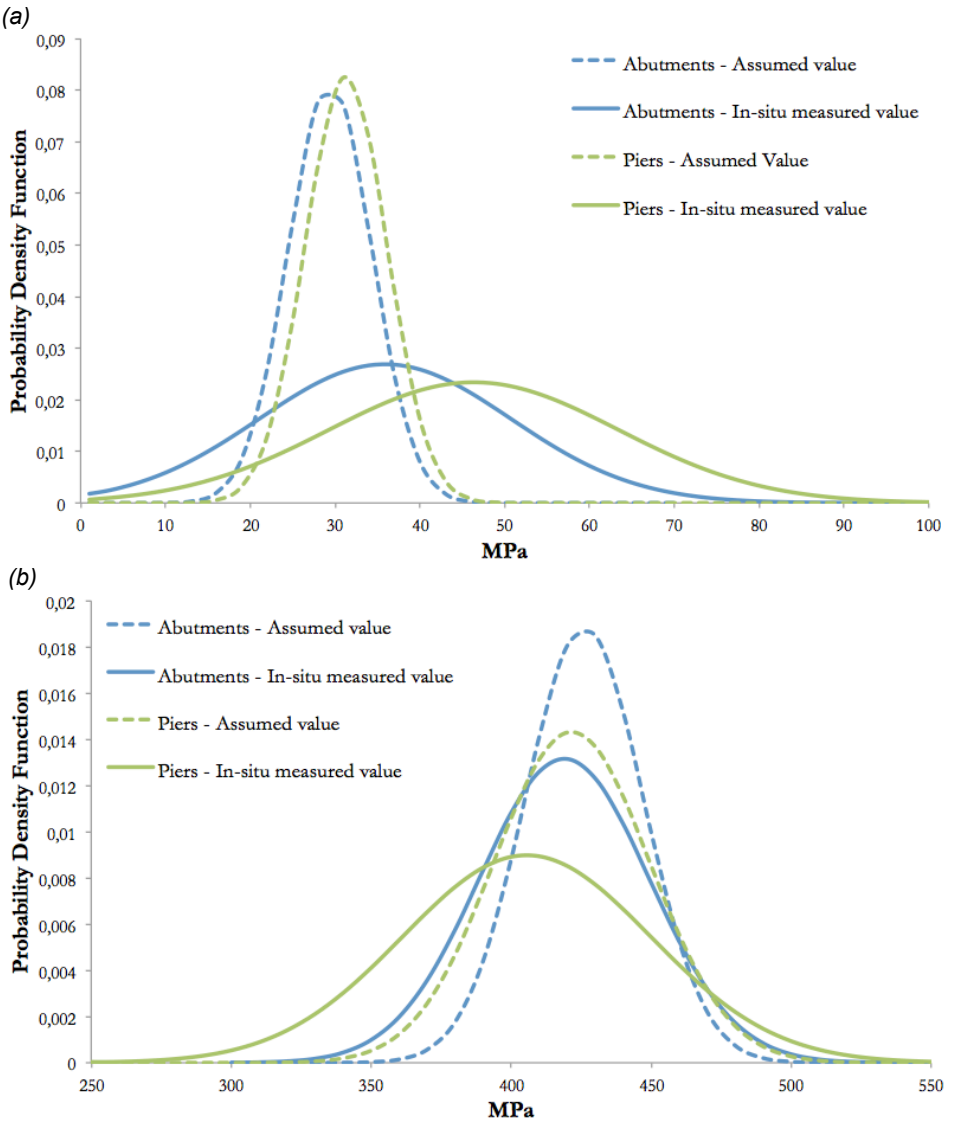

Fig.5.8 Probability density functions of compressive concrete strength (a) and tensile steel yielding stress (b) of the whole reinforced concrete bridges' stock as firstly assumed and after in-situ investigations.

Figure 5.11 shows the fractions of conservative, correct/neutral and unconservative ratios between measured and assumed values of the main mechanical materials' parameters. It can be observed that more correct/conservative assumptions have been made for mechanical characteristics of the reinforcing steel than for concrete due a more accurate quality control during the steel production process.

(a)

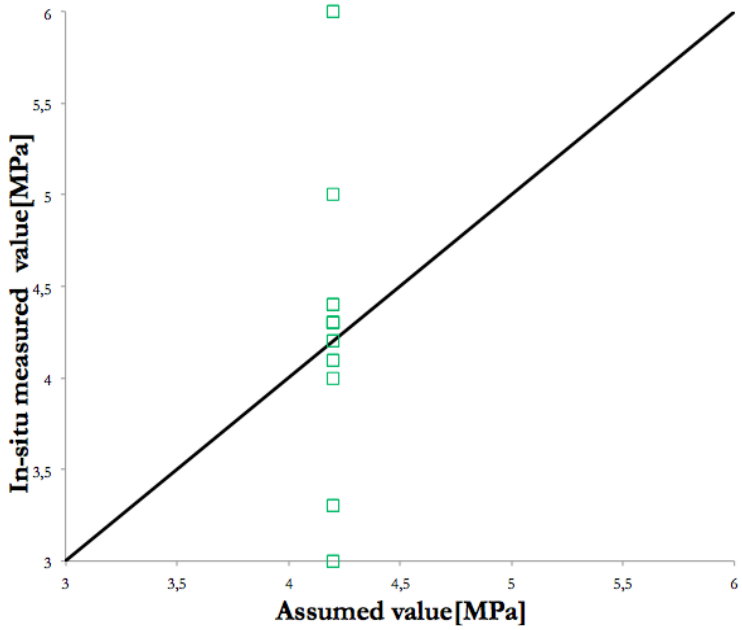

(b)

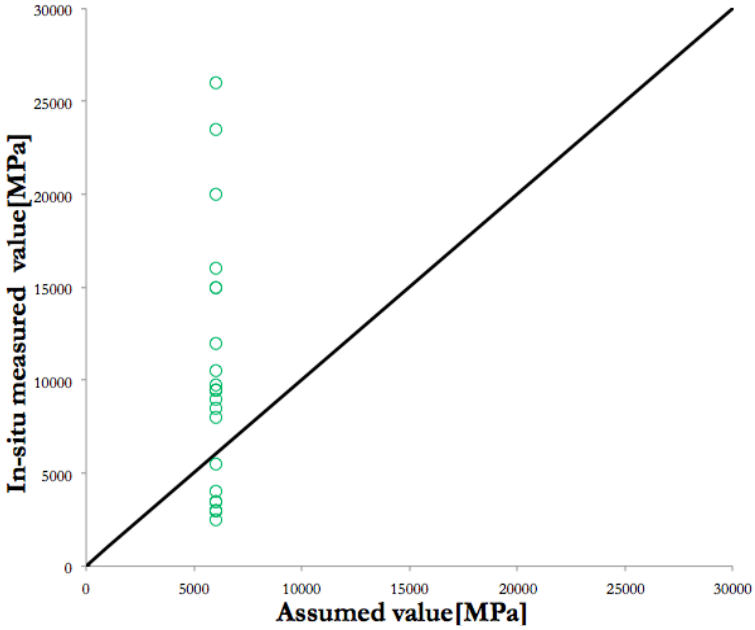

Fig.5.9 Mechanical characteristics for the considered masonry bridges: masonry compressive strength (a) and elastic modulus (b).

(a)

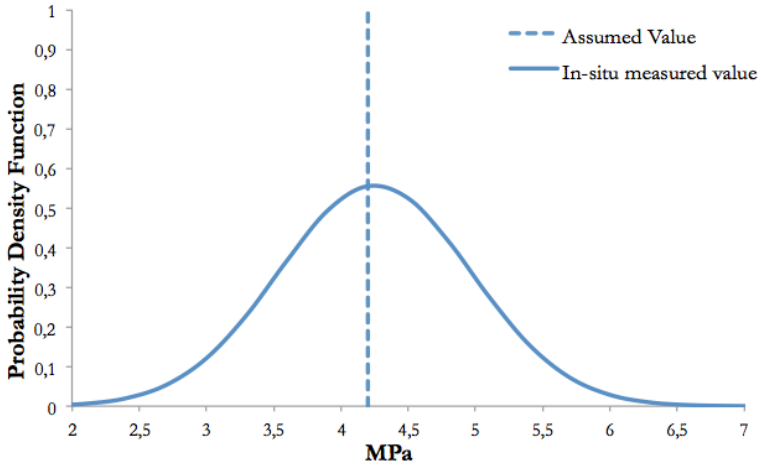

(b)

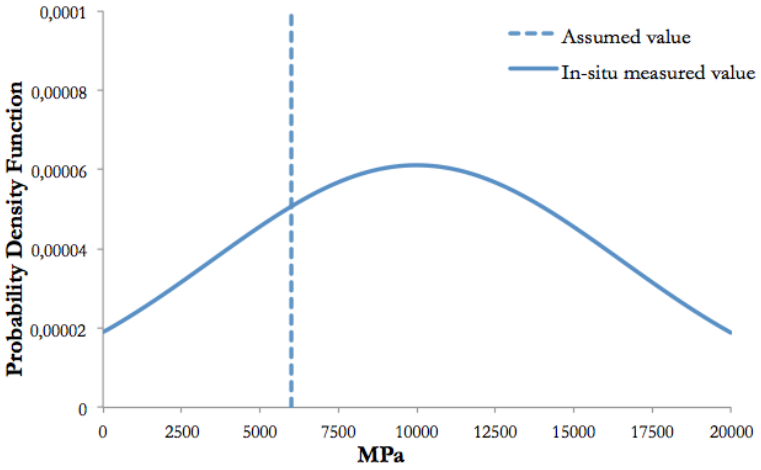

Fig.5.10 Probability density functions of masonry/stone compressive strength (a) and elastic modulus (b) of the whole masonry/stone bridges' stock as firstly assumed and after in-situ investigations.

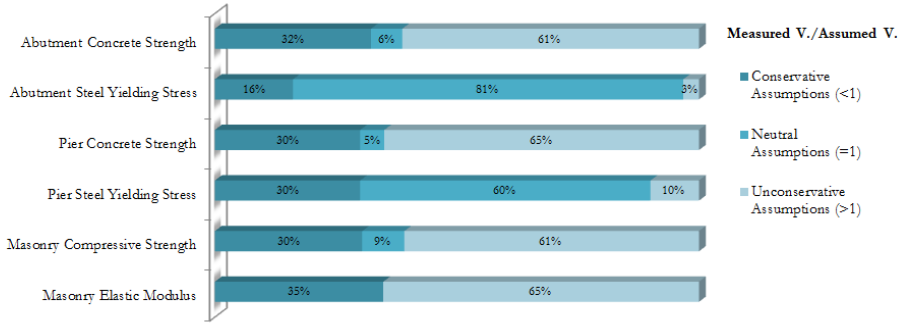

Fig.5.11 Fractions of conservative, neutral and unconservative ratios between measured and assumed values of the main mechanical materials' parameters.

5.3.2 Masonry/stone bridges

The results obtained in first and second analysis are now shown for the possible collapse mechanisms. Figure 5.12 shows the results related to the analyses of the arch (Fig. 5.12a), spandrel wall (Fig.5.12b) collapse mechanisms considering *Safety Limit State* (*SLS*) and *Ultimate Limit State* (*ULS*), abutment and foundation (Fig.5.12c). The diagram shows the safety factors FC_i, calculated in first and second analysis for each masonry/stone bridge, highlighting also the relative improvement or the worsening of each FC_i between the first and second analysis. The dots on the inclined lines are characterized by unchanged safety factors between first and second analysis.

The results highlight how the most vulnerable collapse mechanism is that of the spandrel wall in transversal direction, with the majority of the analysed bridges characterized by safety factors FC_i lower than 1. It can be observed how safety factors for the arch and the spandrel wall at *SLS* are bigger than those obtained at *ULS*. The results have evidenced how the geometrical survey has played an useful role in the whole structural assessment, in particular referring to spandrel wall failure mechanism estimations (as shown in Figure 5.13).

(a)

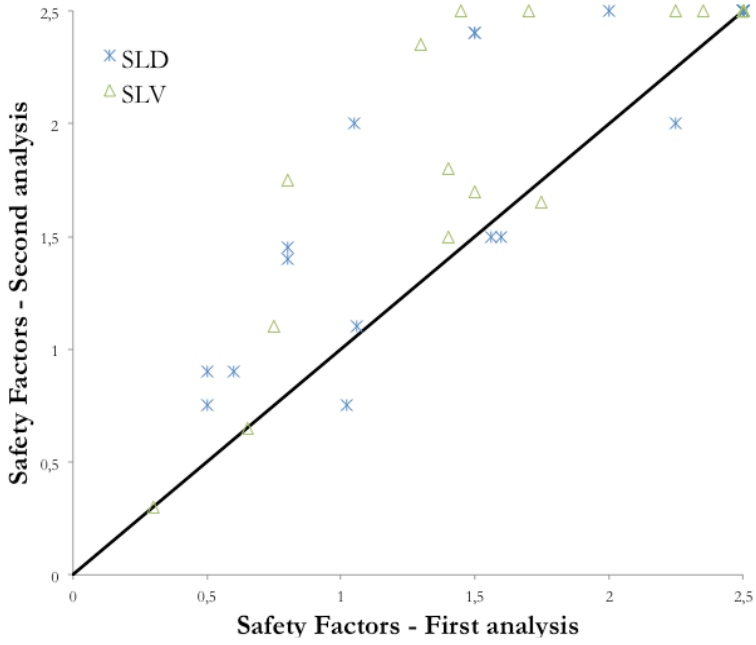

(b)

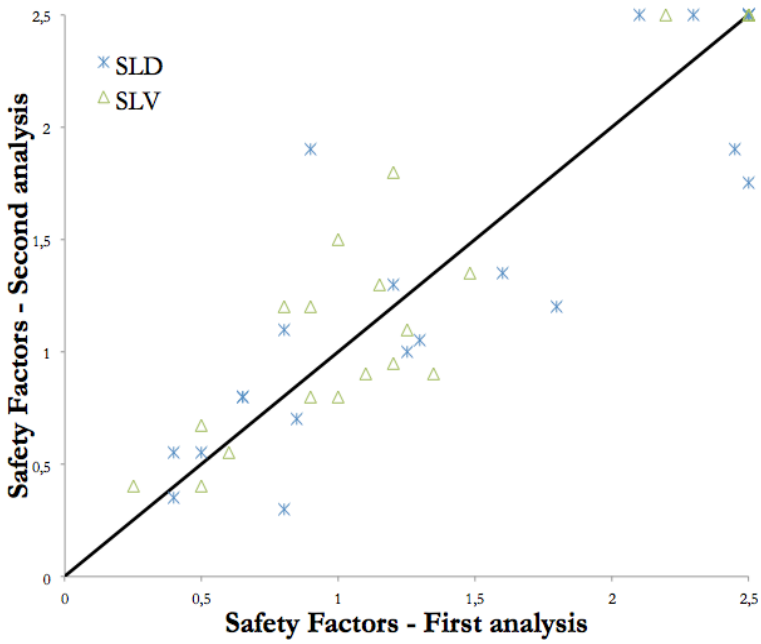

(c)

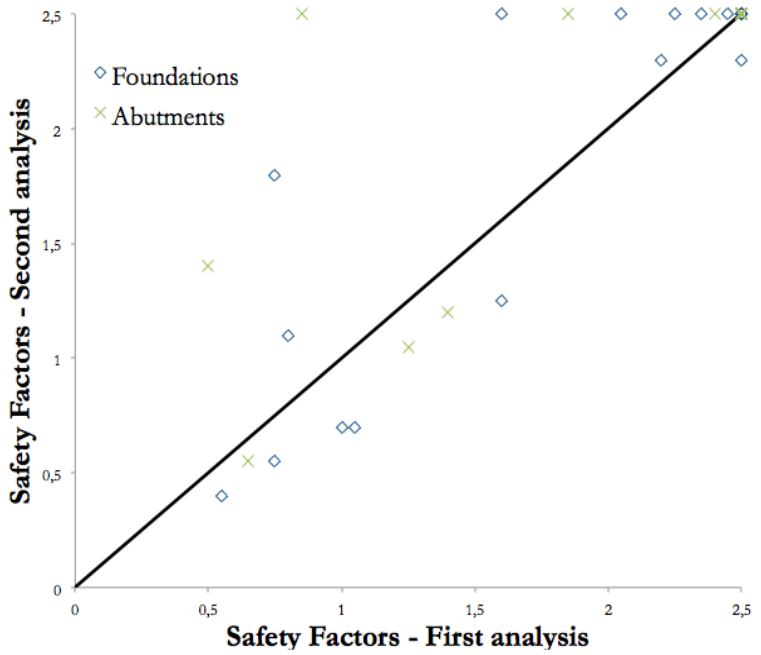

Fig. 5.12 Results for the analysed masonry bridges: arch collapse mechanism (a), spandrel wall collapse mechanism (b) and masonry abutments and foundations (c).

A significant percentage of unchanged results have been obtained since, in these cases, assumed bridges' geometrical characteristics have been confirmed during the *in-situ* geometrical surveys.

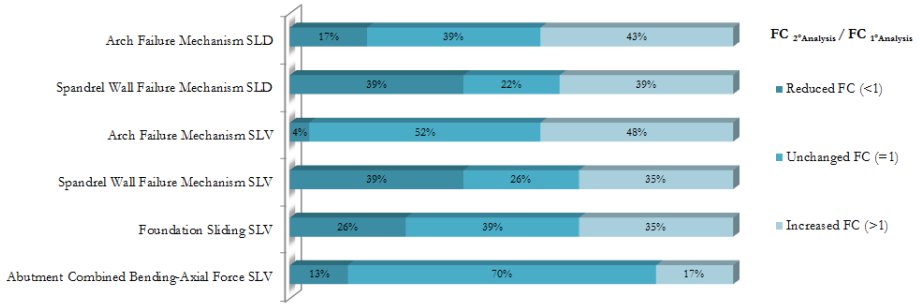

Fig.5.13 Fractions of reduced, unchanged and increased safety factors FC_i for the first and the second analysis of masonry/stone bridges.

Figure 5.14 shows the assessment outcomes and relative changes from the first to the second analysis for the structural elements of the masonry/stone bridge stock. The diagrams show how spandrel wall seems to be the most vulnerable element according to the related unsatisfied outcomes.

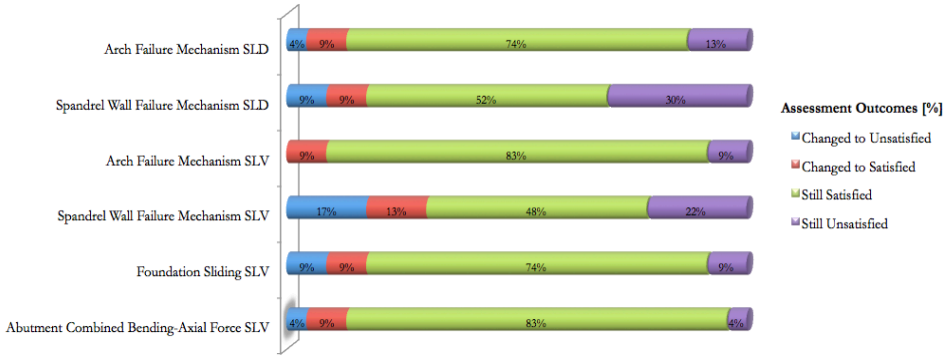

Fig.5.14 Assessment outcomes and relative changes from the first to the second analysis for the structural elements of the masonry/stone bridge stock.

5.3.3 Reinforced concrete bridges

Figures 5.15 and 5.16 show the results of the assessment of the group of *RC-PRC* bridges considered in this work, for abutments (Figure 5.15) and piers (Figure 5.16) respectively.

(a)

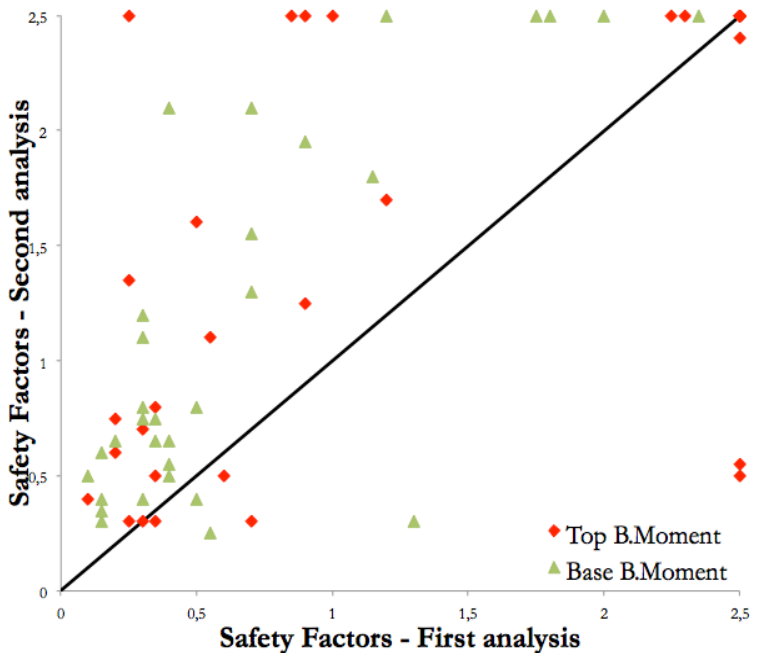

(b)

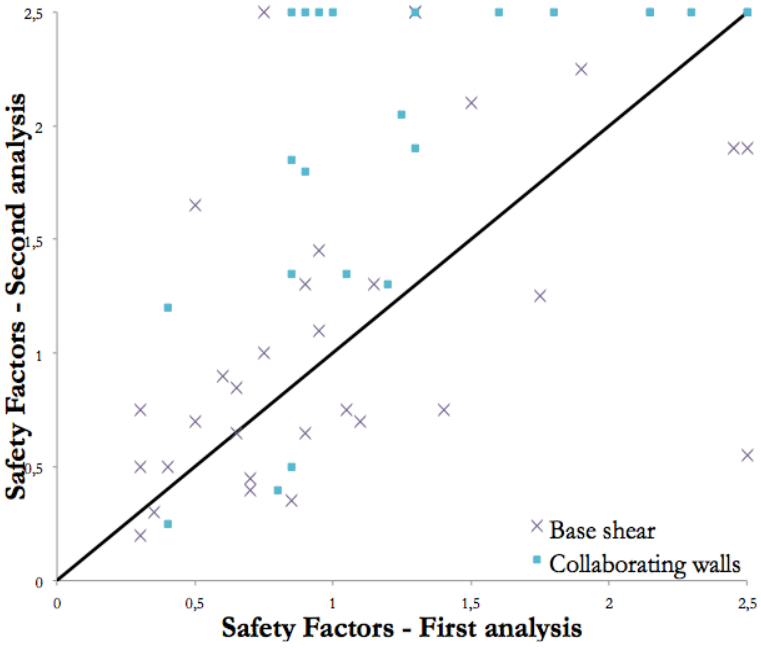

Fig.5.15 Results for the abutments of the analysed reinforced concrete bridges: top and base bending moments (a); shear at the base and shear in the walls (b).

(a)

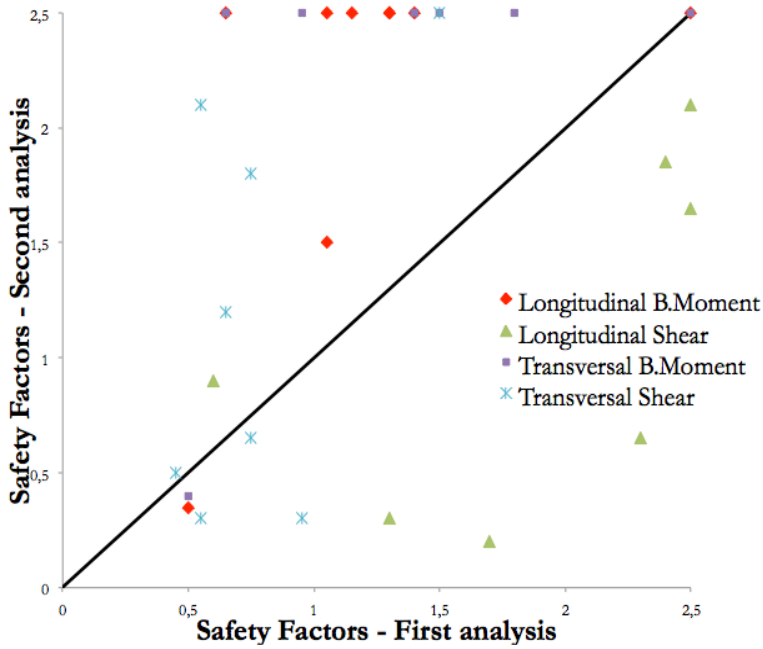

(b)

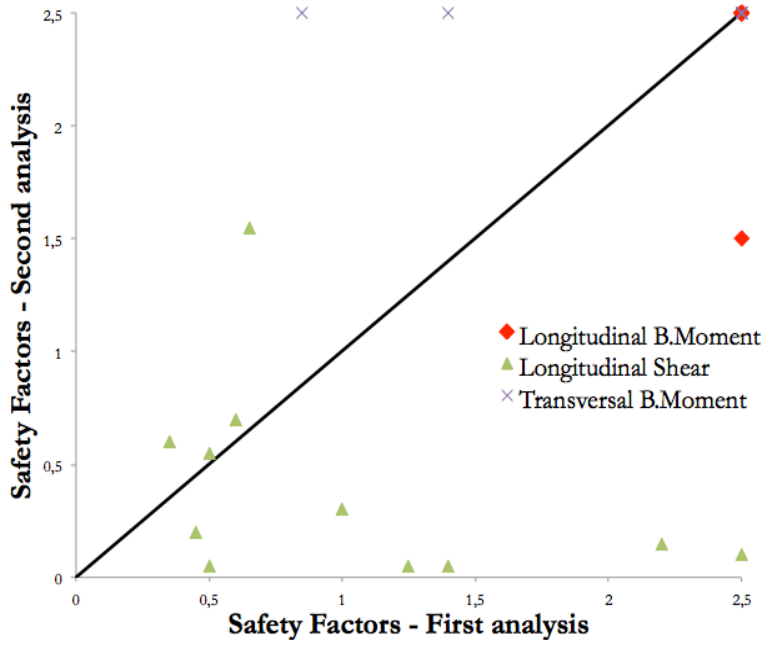

Fig.5.16 Results for the analysed reinforced concrete bridges: framed piers (a) and wall piers (b).

The results show the comparisons between safety factor values obtained in the first study (on the basis of the original drawings, where available, or assumed according to the past practice) and those derived from the *in-situ* measurements. Figures 5.15 and 5.16 show the safety factors FC_i calculated in first and second analysis for each reinforced concrete bridge, showing the relative improvement or the worsening of each FC_i between first and second analysis. The results have highlighted a general increase of the positive outcomes moving from the first to the second analysis, mainly due to the conservative assumptions adopted in the first analysis. Figure 5.20 shows the fractions of increased, unchanged and reduced safety factors FC_i for the first and the second analysis of reinforced concrete bridges. The diagrams highlight how safety factors for bending in abutments and piers are characterized by a substantial increase of the FC_i values. Figure 5.17 also shows how the *in-situ* investigations on materials' properties have led to a significant percentage of cases in which reduction of the safety factors for shear if compared to the first analysis is observed.

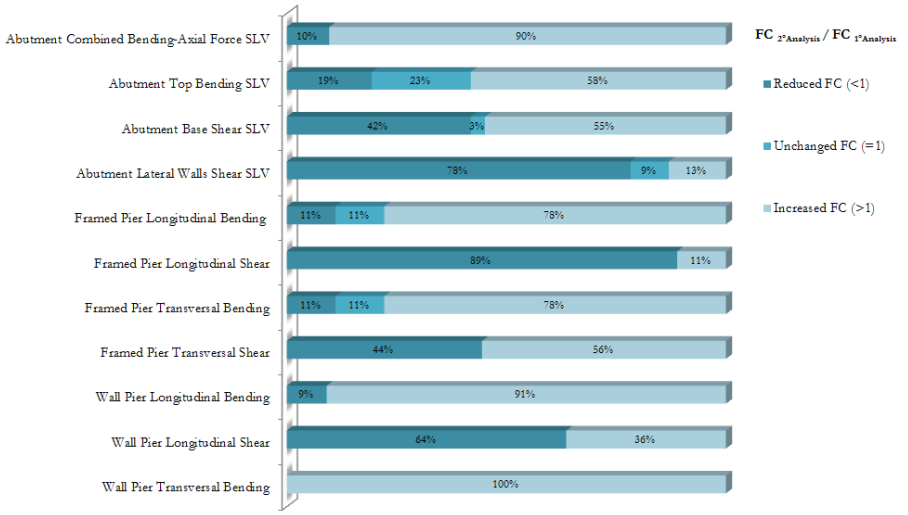

Fig.5.17 Fractions of reduced, unchanged and increased safety factors FC_i for the first and the second analysis of reinforced concrete bridges.

Figure 5.18 suggests that *in-situ* investigations has allowed to find a reduction of the FC_i values for framed and wall piers in the longitudinal direction. Figure 5.18 shows the assessment outcomes and relative changes from the first to the second analysis for the structural elements of the reinforced concrete bridge stock. The diagram confirms previously described considerations, in particular

related to the utility of *in-situ* investigations for shear assessment of the piers (in more than half of the cases characterized by unsatisfied outcomes) and, on the other hand, shows how for bending assessment the results substantially remain still satisfied. Referring to abutments and foundations outcomes, despite for these cases the *in-situ* investigations have not led to relevant changes in the assessment outcomes, the results have shown a general diffused vulnerability for these elements (still unsatisfied results: 55% for abutments combined axial force-bending at *SLV*, 35% for abutments top bending at *SLV*, 39% for abutments base shear at *SLV*).

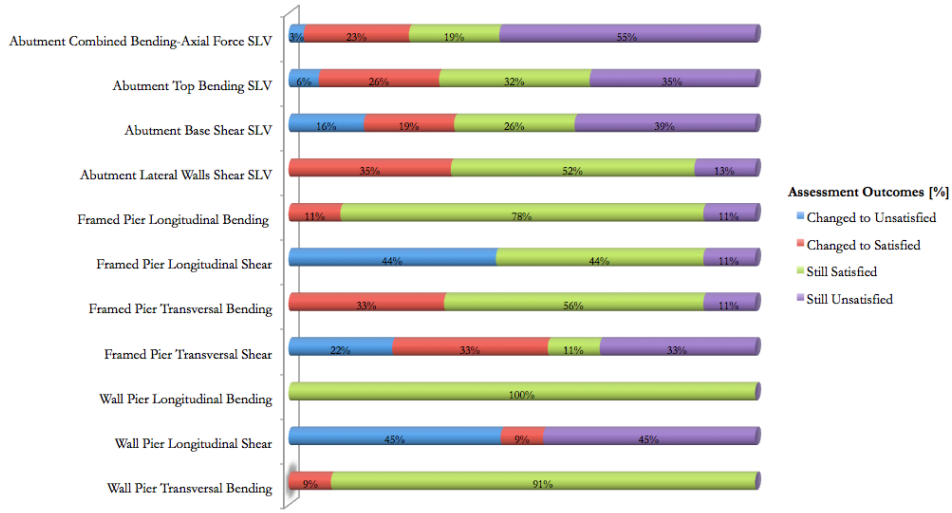

Fig.5.18 Assessment outcomes and relative changes from the first to the second analysis for the structural elements of the reinforced concrete bridge stock.

5.4 Conclusions

This chapter presents some insights on planning of seismic vulnerability assessment of large stocks of bridges with a real application to the road network of the Veneto region, Italy.

In the first part of the study a preliminary seismic analysis of 335 existing bridges was carried out. In this first phase, the main mechanical characteristics of the structural elements were often unknown and, as in the professional

practice, some reasonable assumptions were done according to the construction practice of the first construction period.

The second part of the study, described in this paper, was focused on updating the preliminary seismic analyses on a cluster of 71 bridges considered as representative of the main typologies related to the initial 335 bridges. A series of *in-situ* and laboratory investigations allowed to define the main physical and mechanical characteristics of the materials constituting the main structural elements of this cluster of masonry/stone and reinforced concrete bridges. Measurements related to *in-situ* and laboratory investigations have allowed to characterize in a more realistic way the analysed bridges and improve seismic assessment. For each bridge the significant safety factors FC_i have been calculated.

Measured quantities have been compared with the assumed ones, evaluating their ratios for each structure and thus evidencing the situations for which *in-situ* investigations show conservative (ratio lower than 1), correct/neutral (equal to 1) or unconservative (higher than 1) assumptions. The fractions of conservative, correct/neutral and unconservative ratios between measured and assumed values of the main mechanical materials' parameters have been calculated.

The results have evidenced how the geometrical survey has played an useful role in the whole structural assessment, in particular referring to spandrel wall failure mechanism that seems to be the most vulnerable mechanism for the masonry/stone bridges.

The assessment outcomes and relative changes from the first to the second analysis for the structural elements of the bridge stock have been shown with the aim of highlighting the cases for which the inspections were more useful.

Regarding reinforced concrete bridges, safety factors for bending in abutments and piers have been characterized by a substantial increase of the FC_i values after the inspections whereas *in-situ* investigations on materials' properties have led to a significant percentage of cases in which reduction of the safety factors for shear if compared to the first analysis, is observed. Referring to abutments and foundations outcomes, despite for these cases the *in-situ* investigations have not led to relevant changes in the assessment outcomes, the results have shown a general diffused vulnerability for these elements

Finally, the use of properly planned *in-situ* and laboratory investigations on representative bridge structural elements may represent an useful instrument for the execution of careful seismic vulnerability assessment of large stock of bridges and allow avoiding too conservative or unconservative assumptions for

the estimation of the main mechanical characteristics of the materials and, as a consequence, finding inaccurate structural safety factors.

6 SEISMIC VULNERABILITY OF TYPICAL ITALIAN BRIDGE CONFIGURATIONS

6.1 Introduction

Recent seismic events in Italy raised the awareness about the seismic risk, especially regarding infrastructure functionality. From this point of view, seismic vulnerability assessment of infrastructural networks gained a relevant interest. In this context the characterization of the risk of the various structural elements belonging to the network as bridges, viaducts, tunnels, walls etc. assumes particular importance (Pellegrino et al. 2014). Bridges has been proven to be the most vulnerable elements in the transportation network during an earthquake, therefore their seismic vulnerability assessment is necessary for a proper planning of the emergency response and to define a priority for retrofit interventions (Modena et al. 2014).

These considerations can be easily emphasized analysing many areas of the Italian national territory where often connections between urbanized centres are provided by a few links of the network and, for serious damages of bridges and viaducts, it easily runs the risk of damaging all these few links causing the isolation of those urbanized centres (Zanini et al. 2013).

In this context of seismic vulnerability assessment, fragility curves are a performing tool to assess bridge seismic vulnerability (Monti and Nisticò 2002; Padgett and DesRoches 2008; Shinozuka et al. 2000; Lupoi et al. 2006; Shinozuka et al. 2002; Shinozuka et al. 2003), taking into account uncertainties of the variables e.g. by using probability distributions to describe the properties of the materials composing the structure. Fragility curves can be developed by empirical or analytical methods: empirical fragility curves are usually based on bridge damage data from past earthquakes (HAZUS99 2001; Risk-UE 2004); analytical fragility curves are developed through seismic analysis of the structure like spectral analysis (Hwang et al. 2000), non-linear static analysis (Shinozuka et al. 2000b) or non-linear time history analysis (Choi et al. 2003; Morbin et al. 2010). In this work a parametrical analysis is performed in order to estimate the seismic vulnerability of a recurrent Italian structural typology of multi-span simply supported reinforced concrete bridges (Figure 6.1).

Fig.6.1 Some of the bridges of the Veneto region characterized by the analysed structural typology: Campitello's bridge (a), San Nicolò Comelico's bridge (b), SS52's crossing bridge (c), SR355 bridge (d), Campelli's bridge (e), Vich's bridge (f), Vigne's bridge (g), Piave's bridge (h), Villafranca's railway crossing bridge (i), SS434's crossing bridge (k).

The chapter aims to define for all the possible real geometrical configurations of this common bridge type (considering several combinations of pier height, pier

diameter and span length values) the correct values of the Risk-UE fragility curves input variables to use for the fast characterization of the seismic vulnerability of each possible bridge geometrical layout found in the Italian transportation networks.

6.2 Fragility curves construction

The analytical method used in this work for the construction of fragility curves is briefly described in the following. According to other studies (Choi 2002; Morbin et al. 2010), a kinematic criterion has been used for the definition of damage, according to pier's ductility demand. The damage index is represented by:

$$D_a = d_{PL} = x_{max} / x_y \tag{6.1}$$

where x_{max} is the maximum horizontal displacement of a target point (e.g. the point at the top of the pier) during the time history and x_y is the horizontal displacement at the same point in relation to steel yielding in a significant cross-section of the pier (e.g. the base cross-section).
Four damage states are considered according to Choi (2002) and reported in Table 6.1.

Performance Level (*PL*)	Damage Index Value	Description
PL1	1	Slight damage
PL2	2	Moderate damage
PL3	4	Extensive damage
PL4	7	Complete damage

Table 6.1 Damage states considered in the analytical fragility curves construction.

As a consequence, according to most of the literature, flexural response is analyzed as a first step towards a comprehensive approach including also shear response of vulnerable structural elements to take into account that shear mechanisms of failure could prevail prior to attainment of yielding and the ensuing ductility. In fact the above damage states require significant ductility, which could be probably not available at all (i.e. failure may occur prior to yielding at the above levels). This issue will be taken into account for

subsequent improvements of the work in which fragility curves will be obtained also considering brittle shear failure mechanisms.

Once defined the response parameter to be recorded, non-linear dynamic analyses are developed using artificial accelerograms. The expected earthquake is considered in a probabilistic way according to the indications of the Italian Code for Constructions (Italian Ministry of Infrastructures 2008) for the considered location of the bridge. The Ultimate Limit State of Life Safety is considered (10% exceedance probability during 50 years). Artificial accelerograms, with a content in frequency which fits that of the target spectrum, are developed by means of stochastic vibration method (Vanmarcke 1976), implemented in *SIMQKE* code (Gasparini and Vanmarcke 1976), which calculates power spectral density function from a defined response spectrum and uses this function to derive the amplitudes of sinusoidal signals having random phase angles uniformly distributed between 0 and 2π. The sinusoidal motions are summed to generate independent accelerograms (compatible with the response spectrum). Horizontal and vertical elastic response spectra with 5% damping coefficient and 4s largest period have been considered as target spectra. Artificial accelerograms total duration is 20s: the stationary part of the accelerograms starts after 2s and its duration is 10s (according to Italian Ministry of Infrastructures 2008). The response spectra ordinates of these accelerograms are in the range of 90% (lower bound) and 130% (upper bound) with respect to the ordinates of the above-mentioned target spectra.

According to the Italian Code for Constructions (Italian Ministry of Infrastructures 2008), seven artificial accelerograms were considered for the analysis of the pier in the longitudinal and transverse direction. Each artificial accelerogram is scaled by a numerical factor to obtain various values of peak ground acceleration (*PGA*) and perform the fragility analysis. A number of studies have showed that the lognormal distribution well fits seismic demand (Choi et al. 2003). Given the *IM* - Intensity Measure (*PGA* is considered in this study), the average seismic structural demand (S_d) can be defined by means of the following law:

$$S_d = IM^B e^A \tag{6.2}$$

This law can be represented by the following equation:

$$\ln(S_d) = A + B \ln(IM) \tag{6.3}$$

A and *B* coefficients are calculated by linear regression of the entire set of data which depends on the probabilistic characterization of materials strengths (Cornell et al. 2002) described in the following paragraphs. After finding *A* and *B* coefficients and the dispersion, the fragility curve becomes a lognormal cumulative distribution, in which probability:

$$P_{f,PL}(a) = P[D_a > d_{PL}/a] \quad (6.4)$$

can be calculated by numerically solving the following integral:

$$\int_{D(a)>dPL} f_D(d/a)\partial d \quad (6.5)$$

where the damage density probability function is defined by the lognormal distribution in the following equation:

$$f_D(d) = 1/[(2p)^{1/2} ed] \exp [-0.5 ((\ln d - l)/e)^2] \quad (6.6)$$

being $\lambda = A + B\ ln(IM)$ the average value related to a specific *IM* value and ε the dispersion of data for the above-mentioned linear regression.
These fragility curves are referred to a single pier; considering a bridge set up by *N* piers without interaction between themselves (multi span simply supported girder bridge), the probability of passing a certain Performance Level is:

$$P_{f,PLsystem} = 1- P\ (1 - P_{f,PLpier}(a)) \quad (6.7)$$

6.3 Bridge case study

The case study considered consists in a recurrent bridge type in the Italian transportation road networks. The bridge was built in 1970, near Treviso, in the Veneto region, Italy (Figure 6.2a). The structure consists in a multi-span simply supported reinforced concrete girder bridge. Bridge span modulus has 4 pre-stressed reinforced concrete spans with double-tee beams and a cast-in-place reinforced concrete slab; each span is 24,75m long. The spans are sustained by reinforced concrete frame piers with two circular columns having 1,50m diameter and a transverse reverse-T beam (Figure 6.2b). The piers are 9m high; deck width is 9m. Some geometrical data of the bridge are represented in Figure 6.3.

The static scheme for the piers is different along the two principal directions: a cantilever beam in longitudinal direction and a framed structure in the transversal direction.

According to Morbin et al. (2010) two main variables have been considered for the construction of fragility curves: steel yielding strength f_y and unconfined concrete maximum stress f_c. Reinforcing steel is the Italian *FeB32k* type, described with a lognormal probabilistic distribution (Fig. 6.4a): the mean value of the yielding strength is 385MPa and the standard deviation is assumed equal to 42MPa. Reinforcing steel distribution is subdivided in three intervals having central values equal to 303MPa, 385MPa and 467MPa. Unconfined concrete is supposed of C25/30 class, according to Italian Code for Constructions (Italian Ministry of Infrastructures 2008) and described with a normal probabilistic distribution (Fig. 6.4b), characterized by mean value equal to 41MPa and a standard deviation of 10MPa. Concrete distribution is subdivided in 5 intervals having the following central values: 13MPa, 27MPa, 41MPa, 55MPa, 69MPa. Analogous considerations have been made for confined concrete.

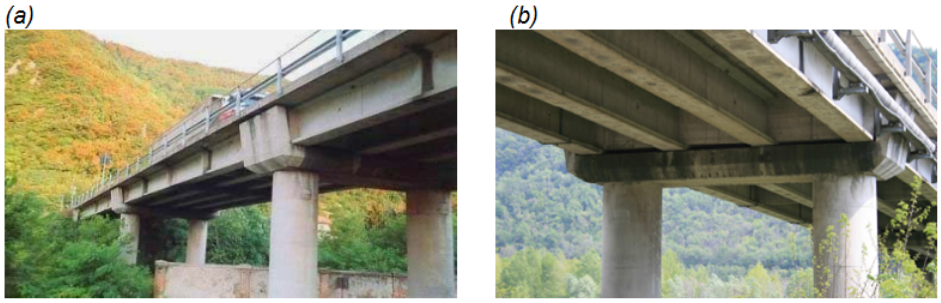

Fig.6.2 General view of the bridge (a) and of the columns and the transverse beam of the piers (b).

The subdivision into finite intervals allows obtaining a reasonable number of sample bridges characterized by different combinations of mechanical properties of two materials.

Each sample bridge was analysed along the two principal directions under the action of 7 artificial accelerograms and the index of damage was obtained. The analyses have been performed using the OpenSees (2011) software: piers have been modelled with beam *nonlinear Column elements*, whereas transverse beams and deck have been modelled with *elastic beam elements*. In Figure 6.5 the structural model of the bridge has been represented. The model of Mander et al. (1988) has been considered for confined concrete. Elastic-perfectly plastic

law has been considered for reinforcing steel. In Fig. 6.6 fragility curves obtained along the two principal directions for the four levels of damage defined above are represented.

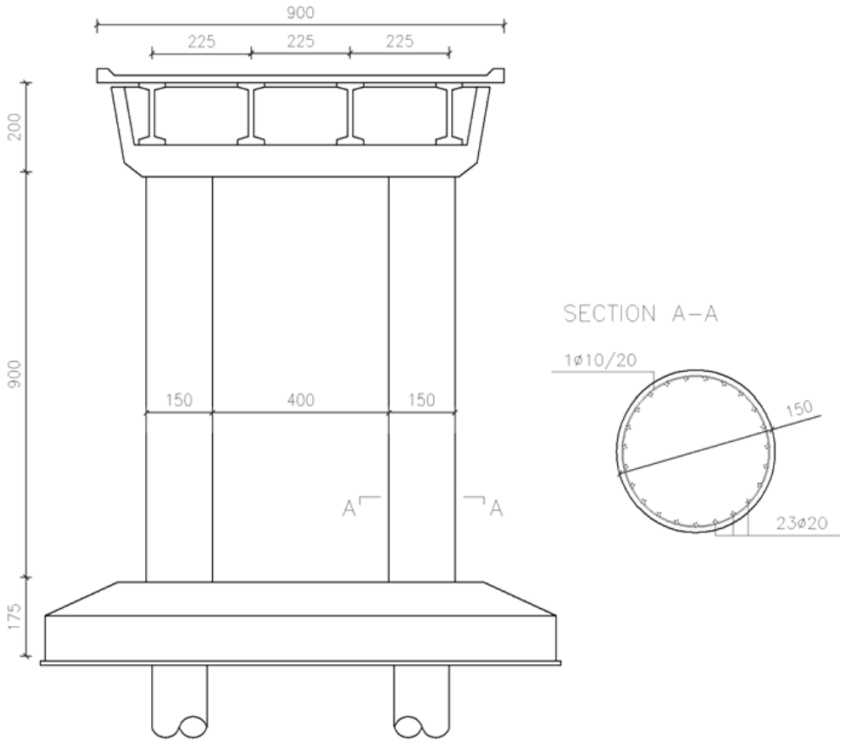

Fig.6.3 Geometrical characteristics of the pier of the bridge considered in this study.

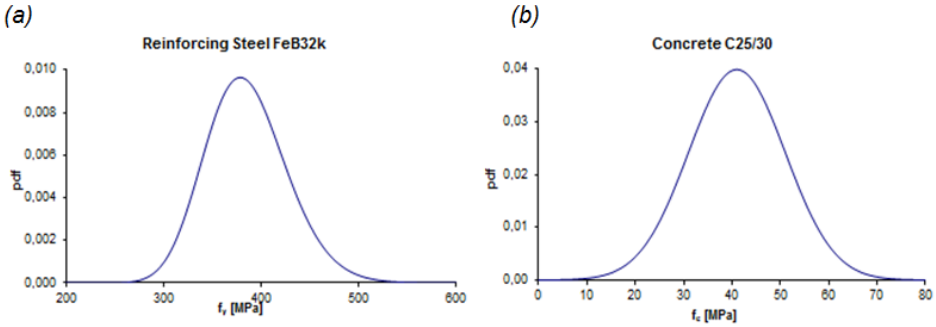

Fig.6.4 Probabilistic distributions of steel yielding strength (a) and unconfined concrete strength (b).

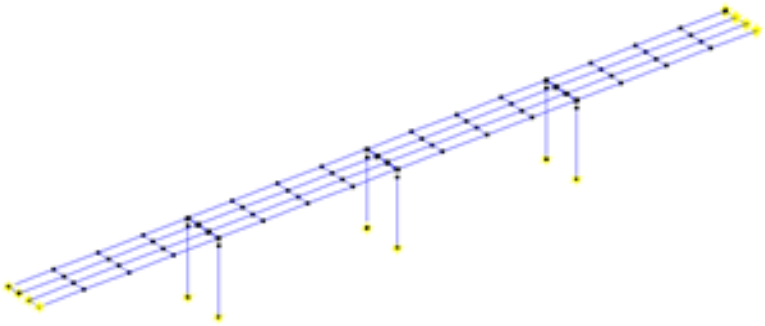

Fig.6.5 The OpenSees model of the bridge in his original configuration.

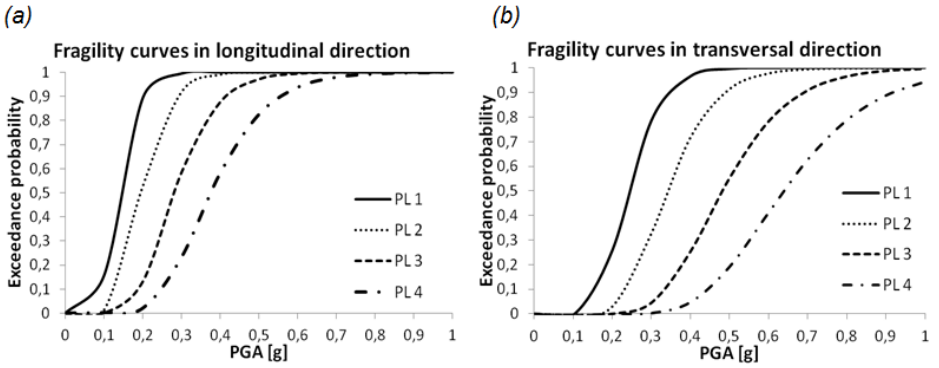

Fig.6.6 Fragility curves of the bridge under analysis in longitudinal (a) and transversal direction (b).

6.4 Parametrical analyses

On the basis of the results previously obtained, a parametrical analysis for the bridge typology considered has been carried out with the purpose of characterizing the seismic vulnerability of the different existing geometrical configurations of the bridge type. Starting from the geometrical characteristics of the study case, structural configurations characterized by different values of pier height *H*, pier diameter *D* and span length *L* have been considered.

Table 6.2 shows the numerical values used for each geometrical parameter. Sixteen geometrical configurations obtained by varying first one parameter and keeping fixed the remaining, and by varying a couple of them have been tested. The analyses have been carried out on the structural configuration of the 4 spans bridge, both in longitudinal and transversal directions. For each

parameters combination the analytical procedure for the fragility curves construction described above has been applied obtaining the analytical trends representatives of the bridge seismic vulnerability.

Afterwards, from the comparison of the results with the Risk-UE curves built with the empirical procedure, the correct mean and standard deviation values have been derived such as to allow to quickly get the curves resulting from the analytical procedure.

The results obtained from the various geometrical configurations tested, have then been statistically analysed to formulate the corresponding analytical expressions and the interpolation surfaces for the fragility characterization of all the possible geometrical configurations of the road transport networks.

H **[m]**	***D*** **[m]**	***L*** **[m]**
5	1	15
7	1,25	20
9	1,5	25
11	1,75	30
13	2	35

Table 6.2 Geometrical parameters values considered in the parametrical analysis.

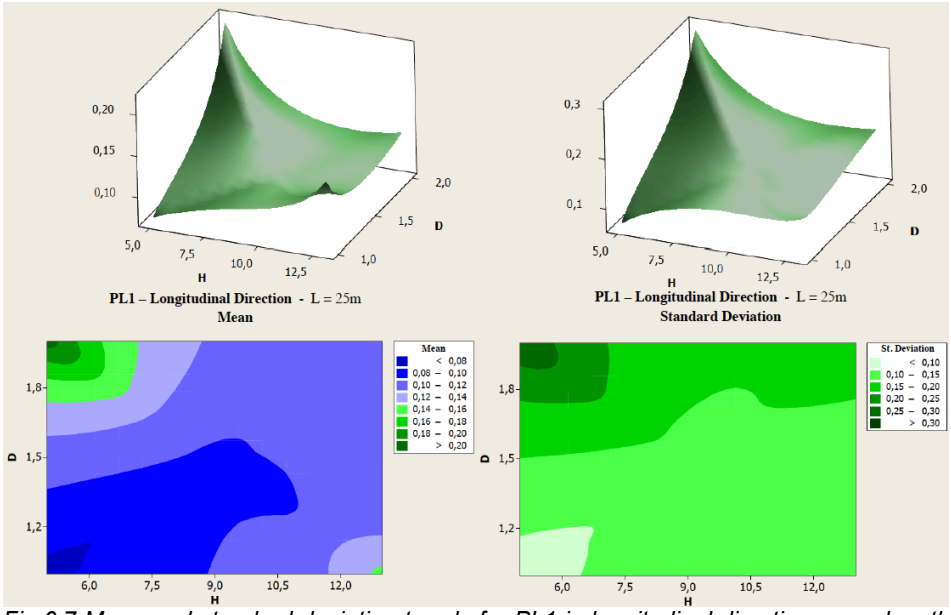

Fig.6.7 Mean and standard deviation trends for PL1 in longitudinal direction, span length 25 m.

In the following some of the obtained mean and standard deviation values trends are shown as examples.

Figure 6.7 shows the surfaces and the relative contour plots representing the trends of the mean and standard deviation for the damage level *PL1* for the 4 spans bridge characterized by span length *L* equal to 25m, analysed in longitudinal direction. For each *PL* and geometrical configuration the respective surfaces and contour plots have been derived. The surfaces are generally characterized by higher values in correspondence of the lower pier height *H* and diameter *D* values.

Figure 6.8 represents the surfaces for the trends of the mean value for the same structural configuration analysed in longitudinal direction, for all the four damage levels considered.

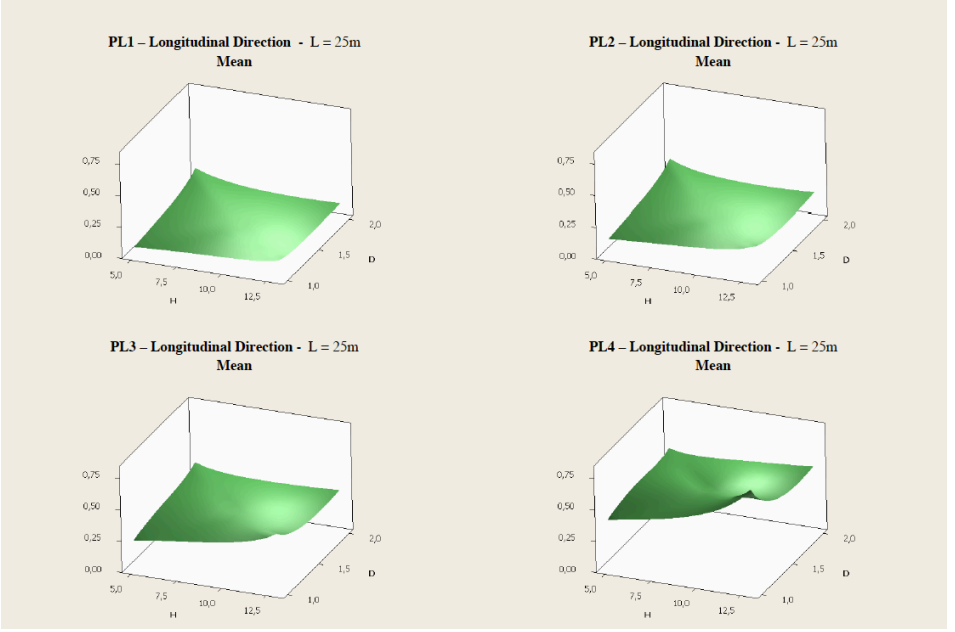

Fig.6.8 Mean value surfaces in longitudinal direction for each PL, span length 25 m.

Figure 6.9 represents the surfaces for the trends of the mean value for the same structural configuration analysed in transversal direction, for all the four damage levels considered.

For each geometrical configuration it can be noticed also how the mean value is characterized by increased values with respect to the growth of the considered *PL*, from *PL1* to *PL4*.

Figure 6.10 shows the relative contour plots for the trends of the standard deviation value for the same structural configuration analysed in transversal direction, for each damage level considered.

It has been noted that for the different performance level *PL* considered, fixing span length *L*, the respective *PL* mean values are influenced by the geometrical parameters *H* and *D* whereas the standard deviation trends are equal for the different performance levels considered on equal span lenght *L*.

The parametrical analysis has led much more precise values both for the estimation of the means and standard deviation: in particular in the case of standard deviation, the Risk-UE procedure provides exclusively a unique value equal to 0,6 that compared with the results obtained in the analysis emphasizes an overestimation of 3-4 times that the effective standard deviation.

Subsequently the results obtained in the combination of *H* and *D* parameters with fixed span length *L* values have then been compared in order to evaluate how the mean and standard deviation surfaces change growing the span lenght *L* considered. Figures 6.11 and 6.12 show the interpolation surfaces and the contour plots of the relative trends of the mean values for the 4 span bridge characterized by different span length values, analysed in longitudinal direction. Similar results can be obtained for the standard deviation values.

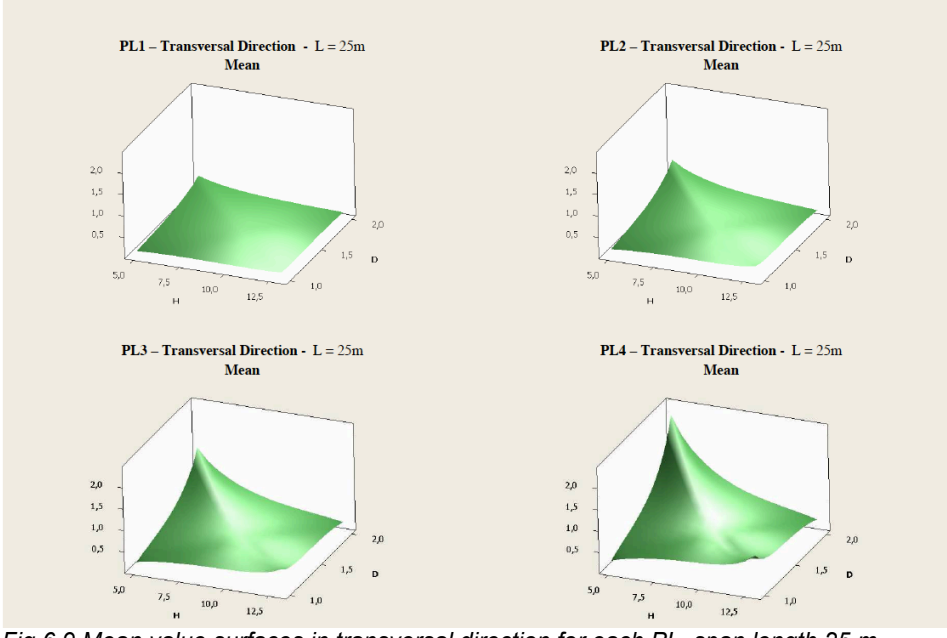

Fig.6.9 Mean value surfaces in transversal direction for each PL, span length 25 m.

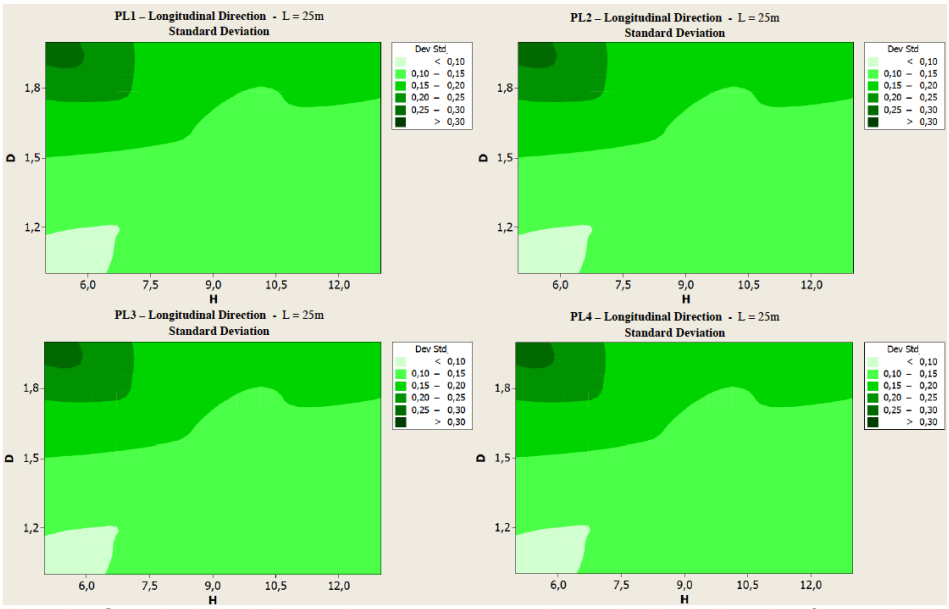

Fig.6.10 Standard deviation value contour plots in longitudinal direction for each PL, span length 25m.

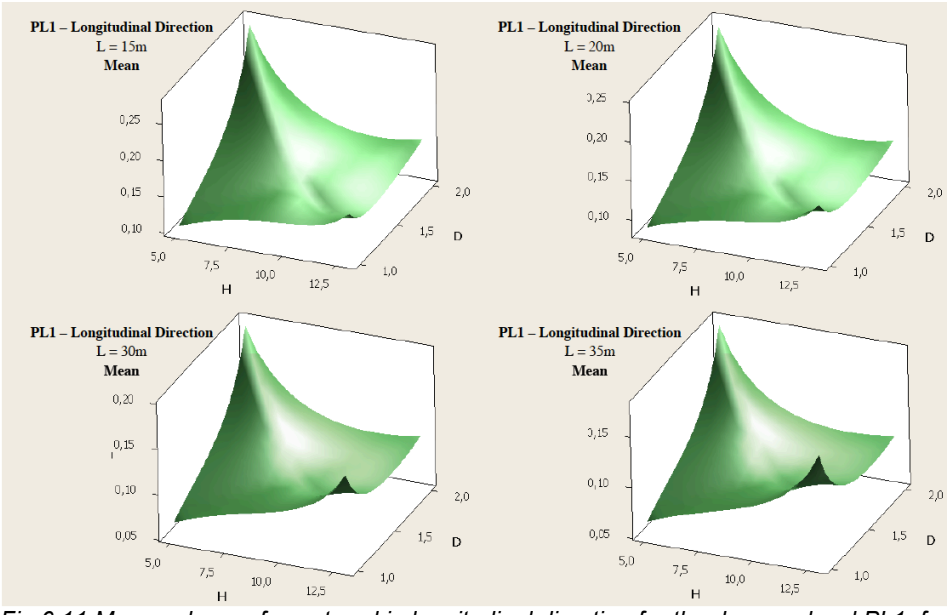

Fig.6.11 Mean value surfaces trend in longitudinal direction for the damage level PL1, for different span lengths.

Tables 6.3, 6.4 represent an *abacus* which lists the possible combination case of the 3 main geometrical parameters of the analysed bridge typology, tested in longitudinal (Table 6.3) and transversal direction (Table 6.4). In each abacus

are reported the mean values of the 4 performance levels *PL* considered μ_1, μ_2, μ_3, μ_4 and the standard deviation value β_c who as shown above is equal for each specific geometric configuration and invariant for all the 4 *PLs* considered. Tables 6.3 and 6.4 exclude geometrical parameter configurations that are structurally hard to find in the built heritage of this structural bridge type (considering all the discrete combinations characterized by values *L*/*D*<20 and *H*/*D*<7,5 times).

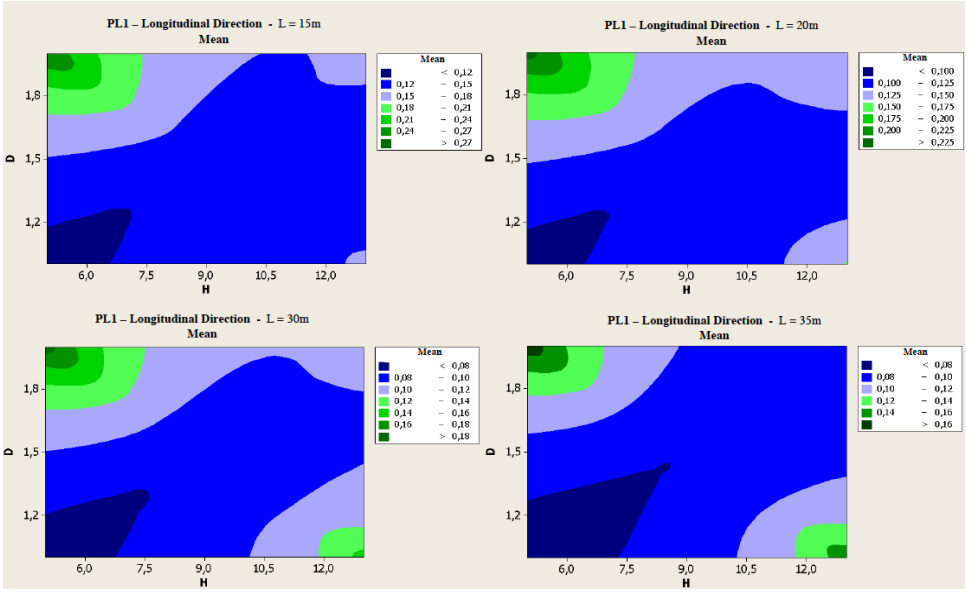

Fig.6.12 Mean value contour plots in longitudinal direction for the damage level PL1, for different span lengths.

LONGITUDINAL DIRECTION							
H **[m]**	***D*** **[m]**	***L*** **[m]**	μ_1	μ_2	μ_3	μ_4	β_c
5	1,00	15	0,1051	0,1916	0,3167	0,4854	0,1071
5	1,00	20	0,0869	0,1650	0,2733	0,4432	0,0874
5	1,25	15	0,1320	0,2108	0,3312	0,4637	0,1622
5	1,25	20	0,1105	0,1842	0,2879	0,4215	0,1378
5	1,25	25	0,0941	0,1628	0,2536	0,3792	0,1134
5	1,50	15	0,1692	0,2412	0,3586	0,4708	0,2260
5	1,50	20	0,1442	0,2146	0,3152	0,4285	0,1968
5	1,50	25	0,1245	0,1932	0,2810	0,3862	0,1677
5	1,50	30	0,1100	0,1770	0,2559	0,3440	0,1386
5	1,75	15	0,2166	0,2827	0,3989	0,5065	0,2985
5	1,75	20	0,1882	0,2562	0,3555	0,4642	0,2646
5	1,75	25	0,1651	0,2348	0,3213	0,4220	0,2308
5	1,75	30	0,1472	0,2186	0,2962	0,3797	0,1969

5	1,75	35	0,1345	0,2076	0,2801	0,3375	0,1631
5	2,00	15	0,2742	0,3355	0,4520	0,5710	0,3796
5	2,00	20	0,2425	0,3090	0,4087	0,5287	0,3411
5	2,00	25	0,2160	0,2876	0,3744	0,4864	0,3025
5	2,00	30	0,1946	0,2714	0,3493	0,4442	0,2640
5	2,00	35	0,1786	0,2604	0,3333	0,4019	0,2254
7	1,00	15	0,1024	0,1947	0,3505	0,5660	0,0981
7	1,00	20	0,0866	0,1681	0,3071	0,5237	0,0854
7	1,25	15	0,1185	0,2013	0,3476	0,5200	0,1403
7	1,25	20	0,0992	0,1748	0,3043	0,4778	0,1230
7	1,25	25	0,0852	0,1534	0,2701	0,4355	0,1056
7	1,50	15	0,1447	0,2192	0,3576	0,5028	0,1912
7	1,50	20	0,1221	0,1926	0,3143	0,4606	0,1692
7	1,50	25	0,1047	0,1712	0,2801	0,4183	0,1471
7	1,50	30	0,0925	0,1550	0,2549	0,3760	0,1251
7	1,75	15	0,1812	0,2483	0,3805	0,5143	0,2509
7	1,75	20	0,1552	0,2217	0,3372	0,4721	0,2241
7	1,75	25	0,1344	0,2003	0,3030	0,4298	0,1973
7	1,75	30	0,1189	0,1841	0,2778	0,3876	0,1705
7	1,75	35	0,1085	0,1731	0,2618	0,3453	0,1438
7	2,00	15	0,2279	0,2885	0,4163	0,5545	0,3192
7	2,00	20	0,1985	0,2620	0,3730	0,5123	0,2877
7	2,00	25	0,1743	0,2406	0,3387	0,4700	0,2562
7	2,00	30	0,1554	0,2244	0,3136	0,4278	0,2247
7	2,00	35	0,1417	0,2134	0,2976	0,3855	0,1933
9	1,25	15	0,1162	0,2096	0,3811	0,5933	0,1255
9	1,25	20	0,0994	0,1830	0,3377	0,5511	0,1152
9	1,25	25	0,0877	0,1616	0,3035	0,5088	0,1049
9	1,50	15	0,1315	0,2150	0,3737	0,5519	0,1636
9	1,50	20	0,1113	0,1884	0,3304	0,5096	0,1486
9	1,50	25	0,0963	0,1670	0,2962	0,4674	0,1336
9	1,50	30	0,0864	0,1508	0,2710	0,4251	0,1186
9	1,75	15	0,1571	0,2315	0,3793	0,5392	0,2103
9	1,75	20	0,1335	0,2049	0,3359	0,4969	0,1906
9	1,75	25	0,1151	0,1835	0,3017	0,4546	0,1709
9	1,75	30	0,1018	0,1673	0,2765	0,4124	0,1512
9	1,75	35	0,0938	0,1564	0,2605	0,3701	0,1315
9	2,00	15	0,1929	0,2593	0,3976	0,5551	0,2658
9	2,00	20	0,1659	0,2327	0,3543	0,5129	0,2414
9	2,00	25	0,1441	0,2113	0,3201	0,4706	0,2170
9	2,00	30	0,1275	0,1951	0,2949	0,4284	0,1926
9	2,00	35	0,1161	0,1841	0,2789	0,3861	0,1681
11	1,50	15	0,1297	0,2285	0,4068	0,6180	0,1429
11	1,50	20	0,1118	0,2019	0,3635	0,5757	0,1350
11	1,50	25	0,0991	0,1805	0,3293	0,5335	0,1271
11	1,50	30	0,0916	0,1643	0,3041	0,4912	0,1192

11	1,75	15	0,1443	0,2325	0,3950	0,5810	0,1768
11	1,75	20	0,1231	0,2059	0,3517	0,5387	0,1642
11	1,75	25	0,1070	0,1845	0,3174	0,4965	0,1516
11	1,75	30	0,0961	0,1683	0,2923	0,4542	0,1389
11	1,75	35	0,0905	0,1573	0,2763	0,4120	0,1263
11	2,00	15	0,1692	0,2477	0,3960	0,5727	0,2195
11	2,00	20	0,1445	0,2211	0,3527	0,5305	0,2021
11	2,00	25	0,1251	0,1997	0,3184	0,4882	0,1848
11	2,00	30	0,1108	0,1835	0,2933	0,4460	0,1674
11	2,00	35	0,1018	0,1726	0,2773	0,4037	0,1501
13	1,75	15	0,1429	0,2512	0,4278	0,6399	0,1504
13	1,75	20	0,1240	0,2246	0,3844	0,5976	0,1449
13	1,75	25	0,1103	0,2032	0,3502	0,5553	0,1393
13	1,75	30	0,1018	0,1870	0,3251	0,5131	0,1337
13	1,75	35	0,0985	0,1760	0,3090	0,4708	0,1282
13	2,00	15	0,1568	0,2539	0,4114	0,6074	0,1802
13	2,00	20	0,1345	0,2273	0,3681	0,5651	0,1699
13	2,00	25	0,1174	0,2059	0,3338	0,5228	0,1596
13	2,00	30	0,1055	0,1897	0,3087	0,4806	0,1494
13	2,00	35	0,0989	0,1787	0,2927	0,4383	0,1391

Table 6.3 Means and standard deviation values in longitudinal direction.

TRANSVERSAL DIRECTION							
***H* [m]**	***D* [m]**	***L* [m]**	μ_1	μ_2	μ_3	μ_4	β_c
5	1,00	15	0,2734	0,4503	0,7346	1,0710	0,1802
5	1,00	20	0,2032	0,3104	0,4737	0,6638	0,1802
5	1,25	15	0,3540	0,6142	1,0448	1,5622	0,2644
5	1,25	20	0,2838	0,4742	0,7840	1,1550	0,2644
5	1,25	25	0,2137	0,3343	0,5231	0,7478	0,2644
5	1,50	15	0,4346	0,7780	1,3551	2,0535	0,3487
5	1,50	20	0,3644	0,6381	1,0942	1,6462	0,3487
5	1,50	25	0,2943	0,4982	0,8333	1,2390	0,3487
5	1,50	30	0,2241	0,3583	0,5725	0,8318	0,3487
5	1,75	15	0,5152	0,9418	1,6653	2,5447	0,4329
5	1,75	20	0,4450	0,8019	1,4044	2,1374	0,4329
5	1,75	25	0,3749	0,6620	1,1436	1,7302	0,4329
5	1,75	30	0,3047	0,5221	0,8827	1,3230	0,4329
5	1,75	35	0,2345	0,3822	0,6218	0,9158	0,4329
5	2,00	15	0,5958	1,1057	1,9755	3,0359	0,5171
5	2,00	20	0,5256	0,9658	1,7147	2,6287	0,5171
5	2,00	25	0,4554	0,8258	1,4538	2,2214	0,5171
5	2,00	30	0,3853	0,6859	1,1929	1,8142	0,5171
5	2,00	35	0,3151	0,5460	0,9321	1,4070	0,5171
7	1,00	15	0,1960	0,3040	0,4705	0,6646	0,1412
7	1,00	20	0,1450	0,2039	0,2856	0,3768	0,1412
7	1,25	15	0,2548	0,4188	0,6826	0,9960	0,2254

7	1,25	20	0,2037	0,3187	0,4977	0,7082	0,2254
7	1,25	25	0,1527	0,2186	0,3127	0,4203	0,2254
7	1,50	15	0,3135	0,5336	0,8947	1,3274	0,3097
7	1,50	20	0,2625	0,4335	0,7098	1,0396	0,3097
7	1,50	25	0,2114	0,3334	0,5248	0,7517	0,3097
7	1,50	30	0,1604	0,2332	0,3399	0,4638	0,3097
7	1,75	15	0,3723	0,6484	1,1069	1,6588	0,3939
7	1,75	20	0,3212	0,5483	0,9219	1,3709	0,3939
7	1,75	25	0,2702	0,4481	0,7370	1,0831	0,3939
7	1,75	30	0,2191	0,3480	0,5520	0,7952	0,3939
7	1,75	35	0,1681	0,2479	0,3671	0,5074	0,3939
7	2,00	15	0,4310	0,7632	1,3190	1,9902	0,4781
7	2,00	20	0,3800	0,6631	1,1340	1,7023	0,4781
7	2,00	25	0,3289	0,5629	0,9491	1,4145	0,4781
7	2,00	30	0,2779	0,4628	0,7641	1,1266	0,4781
7	2,00	35	0,2268	0,3627	0,5792	0,8388	0,4781
9	1,25	15	0,1864	0,2915	0,4553	0,6499	0,1735
9	1,25	20	0,1545	0,2312	0,3463	0,4814	0,1735
9	1,25	25	0,1226	0,1708	0,2372	0,3129	0,1735
9	1,50	15	0,2233	0,3573	0,5693	0,8214	0,2577
9	1,50	20	0,1914	0,2969	0,4603	0,6529	0,2577
9	1,50	25	0,1595	0,2366	0,3512	0,4845	0,2577
9	1,50	30	0,1276	0,1762	0,2422	0,3160	0,2577
9	1,75	15	0,2602	0,4230	0,6833	0,9930	0,3419
9	1,75	20	0,2283	0,3627	0,5743	0,8245	0,3419
9	1,75	25	0,1964	0,3023	0,4652	0,6560	0,3419
9	1,75	30	0,1645	0,2419	0,3562	0,4875	0,3419
9	1,75	35	0,1326	0,1816	0,2472	0,3190	0,3419
9	2,00	15	0,2971	0,4888	0,7973	1,1645	0,4262
9	2,00	20	0,2652	0,4284	0,6883	0,9960	0,4262
9	2,00	25	0,2333	0,3681	0,5792	0,8276	0,4262
9	2,00	30	0,2014	0,3077	0,4702	0,6591	0,4262
9	2,00	35	0,1695	0,2473	0,3612	0,4906	0,4262
11	1,50	15	0,1640	0,2490	0,3787	0,5355	0,1928
11	1,50	20	0,1513	0,2284	0,3456	0,4864	0,1928
11	1,50	25	0,1385	0,2078	0,3125	0,4373	0,1928
11	1,50	30	0,1257	0,1872	0,2794	0,3881	0,1928
11	1,75	15	0,1791	0,2657	0,3946	0,5472	0,2770
11	1,75	20	0,1663	0,2451	0,3615	0,4981	0,2770
11	1,75	25	0,1535	0,2245	0,3284	0,4490	0,2770
11	1,75	30	0,1407	0,2039	0,2953	0,3999	0,2770
11	1,75	35	0,1280	0,1833	0,2622	0,3508	0,2770
11	2,00	15	0,1941	0,2824	0,4105	0,5589	0,3612
11	2,00	20	0,1813	0,2618	0,3774	0,5098	0,3612
11	2,00	25	0,1685	0,2412	0,3443	0,4607	0,3612
11	2,00	30	0,1558	0,2206	0,3111	0,4116	0,3612

11	2,00	35	0,1430	0,2000	0,2780	0,3625	0,3612
13	1,75	15	0,1288	0,1763	0,2408	0,3215	0,1990
13	1,75	20	0,1352	0,1955	0,2836	0,3918	0,1990
13	1,75	25	0,1415	0,2147	0,3264	0,4620	0,1990
13	1,75	30	0,1479	0,2339	0,3692	0,5323	0,1990
13	1,75	35	0,1542	0,2531	0,4120	0,6025	0,1990
13	2,00	15	0,1220	0,1440	0,1585	0,1734	0,2833
13	2,00	20	0,1284	0,1632	0,2013	0,2437	0,2833
13	2,00	25	0,1347	0,1824	0,2442	0,3139	0,2833
13	2,00	30	0,1411	0,2016	0,2870	0,3842	0,2833
13	2,00	35	0,1474	0,2208	0,3298	0,4544	0,2833

Table 6.4 Means and standard deviation values in transversal direction.

In this way for the assessment of a specific geometrical bridge configuration characterized by certain values of *H*, *D*, *L* the abacus allows to quickly obtain the means and standard deviation values through a linear interpolation between the considered configurations. In Tables 6.5 and 6.6 the analitycal regression laws obtained for the definition of the key parameters for the fragility estimation in the main principal directions are shown.

LONGITUDINAL DIRECTION
μ_1 = 0,109 + 0,0736 D - 0,00575 L + 0,00141 H^2 + 0,0817 D^2 + 0,000104 L^2 - 0,0218 H*D + 0,000235 H*L - 0,00271 D*L
μ_2 = 0,283 - 0,00896 L + 0,00222 H^2 + 0,0897 D^2 + 0,000104 L^2 - 0,0250 H*D
μ_3 = 0,388 + 0,0261 H - 0,0150 L + 0,00213 H^2 + 0,103 D^2 + 0,000182 L^2 - 0,0347 H*D
μ_4 = 0,617 + 0,0632 H - 0,361 D - 0,00845 L + 0,00213 H^2 + 0,230 D^2 - 0,0485 H*D
β_c = - 0,0457 + 0,249 D - 0,00371 L + 0,000882 H^2 + 0,0696 D^2 - 0,0257 H*D + 0,000707 H*L - 0,00377 D*L

Table 6.5 Analytical formulations for the calculation of the mean and standard deviation values in longitudinal direction.

TRANSVERSAL DIRECTION
μ_1 = 0,415 - 0,0700 H + 0,541 D - 0,0236 L + 0,00386 H^2 - 0,0437 H*D + 0,00191 H*L
μ_2 = 0,517 - 0,151 H + 1,29 D - 0,0377 L + 0,00723 H^2 - 0,0845 H*D + 0,00465 H*L - 0,0108 D*L
μ_3 = 1,11 - 0,252 H + 2,22 D - 0,0901 L + 0,0169 H^2 - 0,196 H*D + 0,00759 H*L
μ_4 = 1,60 - 0,393 H + 3,56 D - 0,141 L + 0,0275 H^2 - 0,320 H*D + 0,0119 H*L
β_c = - 0,116 + 0,337 D - 0,00162 H^2

Table 6.6 Analytical formulations for the calculation of the mean and standard deviation values in transversal direction.

It can be noticed as the standard deviation values in the analyses in transversal direction is a function only of *H* and *D*, because the span length *L* is not

encountered in the formulation, whereas in longitudinal direction all the 3 geometrical parameters are influent. These results allow to characterize the seismic vulnerability of all the possible geometrical configurations available on the Italian road networks for the structural scheme of a four-span bridge of the studied typology. They represent the adjusted values of the Risk-UE probabilistic input variables –mean and standard deviation- to construct the fragility curves of each bridge belonging to the case study.

6.5 Conclusions

This study shows some insights about practical estimation of seismic fragility curves for a common existing *RC* bridge typology in the Italian transportation network. From a preliminary analysis of the database of bridges in the Veneto region's road networks, a common simply supported reinforced concrete bridge typology with framed piers has been considered as case study. The seismic vulnerability of the bridge has been assessed by analytically constructing the fragility curves. After a comparison of the results obtained with those corresponding to the Risk-UE empirical method, the empirical curves have been corrected with the obtained values of the mean and standard deviation.
In the second part of the work, an extensive parametrical analysis, varying the main geometric parameters, has been performed.
The results obtained in terms of key parameters for fragility estimation have been finally interpolated for constructing the surfaces that characterize the mean and standard deviation values for each possible structural geometric configuration.

7 THE INFLUENCE OF DETERIORATION AND TYPICAL RETROFIT INTERVENTIONS ON THE SEISMIC VULNERABILITY ASSESSMENT OF REINFORCED CONCRETE BRIDGES

7.1 Introduction

The fast socio-economic development of many urban areas has often been characterized by the construction of new infrastructures to meet the increasing demands of mobility. Transport networks are indeed essential for carrying out various economic and strategic activities immediately following a catastrophic event mainly to allow rescue operations initially.

From the analysis of seismic events that occurred in the last decades, it has been observed the most vulnerable elements in transport networks are not only bridges but also tunnels, retaining walls etc., the damage of which may seriously affect transport mobility. These considerations can be easily understood analysing many areas of the Italian national territory where often the connection between urbanized centres is provided by a few links of the network and, for serious damages of bridges and viaducts, it easily runs the risk of damaging all these few links causing the isolation of those urbanized centres. It is also known that the Italian territory, as other regions in the Mediterranean area, is characterized by high seismic risk, and seismic events involve significant negative economic consequences, due to the high population density in many areas of these countries. It is therefore necessary to proceed with an analysis of the seismic vulnerability of individual existing bridges, considering their state of degradation due to environmental agents, and describe the probability of bridges being damaged beyond a specific damage state for various levels of ground shaking. In this context, fragility curves can be considered as one of the most performing tools to assess existing bridge seismic vulnerability (Monti and Nisticò 2002; Padgett and DesRoches 2008; Shinozuka et al. 2000; Lupoi et al. 2006; Shinozuka et al. 2002; Shinozuka et al. 2003), taking into account uncertainty of the variables e.g. by using probability distributions to describe the properties of the materials composing the structure.

Fragility curves can be developed by empirical or analytical methods: empirical fragility curves are usually based on bridge damage data from past earthquakes (HAZUS99 2001; Risk-UE 2004); analytical fragility curves are developed through seismic analysis of the structure like spectral analysis (Hwang et al. 2000), non-linear static analysis (Shinozuka et al. 2000b) or non-linear time history analysis (Choi et al. 2003; Morbin et al. 2010).

Since, typically, the unavoidable degradation of the existing bridges is not taken into account in most of the works available in literature, in this study common degradation phenomena related to steel bars' corrosion are taken into account in the modelling phase of bridges to properly estimate their seismic vulnerability. Only in some recent publications bridge degradation phenomena have been considered in the analysis of transport networks, assuming simplified conditions (deteriorated bridge vs. not deteriorated bridge, with a binary logic) without analysing in detail time evolution of the phenomenon and its implications in terms of increased seismic vulnerability of the bridge affected by degradation (Lee et al. 2011). Reinforcement corrosion and its influence on the durability of the structures have been studied by a number of authors (Andrade et al. 2002; Cabrera 1996; Du et al. 2005; DuraCrete 1998; GiØrv 2009; Melchers et al. 2008; Rasheeduzzafar et al. 1992; RILEM 1996; Wang and Liu 2004).

In this chapter some insights on the influence of the steel reinforcement corrosion on the seismic vulnerability of a typical highway crossing bridge are shown to assess time degradation influence on the seismic vulnerability. Time course of the corrosive phenomenon has been estimated and fragility curves have been constructed for scenarios of 10 years and a total period of investigations to 100 years. Subsequently some seismic retrofit measures have been proposed through the use of traditional restoration techniques, such as pier jacketing with eventual increase of the cross-sectional area and/or eventual addition of steel bars, evaluating the benefits of each intervention. Nowadays other types of interventions can be adopted, such as seismic isolation or the use of *FRP* composites (Kuprenas et al. 1998; Pellegrino and Modena 2010; Shahrooz and Boy 2004): each specific retrofit measure will be characterized by a specific cost and benefit, in terms of reduction of seismic vulnerability.

7.2 Modelling of corrosion in steel bars

A review of various models proposed in the literature to describe degradation phenomena has been preliminary performed (Andrade et al. 2002; Cabrera 1996; Du et al. 2005; DuraCrete 1998; Giørv 2009; Melchers et al. 2008; Rasheeduzzafar et al. 1992; RILEM 1996; Wang and Liu 2004) to choose a suitable model that can be used in this work. The model proposed by Du et al. (Du et al. 2005), has the advantage of using simple analytical expressions and was chosen to estimate the residual capacity of *RC* structural elements with corroded reinforcement by evaluating the reduction of the resisting reinforcement cross-section. The analytical expressions are given as follows:

$$A_s = A_{s0} (1 - 0.01 Q_{corr}) \tag{7.1}$$

$$f = (1 - 0.005 Q_{corr}) f_Y \tag{7.2}$$

where f is the yield strength of corroded bars, f_y is the yield strength of non-corroded bars, A_s is the area of the corroded bars, A_{s0} represents the area of the non-corroded bars, Q_{corr} represents the degree of corrosion of reinforcing bars (expressed in %) related to the rate of corrosion of the bars i_{corr}.

7.3 Numerical application for a typical bridge

The case study considered consists in a typical bridge crossing the A27 highway, in the Veneto region, Italy (see Figures 4.6, 4.7, 4.8, 4.9, 4.10, 4.11). For a more detailed description of the bridge type see Section 4.3. Fragility curves have been constructed according the procedure described in Section 6.2.

The static scheme for the piers is different along the two principal directions: a cantilever beam in longitudinal direction and a framed structure in the transversal direction.

According to Morbin et al. (2010) two main variables have been considered for the construction of fragility curves: steel yielding strength f_y and unconfined concrete maximum stress f_c. Reinforcing steel is the Italian *FeB32k* type,

described with a lognormal probabilistic distribution (Figure 7.1a): the mean value of the yielding strength is 540MPa and the standard deviation is assumed equal to 72MPa. Reinforcing steel distribution is subdivided in three intervals having central values equal to 390MPa, 540MPa and 690MPa. Unconfined concrete is supposed of C30/35 class, according to Italian Code for Constructions (Italian Ministry of Infrastructures 2008) and described with a normal probabilistic distribution (Figure 7.1b), characterized by mean value equal to 38MPa and a standard deviation of 4.8MPa. Concrete distribution is subdivided in 5 intervals having the following central values: 24MPa, 31MPa, 38MPa, 45MPa, 52MPa. Analogous considerations have been made for confined concrete.

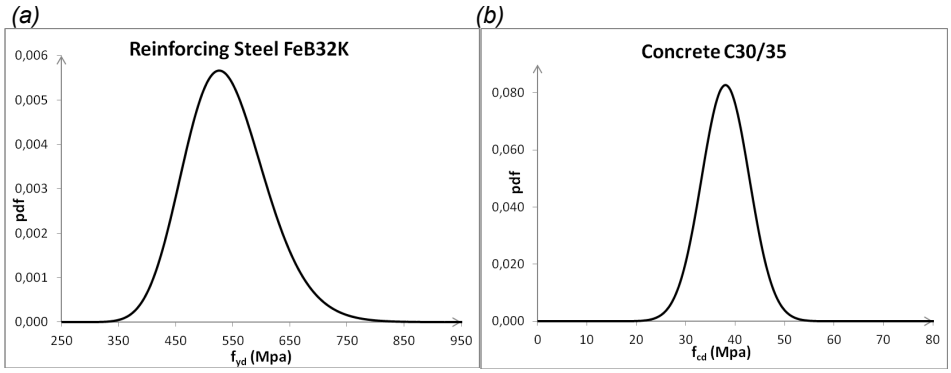

Fig.7.1 Probabilistic distributions of steel yielding strength (a) and unconfined concrete strength (b).

The subdivision into finite intervals allows obtaining a reasonable number of sample bridges characterized by different combinations of mechanical properties of two materials. 15 sample bridges have been analysed, each subjected to nonlinear dynamic analysis. Each sample bridge was analysed along the two principal directions under the action of 7 artificial accelerograms and the index of damage was obtained.

The analyses have been performed using the OpenSees (2011) software: piers have been modelled with beam elements. The model of Mander et al. (1988) has been considered for confined concrete. Elastic-perfectly plastic law has been considered for reinforcing steel. In Figure 7.2 fragility curves obtained along the two principal directions for the four levels of damage defined above are represented.

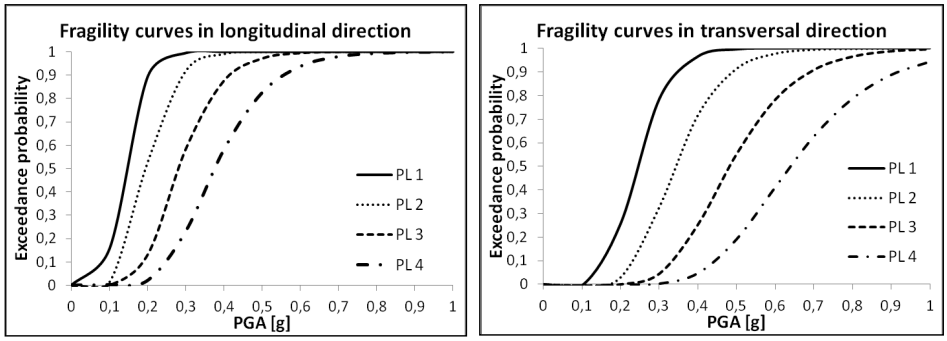

Fig. 7.2 Fragility curves of the bridge under analysis in longitudinal (a) and transversal direction (b).

The corrosion process has been modelled according to Du et al. (2005), assuming a corrosion level equal to i_{corr} = 1.3. Scenarios have been analysed for decades in a total period of 100 years focusing on the consequences caused by the reduction of the reinforcement cross-section in the piers. The reduction trend of the reinforcement bars cross-section is shown in Table 7.1.

Time [years]	Corrosion depth [mm]	Reduced diameter [mm]	Reduced area [mm^2]	Reduced area [%]
0	0	20	314,15	100
10	0,3	19,4	295,59	94
20	0,6	18,8	277,59	88
30	0,9	18,2	260,16	83
40	1,2	17,6	243,28	77
50	1,5	17	226,98	72
60	1,8	16,4	211,24	67
70	2,1	15,8	196,07	62
80	2,4	15,2	181,46	58
90	2,7	14,6	167,42	53
100	3,0	14	153,94	49

Table 7.1 Reduction trend of reinforcement bars section.

Once defined the various scenarios, corresponding fragility curves have been built. Fragility curves have been then grouped for each level of damage to highlight the effects of corrosion processes on seismic vulnerability of the bridges. In Figures 7.3 and 7.4 fragility curves at 0, 20, 40, 60, 80 and 100 years grouped by level of damage have been reported for longitudinal and transversal directions.

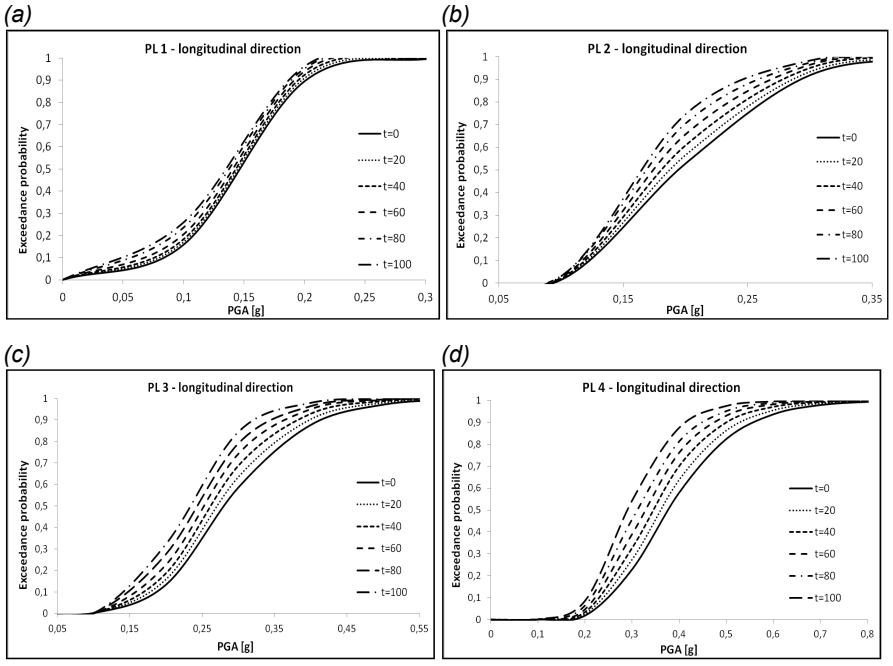

Fig.7.3 Fragility curves in longitudinal direction grouped for each damage level: PL1 (a), PL2 (b), PL3 (c), PL4 (d).

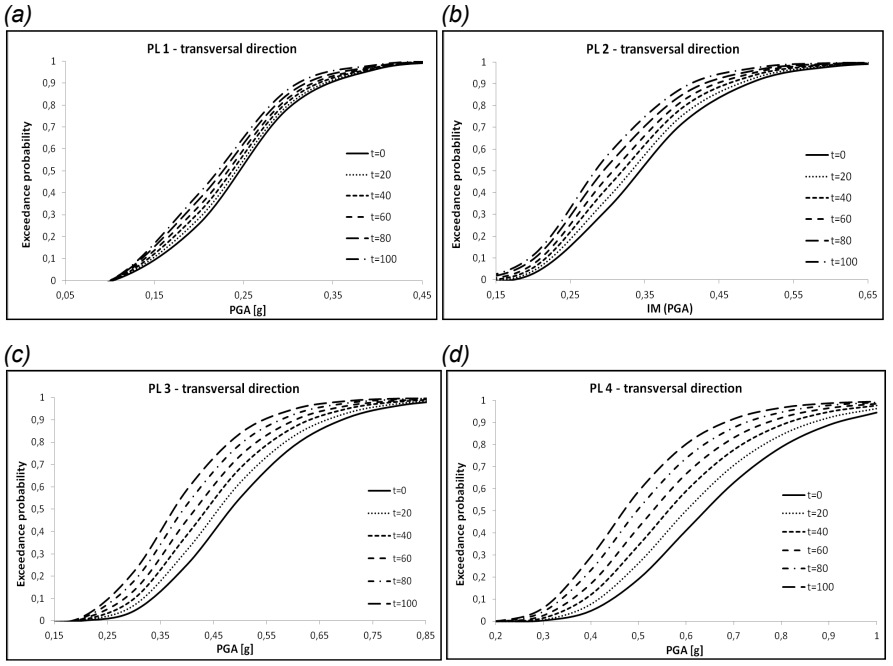

Fig.7.4 Fragility curves in transversal direction grouped for each damage level: PL1 (a), PL2 (b), PL3 (c), PL4 (d).

If the above fragility curves are compared with those obtained with the empirical procedure proposed by Risk-UE for the considered bridge typology, significant discrepancies can be observed. Hence some correction coefficients are proposed to take into account the influence of degradation phenomena.
The following expression is proposed for the mean values of the probabilistic distributions:

$$m(t) = (1 - t/k)\, m \qquad (7.3)$$

where $m(t)$ is the mean value depending on time t (in years), m is the mean value proposed by Risk-UE procedure (not depending on t) and k is a constant that can be calibrated for the specific study case.
The modification of the standard deviation from 0,6, proposed by the empirical Risk-UE procedure, to 0,3 is also proposed to best fit the analytical results. The results obtained for the considered bridge with Risk-UE, analytical and modified Risk-UE procedure (to take into account time degradation), are shown in Figure 7.5 for the Performance Level *PL2*.
The correction of the main parameters of the fragility curves allows better approximating the analytical results and better estimating the vulnerability of the bridge taking into account its temporal evolution when degradation occurs. However, it should be emphasized that the results are valid for the specific type of bridge considered in this study even if, in principle, correction coefficients can be found for any bridge typology. In this way bundles of fragility curves can be obtained for a quick and, at the same time, reliable estimation of seismic vulnerability of existing bridges taking into account their unavoidable degradation.
It is noted that higher ductility level values considered in this paper could not be achieved in reality, because other collapse mechanisms may occur -like fragile mechanisms- in relation to the shear forces which would lead to failure of the pier section, without reaching the higher ductility values considered. In future studies, more specific analyses will be performed on this aspect.

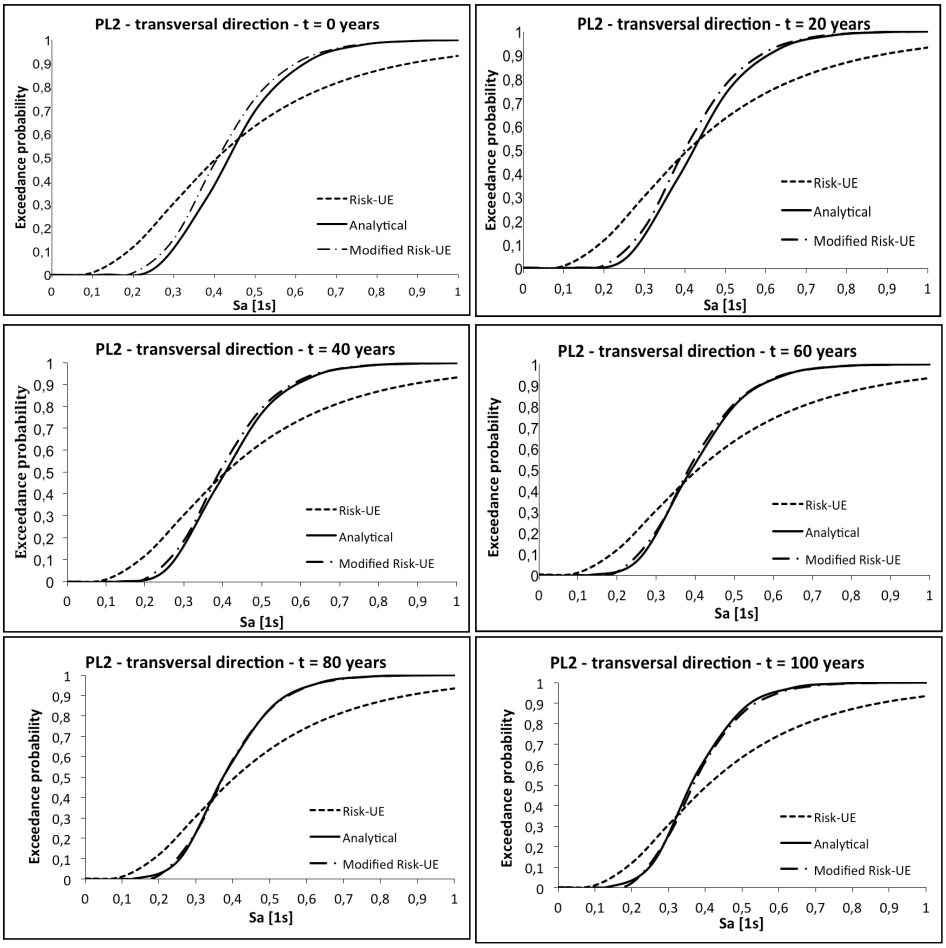

Fig.7.5 Analytical, Risk-UE and modified Risk-UE curves for PL2 and t = 0, 20, 40, 60, 80 and 100 years.

7.4 Retrofit proposal for reducing seismic vulnerability of a typical existing bridge

Some retrofit interventions with traditional techniques have been proposed to reduce seismic vulnerability of the bridge. It is assumed that the fragility curves related to the existing bridge are those corresponding to 60 years after the date of construction of the bridge. Three hypotheses of pier jacketing have been formulated evaluating the relative benefits in terms of improvement of fragility

curves. Firstly concrete column jacketing without modifying the geometric dimensions of the square columns was considered, then an increase of 10cm thickness in the two directions was assumed, and finally increases of 10cm in one direction and 20cm in the other (the side parallel to the longitudinal direction the bridge) were adopted (see Figure 7.6).

For all cases a new cage with 12 additional reinforcement bars of 20mm diameter has been included. The bridge in which the proposed interventions have been applied was modelled by means of nonlinear dynamic analyses along both principal directions. Fragility curves for each level of damage are shown in Figures 7.7 and 7.8. The structural behaviour is different along the two main directions: in particular, the structural scheme is a cantilever beam in the longitudinal direction, and displacements at the top of the pier and their associated damage index values are greater than those measured in the transversal direction, due to the contribution of the transverse beam coupling the response of the two pier's columns and creating a structural framed scheme. The analysis that takes into account the evolution of the corrosion process, provide an assessment of the increased vulnerability of the structure in both principal directions. Furthermore, the variation of the seismic vulnerability due to corrosion is less significant for low *PLs*. The results obtained from the simulation of the proposed retrofit interventions show that they significantly reduce seismic vulnerability of the structure, effectively reducing the probability of being damaged and its detrimental effects on bridge viability.

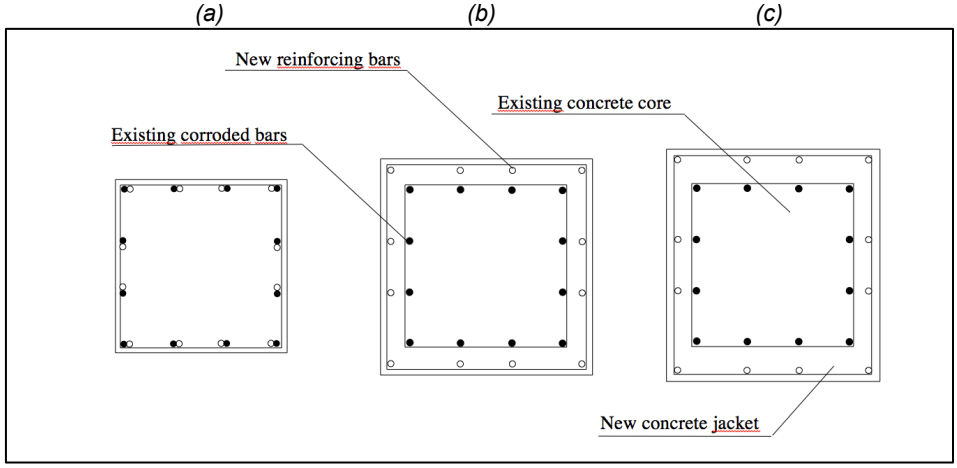

Fig.7.6 Representation of the three interventions proposed: square section with 0,9m side (a), square section of 1 m side (b), rectangular section with 1,1m x 1m sides (c). In white new bars, in black existing corroded bars.

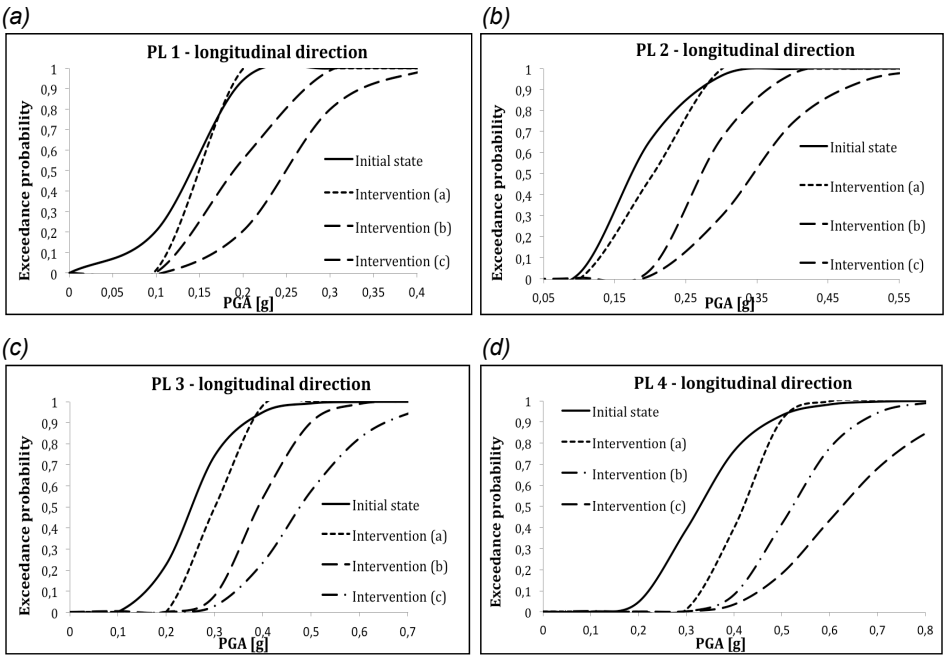

Fig.7.7 Fragility curves in longitudinal direction with retrofit interventions of Fig. 7.6 grouped for each damage level: PL1 (a), PL2 (b), PL3 (c), PL4 (d).

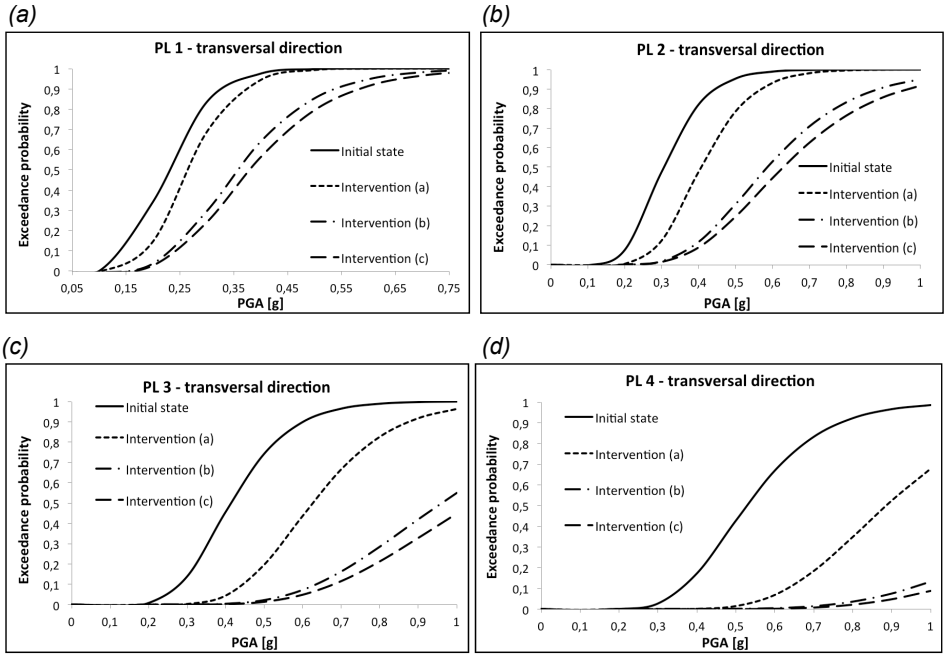

Fig.7.8 Fragility curves in transversal direction with retrofit interventions of Fig. 7.6 grouped for each damage level: PL1 (a), PL2 (b), PL3 (c), PL4 (d).

Other types of intervention can be also used for reducing bridge vulnerability, such as the application of seismic isolation devices, or those based on fiber reinforced polymer (*FRP*) composites technique (Morbin et al. 2010).

7.5 Conclusions

This chapter presents some insights regarding the analysis of the vulnerability of infrastructure networks taking into account their degradation. The effects of degradation phenomena on the seismic vulnerability of bridges were analysed and analytical fragility curves for various scenarios were constructed. Some correction coefficients for Risk-UE fragility curves were proposed to take into account the influence of degradation phenomena. Some types of retrofitting interventions with traditional techniques were also proposed, assessing their benefits in terms of reduction of seismic vulnerability.

The following conclusions can be drawn observing the results of the analysis performed on the single bridge:

- as expected, seismic vulnerability of the bridge increases over time for each level of damage and decreases depending on the characteristics of the retrofit intervention;
- the simulation of the degradation processes allows to define the vulnerability of the structure in relation to its actual state of health;
- as a first step, fragility curves taking into account evolution of degradation phenomena related to reinforcement corrosion can be obtained, in a simplified way, by modifying the empirical Risk-UE curves through correction coefficients variable with time.

According to most of the approaches of the literature, in this work flexural response of bridge piers was analyzed as a first step towards a comprehensive approach taking into account also shear behaviour of vulnerable structural elements. Considering degradation phenomena whose effects could modify the overall structural behaviour, shear mechanisms of failure could occur before reaching yielding of longitudinal and the ensuing ductility. This issue will be taken into account for subsequent improvements of the work in which fragility curves will be obtained also considering brittle shear failure mechanisms.

8 SEISMIC VULNERABILITY ASSESSMENT OF ROAD NETWORKS SUBJECTED TO DETERIORATION

8.1 Introduction

In this chapter a simplified method for the analysis of transport networks, in which bridges are included, has been proposed to determine their risk curves (Roberts 2004). Network vulnerability is expressed as a function of the seismic vulnerability of individual existing bridges belonging to the network and their degradation taking into account their influence on traffic flow (Augusti et al. 1994; Augusti et al. 1998). The proposed method has been applied to a case study related to a small transport network of an Italian mountain area, in the Veneto region.

The obtained results allow predicting possible scenarios of damage, in such a way to quickly inform the rescuers in the immediate post-earthquake emergency phase and, in general, identify potential vulnerable links of the network planning a proper allocation of resources for bridge retrofitting aimed to minimize the overall risk of the transport network (Carturan et al. 2010a; Carturan et al. 2010b; Sgaravato et al. 2008; Shinozuka et al. 2006).

The above analyses (see Chapters 6, 7) were related to single bridges. The further step of the thesis aims at determining the seismic vulnerability of the transport network in which bridges are included. According to the proposals of Augusti et al. (1994, 1998), the analysis of a transport network can be divided into the following steps:

- definition of the network and its arcs. The choice of the network must take into account the level of the analysis: for a regional level, the arcs representing minor roads can be neglected;
- identification of vulnerable bridges and their collocation on the various arcs of the network;
- characterization of the seismic vulnerability of each bridge through the construction of fragility curves as described above;
- definition of the seismic action in the area where the network is located through the study of soil morphology and seismicity data provided by

INGV (National Institute of Geophysics and Volcanology) and identification of the seismic action acting on each bridge of the transport network in relation to its geographical coordinates;
- definition of the Performance Level (*PL*) for the transport network;
- estimation of the probability of occurrence of the *PL* for each bridge of the network, obtained by means of the fragility curves for each intensity measure (*PGA*) for the considered area;
- calculation of the overall vulnerability of the transport network as a function of the vulnerability of its bridges, through an analytical function depending on the network logic diagram, location and number of its bridges.

The analytical function for assessing the vulnerability of the transport network is based on considerations about series and parallel systems. For series of bridges the overall network arc vulnerability is obtained by the vulnerabilities of single bridges using the following expression:

$$P_{series\ system}(a) = 1 - \prod_i \left[1 - P_i(a)\right] \tag{8.1}$$

For systems of parallel bridges the overall vulnerability is given by the following expression as a function of the vulnerability of the single bridges:

$$P_{parallel\ system}(a) = \prod_i P_i(a) \tag{8.2}$$

The combination of the two above expressions can allow obtaining an analytical expression that allows to estimate the overall vulnerability of the network.

8.2 Practical example on a transportation network

The proposed procedure has been applied to the transport network linking the towns of Feltre and Belluno, in the northern Veneto region (North-Eastern part of Italy – see Figure 8.1).

Fig.8.1 View of the transport network considered.

This area is characterized by high values of seismic activity (Figure 8.2). The transport network chosen as example involves an area extended 120 km^2. The distance between the two cities is about of 30 km. It has been initially identified the logic diagram of the network, the existing bridges and their geographical coordinates.

Then fragility curves have been obtained for each bridge using the empirical Risk-UE procedure (Risk-UE 2004), for a preliminary evaluation of the overall network vulnerability. The seismic action has been identified according to Slejko and Rebez 2002 and Slejko et al. 2008.

Seismic vulnerability of each bridge has been assessed for the considered four levels of damage in relation to the entity of the seismic action in the site where the various bridges are located. According to the values of the seismic acceleration at the sites where each bridge is located, the exceedance probabilities are derived from the corresponding fragility curves. Subsequently, the exceedance probability values for each bridge are combined using Eqs. (8.1) and (8.2) in relation to bridges' distribution along the arcs of the network and its logic diagram. In this way the exceedance probabilities for the various arcs of the network are firstly obtained, then those values for the main routes and finally the whole transportation network are estimated. For larger territorial contexts a wide automation of such procedures is required to manage and process the great amount of data that this type of studies needs.

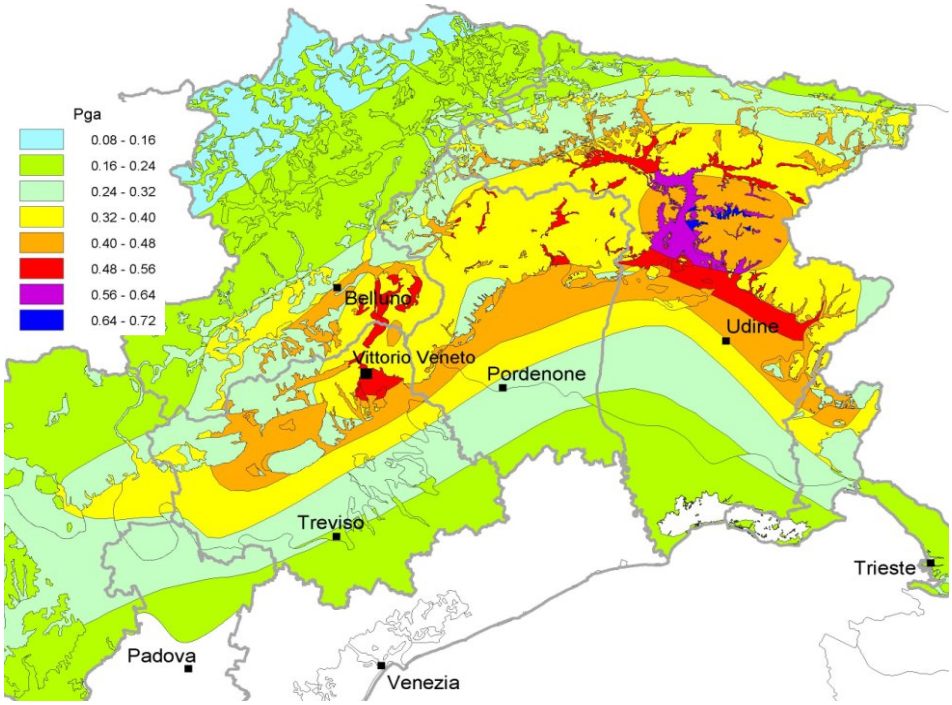

Fig.8.2 Seismic risk map of the North-Eastern Italian area.

The risk curves obtained with the Risk-UE procedure (Risk-UE 2004) for the main paths (Northern and Southern River Piave Routes) are represented in Figure 8.3: the curves have been built on the assumption that, since the area is relatively small, the seismic action conservatively remains equal to its maximum value in all the locations of the network. From the comparison between risk curves of the Northern and Southern Route Piave River it has been observed as the Northern Route present a lower level of seismic risk as compared with the Southern.

The results are based on the simplifying assumption that bridges have been built in the same time period.

This assumption appears reasonable since, in this area, most of bridges have been built after the IInd World War. Time evolution of risk curves for the entire network was also calculated according to the modified Risk-UE fragility curves, as described in the previous section, to take into account the influence of bridges' degradation on the whole network. In Figures 8.4 and 8.5 time evolution fragility curves for *PL3* and *PL4* are shown for the two main routes (a, b), the entire transport network (c) and their difference (d).

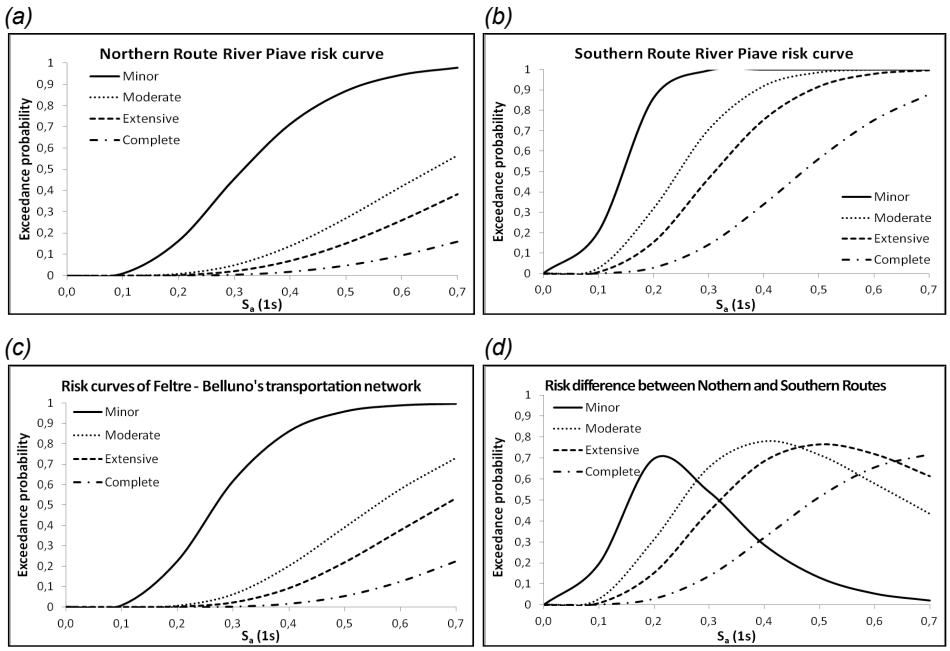

Fig.8.3 Risk curves for the two main routes (a, b), the entire transport network (c) and their difference (d).

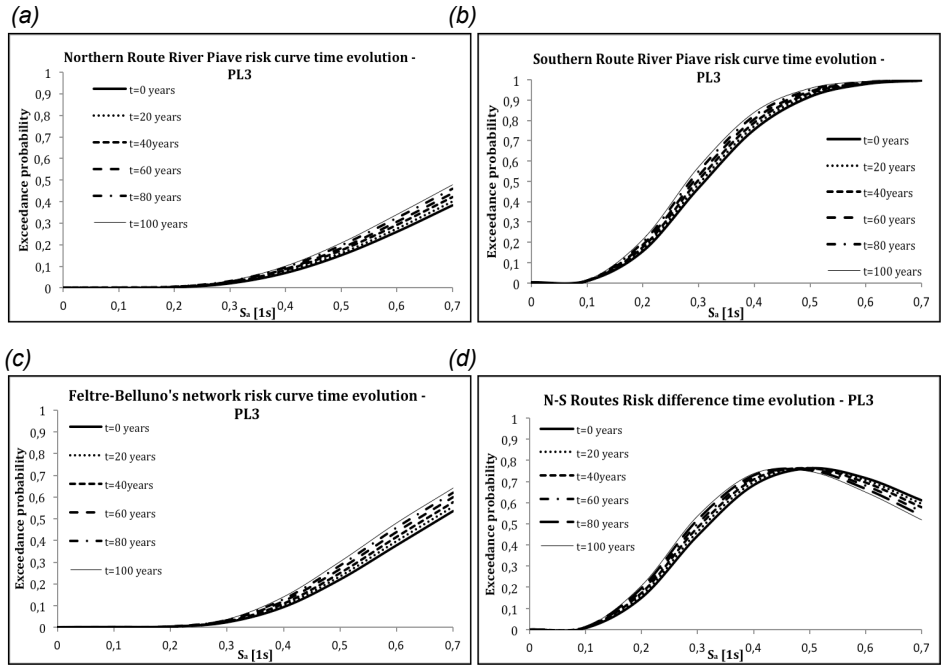

Fig.8.4 Time evolution of fragility curves for PL3 for the two main routes (a, b), the entire transport network (c) and their difference (d).

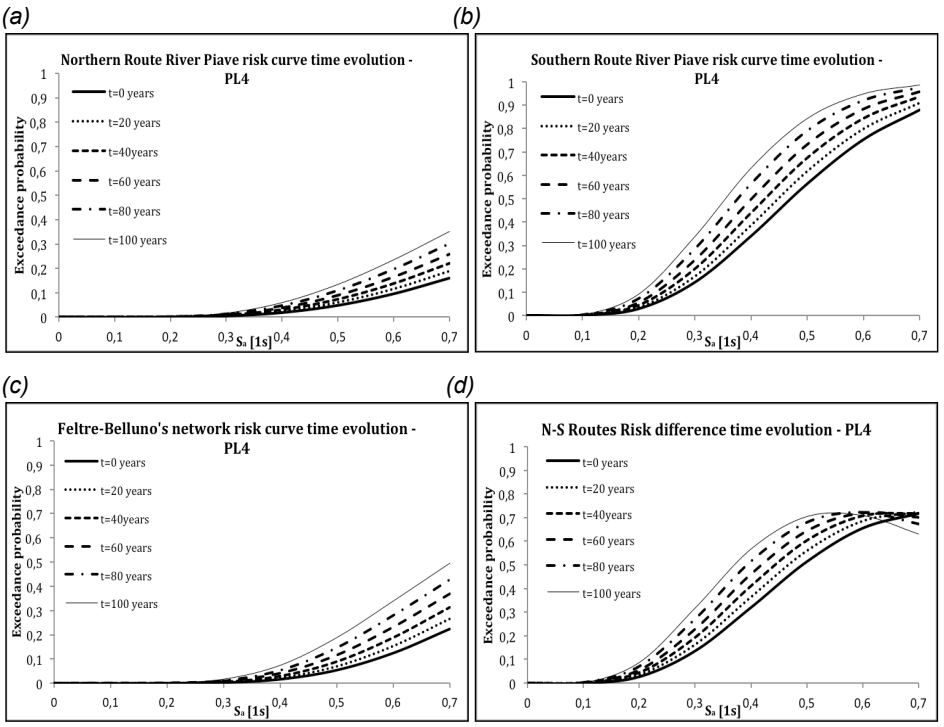

Fig.8.5 Time evolution of fragility curves for PL4 for the two main routes (a, b), the entire transport network (c) and their difference (d).

8.3 Conclusions

In this chapter a simplified methodology for estimating the vulnerability of an entire transport network was described. Seismic vulnerability of the single bridges was characterized through the construction of their fragility curves. Time evolution of risk curves for the entire network was also calculated according to modified Risk-UE fragility curves with the aim of taking into account the influence of bridges' degradation on the vulnerability of the whole network.

The following conclusions can be drawn observing the results obtained from the analysis of the entire transport network:

- the overall vulnerability of the network is a function of the vulnerabilities of its bridges;

- a widespread deterioration of the bridges belonging to a transport network can lead to an increase of the vulnerability of the overall network and should to be taken into account, at least in a simplified way, for a proper network vulnerability assessment;
- the network vulnerability estimation allows to plan budget allocation priority for retrofit interventions of the transport network with the objective of minimizing the overall risk for given budget constraints.

9 *BR.I.N.S.E. v2.0*: A TOOL FOR THE SEISMIC EMERGENCY MANAGEMENT OF BRIDGE INFRASTRUCTURAL NETWORKS

9.1 Introduction

The evaluation of the direct and indirect losses induced by ground shaking is one of the most important traits of seismic hazard assessment. Direct losses can be estimated as the replacement costs of bridges and reconstruction costs of businesses, whereas indirect losses are expressed by the increase of transportation time and losses in business revenues. Observing the seismic events occurred during the last decades, it has been noticed that ground shaking and eventual subsequent fires are the main causes of direct damage; on the other hand business interruption causes approximately half of the experienced indirect losses.

For these reasons it is crucial to provide a detailed seismic input and an accurate spatial distribution when dealing with losses on distributed systems.

In Italy there are not publicly available scenario earthquakes, even thought they are needed for seismic risk analysis, especially when treating distributed systems.

In this chapter a brief review of the seismic hazard background referred to the national area is proven, and the description of a new tool for the seismic assessment of bridge infrastructural networks subjected to scenario earthquakes is illustrated. In the final part of the chapter one possible application of the proposed tool to the railway infrastructural networks context is explained.

9.2 Italian seismic hazard background

The first prototype of a seismic source model of the Italian territory was realized within the activities of the National Earthquake Defense Working Group in the

90s' (Scandone et al., 1992), using the analysis of historical earthquakes reported from 217 BC. In the following years various earthquake databases were compiled including for example *CPTI99* (CPTI Working Group, 1999). These studies led to the formulation of the *ZS4* seismotectonic model (Meletti et al. 2000). *ZS4* model has been then adopted as a model in many successive seismic hazard assessment studies with slight modifications (Romeo and Pugliese, 2000; Rebez and Slejko, 2004). This model was characterized by a significant number of seismic zones with too few earthquakes to derive a statistically significant seismicity rate. In the following years new data was published using *GIS*-based "*fault catalogues*". The new seismogenic process showed the need of replacing *ZS4* with a new seismic source model. On these bases, the actual *ZS9* source model was designed to build a new seismic hazard map, following a government request, with the aim of updating and simplifying the existing *ZS4* seismogenic zones.

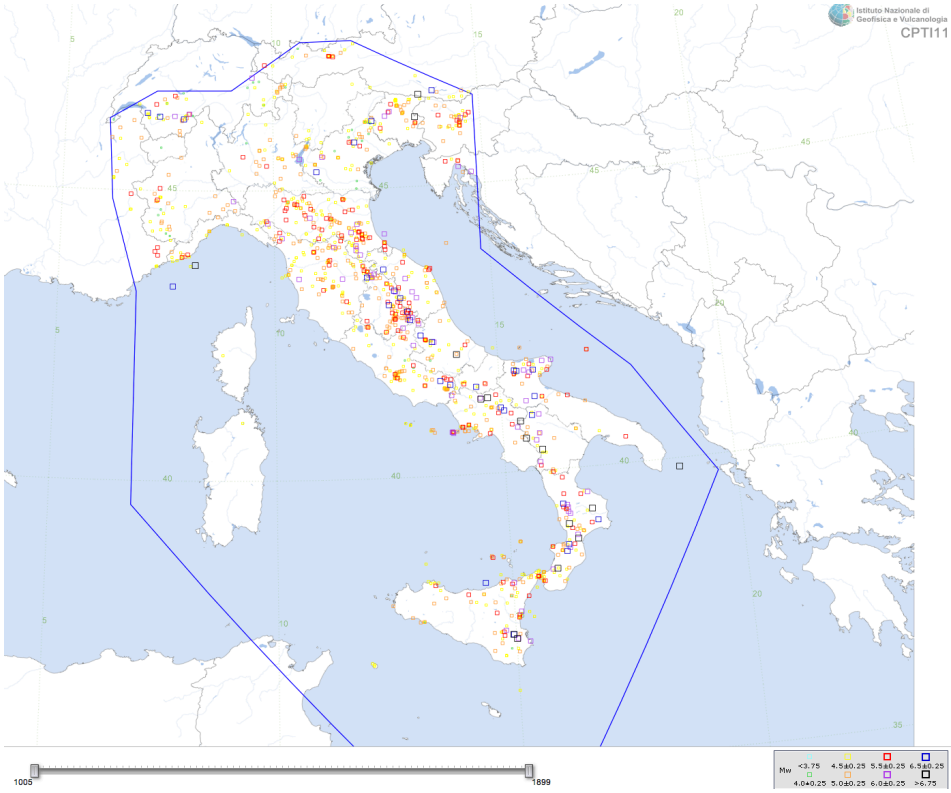

Fig.9.1 Historical earthquakes in Italy from 217 BC to 2011 AD according to CPTI11 catalogue.

Seismogenic zones (*SSZs*) have been reduced from 87 of the previous *ZS4* model to 42 in the *ZS9*, using new tectonic data and the historical events collected in *CPTI04* (CPTI Working Group, 2004), an extensive earthquakes database. The catalogue was then updated and the new *CPTI11* was subsequently developed (Figure 9.1a). The design of *SSZs* necessarily implies uncertainties in geometry, usually hard to assess: for this reason the computer code adopted for hazard calculations, *SEISRISK III* by Bender and Perkins (Bender and Perkins, 1987) allows a buffer area around each *SSZ* where the hazard function smoothly tapers to zero. *ZS9* were designed to embrace all earthquakes having M_w > 5.0 and all known earthquake sources that may generate $M_w \geq 5.5$ earthquakes (DISS Working Group, 2007). These areas do not cover the whole country, but approximately 48% of the Italian territory (Figure 9.1b). The seismogenic areas have a three-dimensional nature, which allows the evaluation of the seismogenic depth.

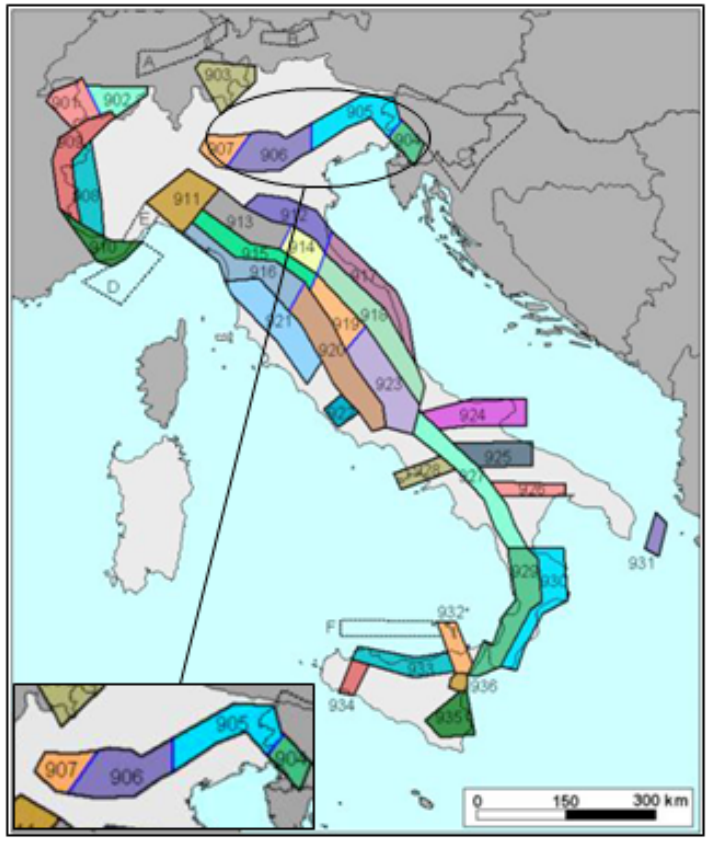

Fig.9.2 Seismogenic zones of the actual ZS9 source model (the bottom left magnification shows the seismogenic zones in the North-Eastern Italy).

A study that investigated some areas showed that the range might coincide with specific geological features. More often, the existence and depth of brittle seismogenic layers are simply inferred from the minimum and maximum depth at which earthquakes occurred (Marone and Scholz, 1988). Recent seismological literature shows that the attenuation of strong motion depends on faulting mechanism, as supported by Bommer et al. (2003), who proposed some coefficients to adjust the attenuation relationships for three main faulting typologies: normal, reverse and strike-slip. *ZS9* accounts for the faulting mechanism. A large natural variability was reduced to a limited number of possible faulting mechanisms: this choice certainly may not represent the full complexity of these faulting dynamics but contributes to improve the seismic hazard estimation. The results obtained were grouped into three main simple cases of faulting mechanism (normal, reverse and strike-slip) to support the subsequent application in *Probabilistic Seismic Hazard Analyses* (*PSHAs)*; the results have been mapped in cumulative moment tensor terms, with the classic geologic "*beach ball*" spheres representation (Figure 9.3).

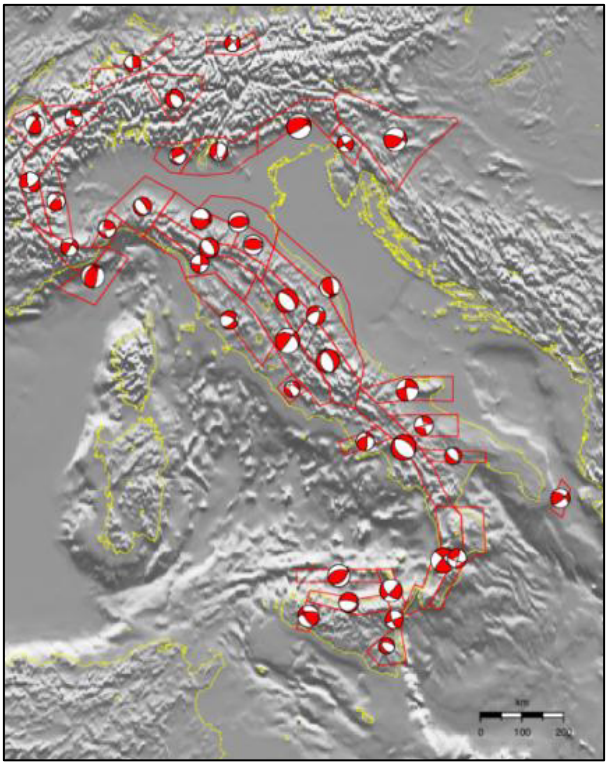

Fig.9.3 Cumulative moment tensor and predominant faulting mechanisms representation for each ZS9 seimogenic zone.

9.3 Recurrence laws, attenuation relationships, scenario earthquakes

Gutenberg-Richter relation has been chosen to represent the recurrence law:

$$log\ \lambda_m = a - b\lambda_m \quad (9.1)$$

where λ_m represents the value of the mean annual rate of occurrence of earthquakes with magnitude m, 10^a is the mean early number of earthquakes with magnitude $m \geq 0$, and b represents the relative likelihood of large and small earthquakes. The analytical expression given by Gutenberg and Richter can be used for each *ZS* (Figures 9.4a, 9.4b) using the specific calibrated coefficients *a* and *b*.

In particular, the *a*-value is taken as the rate of $M_{w,min} = 4{,}8M_w$ earthquakes, to be consistent with the energy content of samples from the database. In this way, the activity rates (*AR*) for each *ZS* and magnitude class M_w have been computed, dividing the overall earthquakes number in the *ZSs* (in the class and time window considered as complete) by the length of the window itself (Table 9.1).

***ZS* Name**	***ZS9***	***a*** **(Co-04.2)**	***a*** **(Co-04.4)**	***b*** **(Co-04.2)**	***b*** **(Co-04.4)**	M_{wMax} ***GR***
Trieste Monte Nevoso	904	4,52	5,29	-1,12	-1,32	6,14
Friuli Veneto Orientale	905	4,66	4,91	-1,06	-1,12	0,37
Garda Veronese	906	4,51	7,06	-1,14	-1,70	0,11
Bergamasco	907	6,81	5,88	-1,71	-1,48	0,04

Table 9.1 Parameters of the seismogenic sources in the North-Eastern Italy.

The most suitable seismic acceleration attenuation relationships have been verified in the light of the most recent earthquake data, as first step the proposed relationships on a national and international level. The expression formulated by Ambraseys et al. (1996) has been modified to correctly use the epicentral distance values. Sabetta and Pugliese (1996) amended this formulation calibrating it with Italian data. Sabetta and Pugliese formulation (Figure 9.4c) has then been integrated using the corrective coefficients considering the prevailing focal mechanism (Bommer et al. 2003.

In addition to the general prediction equation, regional attenuation relationships have been calibrated for regional macro-zones from the scaling laws derived from strong and weak motion data. Analogous relationships have been carried out for volcanic zones with a similar approach.

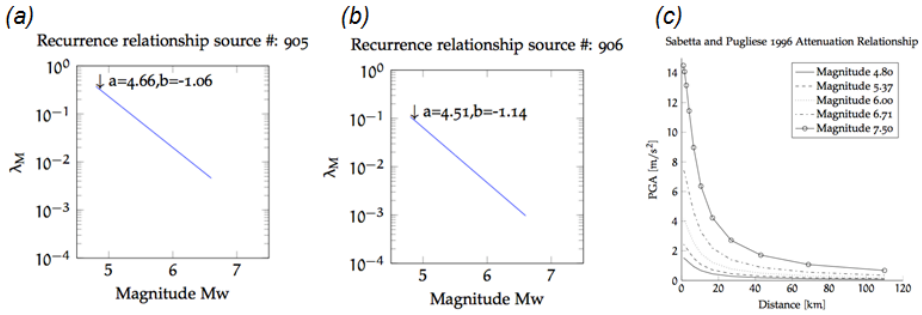

Fig.9.4 Gutenberg Richter recurrence law relationships for the seismogenic zones 905 (a) and 906 (b) and Sabetta and Pugliese attenuation relationship (c).

The three models described above are the key components in the *PSHAs* (Figure 9.5). In particular, referring to the Italian context, the most recent formulations in these fields are the representation of the seismogenic sources (Italian Seismogenic Zonation *ZS9*), the attenuation relationship of Sabetta and Pugliese (1996) modified by Bommer et al. (2003) or the one by Bindi et al. (2011) and finally Gutenberg-Richter's model of the occurrence rate of magnitudes.

Scenario earthquakes overcome the problem of representing the actual distribution of shaking over a spatially distributed system. This is a key aspect in the performance evaluation of distributed systems during the recovery process.

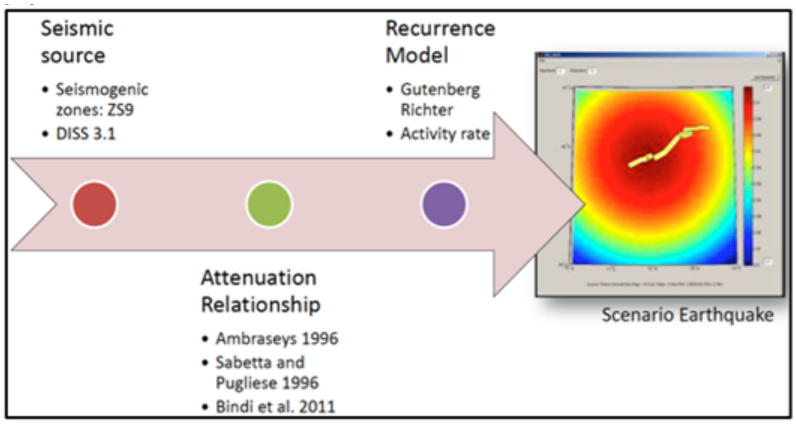

Fig.9.5 Conceptual scheme of the PSHAs.

9.4 *Br.I.N.S.E. v2.0*: a tool for bridge infrastructural networks' scenario earthquakes simulation

The need of simulating scenario earthquakes for the seismic vulnerability assessment of spatially distributed systems (as in the case of infrastructural networks) has lead to the development of a specific tool based on a *Matlab*® code. For this purpose *Br.I.N.S.E. v2.0* (*Bridge Infrastructure Networks' Scenario Earthquakes*) simulator has been proposed and applied to specific case studies to assess its predictional capacity.

Br.I.N.S.E. v2.0 can define the shake-field induced by a specific seismic event, characterized by a M_w value and related epicentral coordinates: peak ground accelerations and S_a(1,0s) are estimated in corrispondence of a portfolio of bridge structures that are under analysis subsequently deriving damage indicators useful for the estimation of the damages suffered by the analysed structures. In particular, the empirical Risk-UE fragility curves have been implemented in the *Br.I.N.S.E. v2.0* allowing to estimate the exceedance probabilities of the 4 Performance Levels previously described in Table 6.1.

Figure 9.6 shows a typical graphical output provided by *Br.I.N.S.E. v2.0* for the simulation of a specific scenario earthquake on a portfolio of bridges.

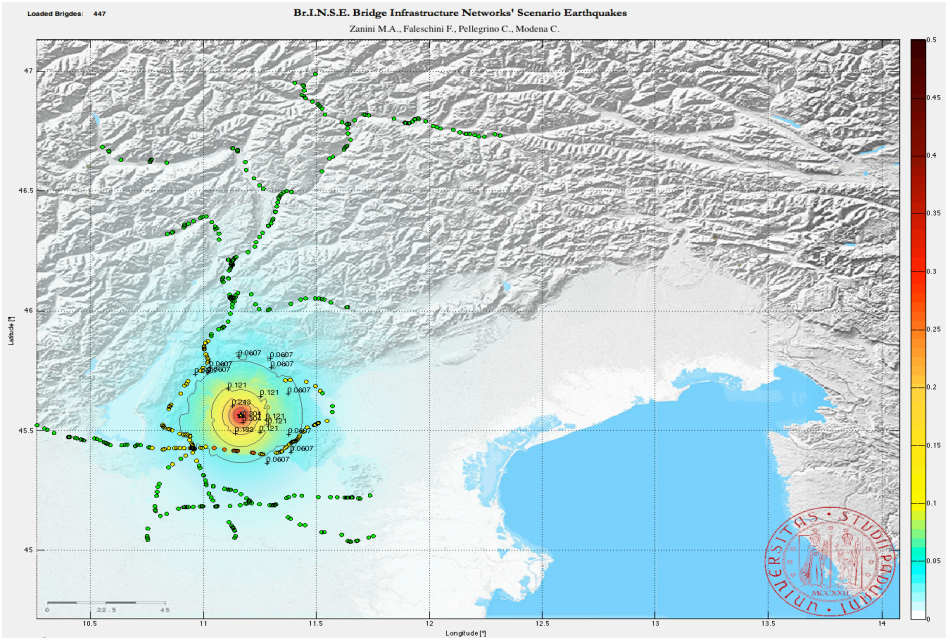

Fig.9.6 A scenario earthquake simulation with Br.I.N.S.E. v2.0.

The reliability of the provisional capacity of the shake field has been validated by comparing *PGA* values recorded in recent seismic events and the shake field formulated by *Br.I.N.S.E. v2.0*. As example, a comparison between data recorded by the National Accelerometric Network (*RAN*) and the simulated shake field for the most recent mid M_w 4,0 seismic event of August 28th 2014, occurred at the border between the Verona and Brescia provinces (lat. 45.67°, long 10.7°) is herein shown in Figure 9.7. In particular, Figure 9.7a represents the recorded shake-field provided by the *Istituto Nazionale di Geofisica e Vulcanologia (INGV*) and Figure 9.7b the *Br.I.N.S.E. v2.0* shake field. Althought it is a moderate but clearly percieved quake, it was possible in real time to validate the reliability of the provision given by *Br.I.N.S.E. v2.0*: Figure 9.7c evidenced how the majority of the records derived from the accelerometric stations located in the area of interest are inside the provisional boundaries for the different soil types (*A*, *B*, *C*) calculated with *Br.I.N.S.E. v2.0*.

In particular in the first 60-70km from the epicetral area it can be noted how measured-simulated data are in very good accordance, only some data slightly diverged for higher distances: in this regard this evidence should be caused by specific site-conditions able to vary the transmission of the seismic waves causing local amplifications, however not significant since in absolute terms these peak ground accelerations are of the order of 0,1%g.

Peak ground acceleration values calculated in correspondence of a portfolio of analysed structures are subsequently used for assess potential damages through the use of the specific fragility curves related to the main structural and material characteristics of each bridge structure. In such way, it is possible to define a priority between different damaged structures which in the post-earthquake phase need to be controlled with visual inspection surveys performed by engineers. These post-earthquake inspections have the main aim to decide if a damaged bridge structure can ensure its normal functionality level or traffic has to be closed since the structural capacity was significantly reduced due to the damages induced by the quake.

Br.I.N.S.E. v2.0 allows, for example, to make these priority analyses taking into account also the structural typology and specific engineering evaluations which in the recent past were not considered by public owners and infrastructural managing companies after seismic events: usually, in fact, no prioritization was made in the post-quake visual inspection operations, thus, not rationally managing this key issue. In the following, a pratical example dealing with this

specific post-quake visual survey operations is described and a proposal of managing protocol with *Br.I.N.S.E. v2.0* is described.

(a)

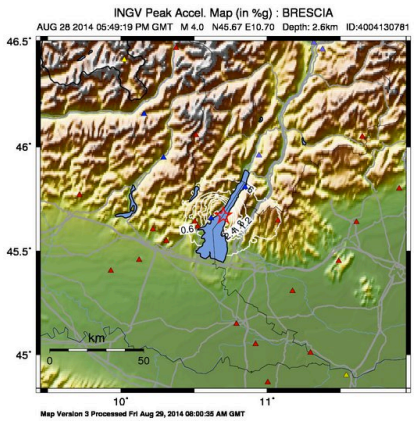

(b)

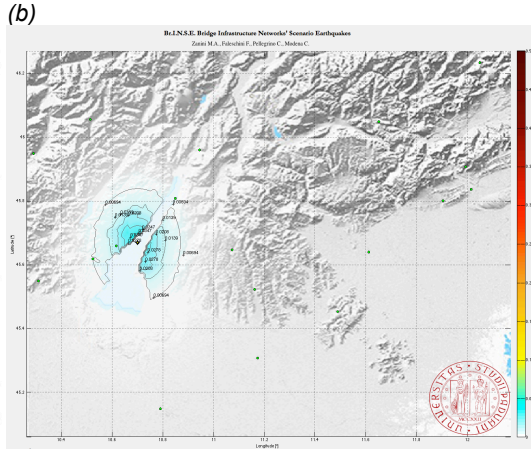

(c)

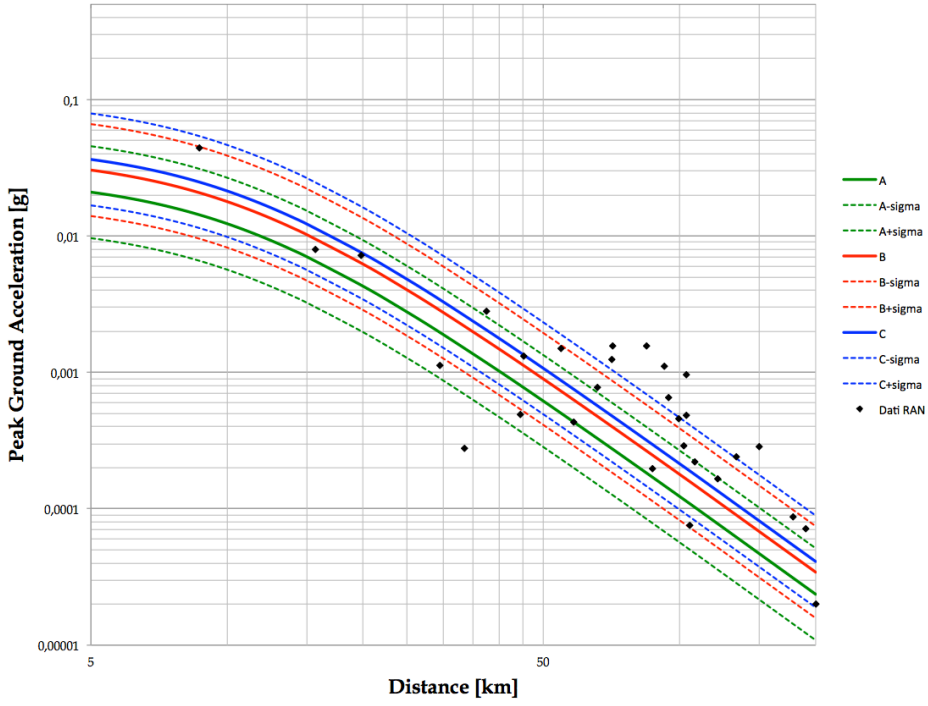

Fig.9.7 The August 28th 2014 Garda Lake earthquake: recorded shake-field provided by INGV (a), Br.I.N.S.E. v2.0 shake-field (b) and comparison between recorded/simulated peak ground acceleration values (c).

9.5 Optimization algorithm for the management of post-quake visual inspections with *Br.I.N.S.E. v2.0*

The *Br.I.N.S.E. v2.0* can be used in railway context for the management of post-earthquake visual surveys needed for ensuring an adequate safety level for the reopening of the railway traffic. In particular, on the basis of the potential damages to a portfolio of railway bridges, defined with *Br.I.N.S.E. v2.0*, an optimization algorithm has been set up for minimizing the total duration time of the visual surveys in relation to the number of available inspectors and the amount of damages induced by the quake. The objective of the procedure is therefore the restoration of the complete functionality of the railway line in the shortest possible timing.

Once defined with *Br.I.N.S.E. v2.0* bridges needing a visual inspection and the number of available inspectors in the different railway stations, the algorithm allows to define for each of them their specific routes and the bridges that have to be inspected through the road network.

On the basis of the road network graph of the area involved by the quake occurrence, a minimum path sub-algorithm is used for evaluate the travel time of each inspector, since the time duration of the visual inspection (t_{insp}) is conventionally assumed equal to 30mins. Once a visual inspection has been carried out, the inspector moves to the next most closer bridge in need of survey. The optimization algorithm therefore defines routes and the bridges that each inspector has to control for minimizing the total duration of the railway line out-of-service. The optimization algorithm assigns bridges belonging to a specific railway line trunk to the inspectors of the railway station from which that specific railway line trunk belongs.

The threshold value of exceedance probability has been taken into account referring to the Performance Level #1 (see Table 6.1) i.e. related to slight damages: this as even also apparent minor damages could lead to derailments, with catastrophic consequences to the safety of the passengers.

Br.I.N.S.E. v2.0 coupled with the above briefly described optimization algorithm has been tested in the following on two specific scenario earthquakes potentially affecting the railway line belonging to the jurisdictional railway directorate of Verona (in the following named “Verona’s *DTP*”).

Due to the lack of information, a preliminary screening of the railway networks owned by the Verona’s *DTP* has been performed and a specific bridge database cointaning the main data needed for the estimation of bridges’ Risk-

UE seismic fragility curves has been set up. This initial recognition, mainly based on the collection of data from satellite images lead to the identification of 447 bridges, viaducts and minor structures (like buried shallow decks), as shown in Figure 9.8.

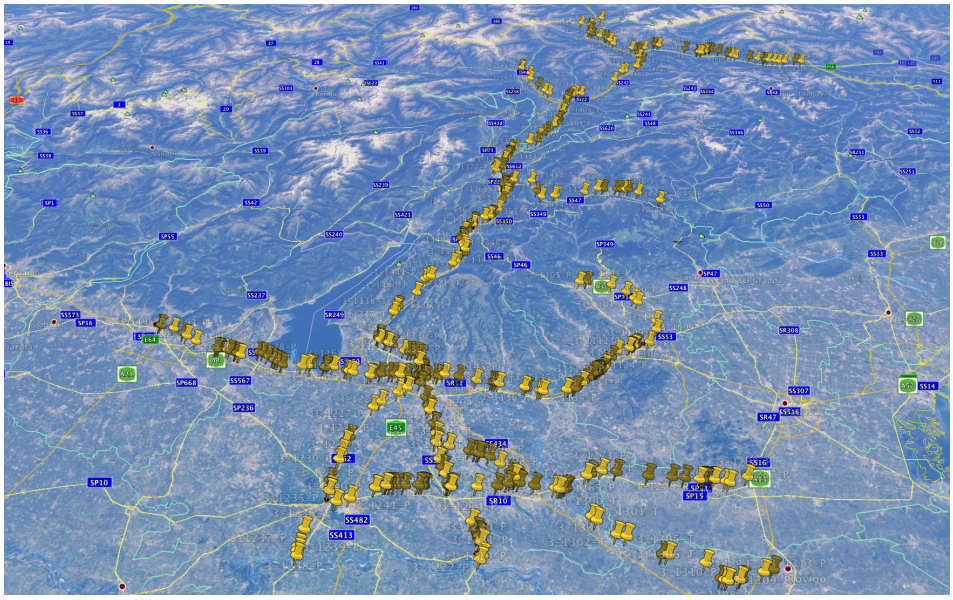

Fig.9.8 The 447 railway bridges managed by the Verona's DTP.

The construction of a database inventory is therefore the first step in the development of a risk analysis of spatially distributed systems.

Due to the different administrative jurisdictions, bridges have been subsequently grouped in subclasses managed by the same jurisdictional units (each one characterized by a specific railway line trunk of competence, as illustrated in Figure 9.9).

Given the lack of information concerning recent significant seismic events occurred in the territorial area in which the railway line managed by the Verona's *DTP* is located, a literature review (Viganò et al. 2008; Livio et al. 2009) on the main historical events occurred in the past was performed and the results have been shown in Table 9.2.

Based on these results a simulation of the potential effects of the recurrence of an earthquake characterized by the same epicentral coordinates of the Basso Bresciano 1222 historical earthquake and a M_w 6,0 has been performed.

Figure 9.10 represents the simulated shake-field induced by the hypotetic M_w 6,0 Basso Bresciano 1222 scenario earthquake on the actual railway bridges owned by the Verona's *DTP*.

UNITÀ TERRITORIALE DI VERONA

Tronco	Sede	Giurisdizione		
		Tratti di Linea	dal km	al km
Reparto UTVR-LV1 Verona				
UTVR-LV1-TR1	Domegliara	Verona P.N.-Brennero	6+888	40+596
UTVR-LV1-TR2	Peschiera	Milano-Venezia	84+000	135+669
UTVR-LV1-TR3	Verona P.N.	Milano-Venezia	135+669	151+928
		Verona P.N.-Brennero	4+161	6+888
		Poggio Rusco-Verona P.N.	110+741	114+952
		Modena-Verona P.N.	89+861	94+346
		Verona-Rovigo	10+110	10+505
		Raccordi:		
		B.PC Fenilone-Verona P.N. Scalo	0+000	1+949
		B.PC Fenilone-B.PC S.Massimo	0+000	1+183
		B.PC Fenilone-B.S.Lucia	0+000	1+238
		B.PC Fenilone-VeronaQ.E.	0+000	1+083
		B.PC S.Massimo-Verona P.N. Scalo	0+000	2+066
		B.S.Lucia-B.PC S.Massimo	0+000	1+615
		B.S.Lucia-Verona P.N. Scalo	0+000	2+208
		Verona Q.E.-B.PC S.Massimo	0+000	1+908
		Piazzali Verona P.N.,Verona P.N. Scalo,Dep.Loc.S.Lucia,Sq.Rialzo, Mag.C.le e Off.G.R.P.V.		
UTVR-LV1-TR4	Vicenza	Milano-Venezia	151+928	200+857
		Vicenza-Schio	0+000	31+240
		Vicenza-Treviso	0+000	1+568
Reparto UTVR-LV2 Verona				
UTVR-LV2-TR1	Isola della scala	Poggio Rusco-Verona P.N.	60+704	110+741
		Codogno-Monselice	115+152	116+207
UTVR-LV2-TR2	Mantova	Modena-Verona P.N.	42+554	89+861
		Codogno-Monselice	87+520	115+152
UTVR-LV2-TR3	Legnago	Verona-Rovigo	27+663	100+623
		Codogno-Monselice	116+207	171+643

UNITÀ TERRITORIALE DI BOLZANO

Tronco	Sede	Giurisdizione		
		Tratti di Linea	dal km	al km
Reparto UTBZ-LV1 Trento				
UTBZ-LV1-TR1	Rovereto	Peri (e) - Trento (e)	40+589	94+280
UTBZ-LV1-TR2	Trento	Trento (i) - Mezzocorona (i)	94+280	112+214
		Trento (i) - Primolano (e)	146+998	80+301
Reparto UTBZ-LV2 Bolzano				
UTBZ-LV2-TR1	Bolzano	Bressanone (e) - Mezzocorona (e)	187+879	112+214
		F.V. Bolzano - Merano (i)	F.V. BZ	32+055
UTBZ-LV2-TRNORD	Brennero	Brennero (i) - Bressanone (i)	239+546	187+879
		F.V. Fortezza – S. Candido Confine di Stato	0+000	72+568

Fig.9.9 The jurisdictional units and related line trunks belonging to the Verona's DTP (in Italian).

Event	Date	M_w	σ	Lat. (°)	Long. (°)
Media Valle Adige	09/11/1046	6,00	0,50	45,833	11,067
Veronese	03/01/1117	6,69	0,20	45,309	11,023
Basso Bresciano	25/12/1222	5,84	0,56	45,535	10,621
Monte Baldo	18/09/1882	4,99	0,72	45,710	10,770
Valle d'Illasi	07/06/1891	5,86	0,06	45,564	11,165
Salò	30/10/1901	5,70	0,10	45,582	10,493
Monte Baldo	19/02/1932	5,08	0,44	45,632	10,729

Table 9.2 Historical earthquakes occurred in the analysed area.

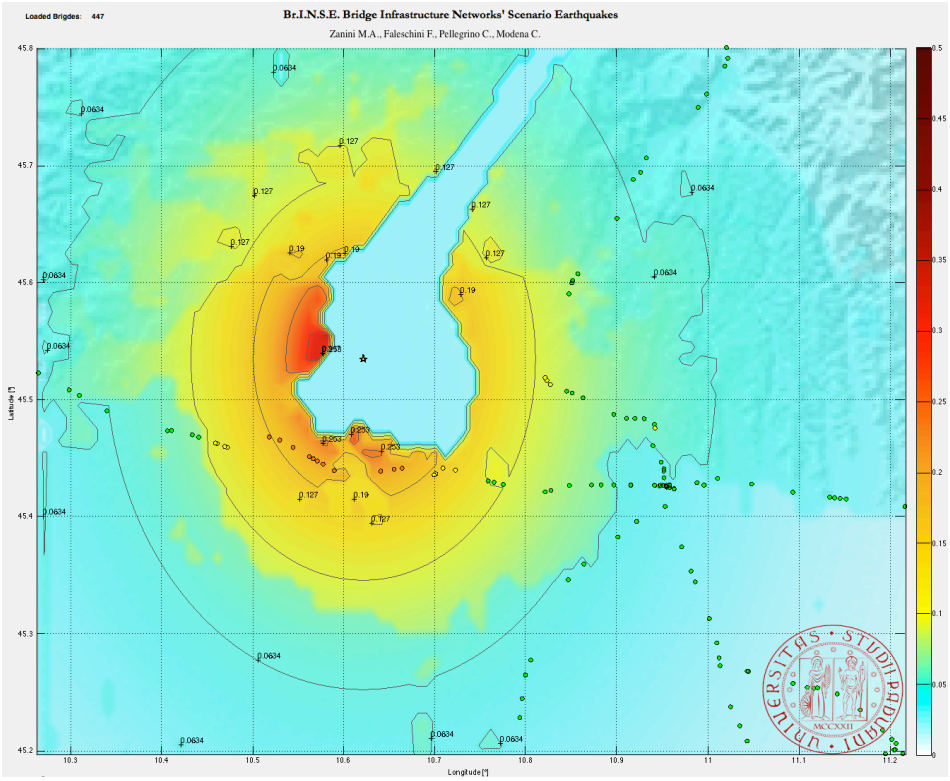

Fig.9.10 Representation of the shake-field provided by Br.I.N.S.E. v2.0 for a M_w 6,0 earthquake with the same epicentral coordinates of the Basso Bresciano 1222 earthquake.

Figure 9.10 evidences bridges in need of post-quake visual survey, due to the observation of *PL1* exceedance probabilities higher than the thresold value (cautelatively assumed equal to 10% for the maximum urgency level -red dots- and equal to 1% for the intermediate urgecy level -yellow dots-). Theresold values are indicative and can be easily modified according to owners' needs.

The M_w 6,0 Basso Bresciano 1222 scenario earthquake should induce slight damages to 23 railway bridges of the Verona's *DTP*, 11 of which characterized by a maximum visual survey urgency level and the latter 12 by an intermediate one. In particular:

- 4 of them located on the Verona P.N.-Brennero railway line trunk from km 6+888 al km 40+596, owned by the jurisdictional unit of Domegliara (*ID* code *UTVR-LV1-TR1*);
- 19 of them located on the Milan-Venice railway line trunk from km 84+000 al km 135+669, owned by the jurisdictional unit of Peschiera (*ID* code *UTVR-LV1-TR2*).

The time duration of each inspection has been conventionally assumed equal to t_{insp} = 30 mins. The application of the optimization algorithm has lead to the evaluation of the total inspections duration of each jurisdictional unit, given the number of inspectors for each of them. In particular:

- for the jurisdictional unit of Domegliara (*UTVR-LV1-TR1*) assuming 3 inspector, the total inspections duration time is equal to 77mins;
- for the jurisdictional unit of Peschiera (*UTVR-LV1-TR2*) assuming 5 inspectors, the total inspections duration time is equal to 184mins.

In such way, the duration of the visual survey operations is equal to the maximum time value (i.e. 184min): this value represents an estimation of the railway-line out-of-service time duration. Figure 9.11 shows the timetable of the visual inspection surveys for the 8 inspectors involved in the post-quake reopening operations.

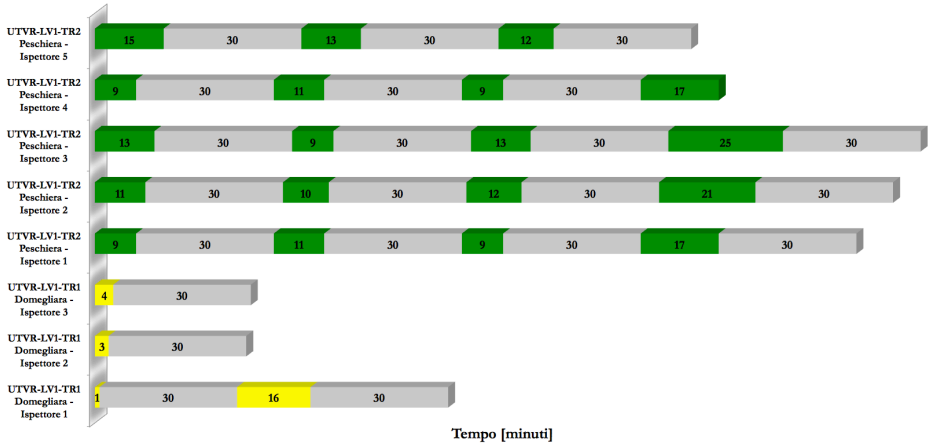

Fig.9.11 Timetable of the visual inspections surveys of the inspectors of the jurisdictional units of Domegliara (UTVR-LV1-TR1) and Peschiera (UTVR-LV1-TR2).

Finally, the visual inspection routes for each inspector (characterized by a different line colour) have been shown in Figure 9.12 (jurisdictional unit of Domegliara) and Figure 9.13 (jurisdictional unit of Peschiera).

Fig.9.12 Post-quake visual survey routes for each inspector of the jurisdictional unit of Domegliara (UTVR-LV1-TR1).

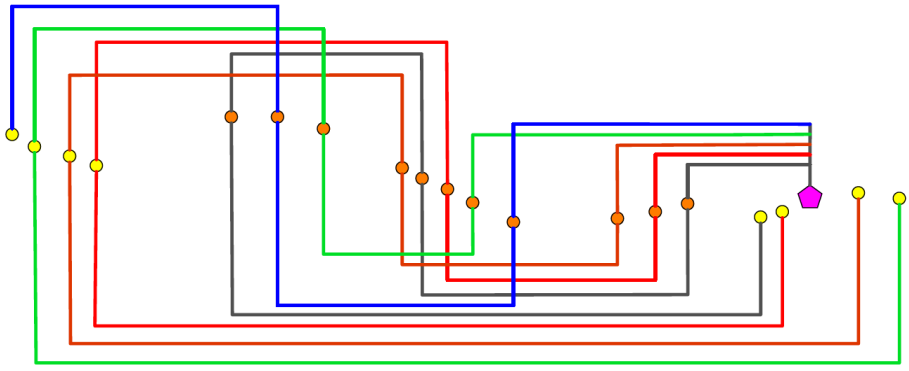

Fig.9.13 Post-quake visual survey routes for each inspector of the jurisdictional unit of Peschiera (UTVR-LV1-TR2).

9.6 Conclusions

A brief review of the seismic hazard background referred to the national area was illustrated, in particular referring to the North-Eastern part of the Italy. The need of simulating scenario earthquakes for the seismic vulnerability assessment of spatially distributed systems has allowed to create a specific tool based on a *Matlab*® code. For this purpose *Br.I.N.S.E. v2.0* (*Bridge Infrastructure Networks' Scenario Earthquakes*) simulator was proposed and applied to to the railway infrastructural networks context for assessing its predictional capacity.

An optimization algorithm for the minimization of the total duration of the post-quake inspections on railway bridges hit by a seismic event was proposed and applied with *Br.I.N.S.E. v2.0* to a case study represented by the railway line owned by the Verona's *DTP*. In particular, on the basis of the potential damages induced by an hypotetic scenario earthquake, the jurisdictional units involved in the post-quake operations and the number of inspectors belonging to each of them, the optimization algorithm allow to define visual inspection routes for each inspector and the timetable of the post-quake operations.

In such way the application of the proposed algorithm on the results provided by *Br.I.N.S.E. v2.0* should represented a rational risk-based methodology for the management of the post-quake visual surveys following a seismic event, with the aim of reducing disruptions and railway lines out-of-service.

10 GENERAL CONCLUSIONS AND RECOMMENDATIONS

This work presented various insights about seismic vulnerability assessment and management of existing bridges subjected to environmental ageing belonging to Italian infrastructural networks. The thesis illustrated in the first part different key issues related to the management and seismic assessment at the bridge level whereas the second part focused on the management at network level also taking into account economical and transportation models.
Different questions were herein explored in order to give useful information to owners or Institution to decide the optimal management planning strategy to put in place for extending bridges' service-life ensuring at the same time an adequate serviceability and safety level.
Chapter 2 described structural and functional deficiencies, related to natural ageing, degradation processes, poor maintenance, increased traffic loads and upgraded safety standards with nowadays affect existing bridges structures. Deterioration processes were critically analysed in particular referring to the materials composing bridge structures, and defining their implications in terms of structural capacity reductions. The condition assessment was defined as a priority for existing bridges, and requires a complex comprehensive approach deeply involving both the use of standard procedures, like *in-situ* and laboratory tests and less conventional tools such as structural monitoring and dynamic identification techniques. In such way, in Italy, seismic retrofitting of bridges has been recently become compulsory for all structures having a strategic function for civil protection activities.
Chapter 3 illustrated a proposal of an integrated procedure for the evaluation of the maintenance condition state and the seismic vulnerability assessment of existing road bridges. The proposed method was applied to a stock of 150 bridges in the Vicenza province, North-Eastern Italy. Visual inspections were carried out to evaluate a *Total Sufficiency Rating* (*TSR*) and simplified seismic assessment was performed for each bridge, in accordance with Pellegrino et al. (2011) and Pellegrino et al. (2014). For each bridge five parameters were assessed:

- a *TSR* value, representing the qualitative outcome of the visual inspection of the state of maintenance of the whole structure (see Section 3.2);

- a unitary maintenance cost in [€/m^2], which represents the normalized cost referred to 1m^2 deck for the execution of maintenance works with the aim of remove the whole local and diffused defects found on the existing deteriorated structure;
- a $FC_{i,min}$ value, that describes the main criticality detected in the fast seismic assessment of the main structural elements composing each bridge (see Sections 3.3-3.4);
- a unitary seismic retrofit cost, given by *OPCM 3362/04*, in [€/m^2], which represents the normalized cost referred to 1m^2 deck for the execution of structural seismic retrofit interventions aimed to increase the resistance against horizontal actions of the elements in which criticatilies were detected;
- a unitary total cost in [€/m^2], i.e. the sum of the unitary maintenance cost and the unitary seismic retrofit cost.

The outcomes were subsequently analysed to derive provisional unitary maintenance, unitary seismic retrofit and unitary total cost equations, configuring as useful economic indicators for the evaluation of the amount of resources needed for bridge restoration interventions.

Chapter 4 presented a statistically-based algorithm for the prediction of bridges' remaining service-life on the basis of the outcomes deriving from the execution of the visual inspection surveys. Through the application of the Bayesian theory on the visual inspection report data performed on different bridge structural typologies, element deterioration curves and subsequently service-life curves were constructed. Finally remaining service-life scenarios were formulated and critically discussed for two different bridge portfolios.

Chapter 5 showed some insights on planning of seismic vulnerability assessment of large stocks of bridges with a real application to the road network of the Veneto region, Italy. The work was focused on updating the preliminary seismic analyses on a cluster of 71 bridges by a series of *in-situ* and laboratory investigations on the main physical and mechanical characteristics of the materials constituting the masonry/stone and reinforced concrete bridges. Measurements related to *in-situ* and laboratory investigations allowed to characterize in a more realistic way the analysed bridges and improve seismic assessment. For each bridge the significant safety factors FC_i have been calculated. Measured quantities were compared with the assumed ones, evaluating their ratios for each structure and thus evidencing the situations for which *in-situ* investigations show conservative, correct/neutral or unconservative

assumptions. The results have evidenced how the geometrical survey played an useful role in the whole structural assessment, in particular referring to spandrel wall failure mechanism that seems to be the most vulnerable mechanism for the masonry/stone bridges. Regarding reinforced concrete bridges, safety factors for bending in abutments and piers were characterized by a substantial increase of the FC_i values after the inspections whereas *in-situ* investigations on materials' properties led to a significant percentage of cases in which reduction of the safety factors for shear if compared to the first analysis is observed.

More in general, properly planned *in-situ* and laboratory investigations could lead to avoiding too conservative or unconservative assumptions for the estimation of the main mechanical characteristics of the materials and, as a consequence, finding inaccurate structural safety factors.

Chapter 6 illustrated an example of practical estimation of analytical seismic fragility curves for a common existing *RC* bridge typology in the Italian transportation network. After a comparison of the results obtained with those corresponding to the Risk-UE empirical method, analytical coefficients were calculated with the aim of quickly correcting empirical curves. An extensive parametrical analysis was then done on the main geometrical parameters and linear regression models was set up for the estimation of mean and standard deviation values.

Chapter 7 explored the analysis of the vulnerability of infrastructural networks taking into account their degradation. The effects of degradation phenomena on the seismic vulnerability of bridges were analysed and analytical fragility curves for various scenarios were constructed. Some correction coefficients for Risk-UE fragility curves were proposed to take into account the influence of degradation phenomena. Some types of retrofitting interventions with traditional techniques were also proposed, quantifying their benefits in terms of reduction of seismic vulnerability. The simulation of the degradation processes allowed to define the vulnerability of the structure in relation to its actual state of health.

In ***Chapter 8*** a simplified methodology for estimating the vulnerability of an entire transport network was described. Seismic vulnerability of the single bridges was characterized through the construction of their fragility curves. Time evolution of risk curves for the entire network was also calculated according to modified Risk-UE fragility curves with the aim of taking into account the influence of bridges' degradation on the vulnerability of the whole network.

It was possible to evidence how the overall vulnerability of the network is a function of the vulnerabilities of its bridges and more generally bridges'

degradation can increase the vulnerability of the overall network and this issue should be taken into account by owners. In such way, the network vulnerability estimation allows to plan budget allocation priority for retrofit interventions of the transport network with the objective of minimizing the overall risk for given budget constraints.

Chapter 9 presented a brief review of the seismic hazard background referred to the national area. The need of simulating scenario earthquakes for the seismic vulnerability assessment of spatially distributed systems has lead to the development of a specific tool named *Br.I.N.S.E. v2.0* (*Bridge Infrastructure Networks' Scenario Earthquakes*). One of the possible applications of the proposed tool to the railway infrastructural networks context was explained: in particular, *Br.I.N.S.E. v2.0* was used in railway context for the management of post-earthquake visual surveys needed for ensuring an adequate safety level for the reopening of the railway traffic and contextually minimizing the total railway line out-of-service time.

10.1 Recommendation for further studies

Results deriving from this study identify several topics worthy of further investigation:

- collection of new visual inspection data in order to better define element-deterioration curves and thus the provisional capacity of the service-life curves proposed algorithm;
- UTCs predictive equations proposed in Table 3.10 should be further optimized, avoiding redundancies in the cost estimation (i.e. taking into account, as example, that for RC-PRC bridges some possible interventions like pier jacketing can be seen both as maintenance and seismic retrofit interventions);
- generation of analytical fragility curves could consider as vulnerable other elements of the bridge in order to improve the seismic assessment (Nielson & DesRoches, 2007): pounding between adjacent spans, fixed and expansion bearings, abutments failure, deck unseating, etc. Specific *PLs* have to be defined for each element considered as vulnerable;

- in the seismic vulnerability assessment a comprehensive approach taking into account also shear behaviour of vulnerable structural elements could be considered. Degradation phenomena, whose effects could modify the overall structural behaviour could lead to shear mechanisms of failure and could occur before reaching yielding of longitudinal and the ensuing ductility;
- influence of other bridge geometrical parameters could be investigated (e.g. piers section, pier reinforcing steel typologies, span length, etc.) in order to give simple analytical laws to generate quickly fragility curves;
- other common structural typologies could be considered in the seismic vulnerability assessment;
- analytical seismic vulnerability assessment methodology could be implemented in an updated version of *Br.I.N.S.E. v2.0* with the aim of refine in absolute terms the reliability of the damage forecasts.

ACKNOWLEDGEMENTS

I would thank you to people with whom I spent my Ph.D. years. First, I wish to thank my supervisor Prof. Carlo Pellegrino for his guidance, advices and encouragements during this study and in various other activities connected to my Research.

I would also like to thank Prof. Claudio Modena for some insights related to research themes but also engineering practical issues.

I'm grateful to Prof. Riccardo Rossi and Dr. Massimiliano Gastaldi for the interesting discussions concerning transportation analysis and traffic flows management.

A thank to my friends and collegues Flora, Paolo, Riccardo and Marco with whom I shared successes, satisfaction but also difficulties and doubts. I also thank to graduate students that I followed and guided in their studies (Pierangelo, Nicolò, Francesco, Giorgio, Luca) for their collaboration.

I would thank also 4Emme S.p.A. for providing useful visual inspection data and Veneto Strade S.p.A. and Vi.abilità S.p.A. for their cooperation in some specific analyses.

Finally, my special thank to my parents and my relatives to have supported me in all my choices, in particular to my father and my mother for their teachings and their morality, representing for me a daily-life example.

LIST OF FIGURES

LIST OF TABLES

REFERENCES

Ambraseys N.N., Simpson K.A., Bommer J.J. (1996) *Prediction of horizontal response spectra in Europe*. Earthquake Engineering and Structural Dynamics, 25, 4:371-400.

Andrade C., Alonso C., Sarrìa J. (2002) *Corrosion rate evolution in concrete structures exposed to the atmosphere*. Cement & Concrete Composites, 24: 55-64.

Augusti G., Borri A., Ciampoli M. (1994) *Optimal allocation of resources in reduction of the seismic risk of highway networks*. Engineering Structures, 16 (7): 485-497.

Augusti G., Ciampoli M., Frangopol D. (1998) *Optimal planning of retrofitting interventions on bridges in a highway network*. Engineering Structures, 20 (11): 933-939.

Bender B., Perkins D.M. (1987) *SEISRISK III: a computer program for seismic hazard estimation*. U.S. Geol. Surv. Bull. 1772: 48.

Bindi D., Pacor F., Luzi L., Puglia R., Massa M., Ameri G., Paolucci R. (2011) *Ground-motion prediction equations derived from the Italian strong motion database*. Bulletin of Earthquake Engineering, 9: 1899-1920.

Biondini F., Camnasio E., Palermo A. (2014) *Lifetime seismic performance of concrete bridges exposed to corrosion*. Structure and Infrastructure Engineering. 10, 880-900.

Bommer J.J., Douglas J., Strasser F.O. (2003) *Style-of-faulting in ground-motion prediction equations*. Bulletin of Earthquake Engineering 1:171-203.

BR.I.M.E. (2001) Bridge management in Europe. *Bridge Management Systems: Extended Review of Existing Systems and Outline framework for a European System* D13, IV Framework Programme, Brussels.

Cabrera J.G. (1996) *Deterioration of concrete due to reinforcement steel corrosion*, Cement & Concrete Composites, 18: 47-59.

Caramelli S., Croce P., Froli M., Sanpaolesi L. (1990) *Impalcati da ponte a lastra ortotropa: comportamento a fatica*. Costruzioni Metalliche, 9, 376-411. (*in italian*)

Caramelli S., Croce P. (2000) *Le verifiche a fatica dei ponti in acciaio.* Costruzioni Metalliche, 6: 33-47. (*in italian*)

Carturan F., Pellegrino C., Modena C., Rossi R., Gastaldi M. (2010a) *Optimal resource allocation for seismic retrofitting of bridges in transportation networks*. In Proc. of IABMAS 2010 - The Fifth International Conference on Bridge Maintenance, Safety and Management. Philadelphia, USA, 11th-15th July 2010.

Carturan F., Pellegrino C., Zampellini A., Modena C., Rossi R., Gastaldi M. (2010b) *A procedure for the evaluation of the seismic vulnerability of bridge networks*. In Proc. of 14ECEE - The 14th European Conference on Earhtquake Engineering 2010. Ohrid, Republic of Macedonia: 30th August – 3rd September.

Carturan F., Pellegrino C., Rossi R., Gastaldi M., Modena C. (2013) *An integrated procedure for management of bridge networks in seismic areas*. Bulletin of Earthquake Engineering, 11 (2), 543-559.

Carturan F., Zanini M.A., Pellegrino C., Modena C. (2014) *A unified framework for earthquake risk assessment of transportation networks and gross regional product*. Bulletin of Earthquake Engineering, 12(2): 795-806.

Chang S.E., Shinozuka M., Moore J.E. (2000) *Probabilistic earthquake scenarios: extending risk analysis methodologies to spatially distributed systems*. Earthquake Spectra 16, 3, 557-572.

Chang S.E., Nojima N. (2001) *Measuring post-disaster transportation system performance: the 1995 Kobe earthquake in comparative perspective*. Transportation Research Part A, 35, 475-494.

Chang S.E., Shinozuka M. (2004) *Measuring improvements in the disaster resilience of communities*. Earthquake Spectra 20, 3, 739-755.

Choi E. (2002) *Seismic Analysis and Retrofit of Mid-America Bridges*. Georgia Institute of Tecnology.

Choi E.S., DesRoches R., Nielson B. (2003) *Seismic fragility of typical bridges in moderate seismic zones*. Engineering Structures; 26 (2): 187-199.

Cornell C., Jalayer F., Hamburger R., Foutch D. (2002) *Probabilistic Basis for 2000 SAC Federal Emergency Management Agency Steel Moment Frame Guidelines*. Journal of Structural Engineering; 128(4): 526-533.

COST345 (2004) *Procedures required for the assessment of highway infrastructures*, European Research Project under the framework of European Cooperation in the field of Scientific and Technical research, EU Commission-Directorate General Transport and Energy.

CPTI Working Group (2004) *Catalogo Parametrico dei Terremoti Italiani*, version 2004 (CPTI04).

de Jong F.B.P. (2004) *Overview Fatigue phenomenon in orthotropic bridge decks in the Netherlands*. Conference proceedings Orthotropic Bridge Conference, Sacramento, CA.

de Jong F.B.P., Boersma P.D. (2004) *Lifetime calculations for orthotropic steel bridge decks*. Conference Proceedings 10th International Conference on Structural Faults and Repair on steel structures, London.

Decree of the President of the Bolzano Province n°41 (2011) *Technische Bestimmungen über die Abnahme und die statische sowie periodische Kontrolle von Straßenbrücken - Disposizioni tecniche sul collaudo e sul*

controllo statico e periodico dei ponti stradali, President of the Bolzano Province ,(*in Deutsch / Italian*).

DISS Working Group. Database of Individual Seismogenic Sources (2007), Version 3.1.1: *A compilation of potential sources for earthquakes larger than M 5.5 in Italy and surrounding areas*. http://diss.rm.ingv.it/diss/, © INGV 2010 - Istituto Nazionale di Geofisica e Vulcanologia - All rights reserved; DOI:10.6092/INGV.IT-DISS3.1.1

Du Y.G., Clark L.A., Chan H.C. (2005) *Residual capacity of corroded reinforcing bars*. Magazine of Concrete Research, 57 (3): 135-147.

DuraCrete (1998) *Modelling of degradation*. The European Union – Brite EuRam III

Ferreira C., Neves L., Matos J., Soares J.S. (2014). *A degradation and maintenance model: application to Portuguese context*. Proceedings of the 7th International IABMAS Conference on Bridge Maintenance, Safety, Management, Resilience and Sustainability, Shanghai 7th-11th July 2014, ISBN 978-1-138-00103-9.

Franchetti P., Grendene M., Pellegrino C., Modena C. (2004) *A methodological approach to bridge maintenance and criteria for seismic risk evaluation*. 18th Australasian conference on the mechanics of structures and materials, 1–3 December 2004, Perth, Western Australia.

Franchin P., Lupoi A., Pinto P.E. (2006) *On the role of road networks in reducing human losses after earthquakes*. Journal of Earthquake Engineering, 10(2): 195-206.

Fruguglietti E., Pasqualato G. (2014) *Bridge management system implementation for Italian highways: from Pontis toward SIOS (Sistema Ispettivo Opere Sineceo) and new generation systems*. Proceedings of the 7th International IABMAS Conference on Bridge Maintenance, Safety, Management, Resilience and Sustainability, Shanghai 7th-11th July 2014, ISBN 978-1-138-00103-9.

Gasparini D.A., Vanmarcke E.H. (1976) *Simulated earthquake motions compatible with prescribed response spectra*. Massachussets Institute Technology; R76-4(420 G32 1976): p. 99.

Giørv O.E. (2009) *Durability design of concrete structures in severe environments*. Taylor and Francis.

Hasan M.S., Setunge, S., Law, D.W. (2014) *Deterioration forecasting of concrete bridge elements in Victoria, Australia using a Markov Chain.* Proceedings of the 7th International IABMAS Conference on Bridge Maintenance, Safety, Management, Resilience and Sustainability, Shanghai 7th-11th July 2014, ISBN 978-1-138-00103-9.

HAZUS 99 (2001) Direct Physical Damage to Lifelines-Transportation Systems.

Hofmann M., Kühn B., Frieβem H., Winkler B. (2012) *Pre-assessment of existing road bridges – New procedure for a rough but quick estimation of the*

capacity of existing road bridges. Proceedings of the 6th International IABMAS Conference on Bridge Maintenance, Safety, Management, Resilience and Sustainability, Stresa 8th-12th July 3162-3169, ISBN 978-0-415-62124-3.

Hudson S.W., Carmichael R.F., Moser L.O., Hudson W.R., Wilkes W.J. (1987) *Bridge management systems*. NCHRP Rep. 300, Proj. 12-28 (2), Transportation Research Board, National Research Council, Washington, DC.

Hwang H., Jernigan J.B., Lin Y.W. (2000) *Evaluation of Seismic Damage to Memphis Bridges and Highway Systems*. Journal of Bridge Engineering; 5 (4): 322-330.

INGV, available from http://emidius.mi.ingv.it/CPTI/.

Italian Ministry of Infrastructures (2008) *Norme Tecniche per le Costruzioni*, DM 2008-1-14. (*in Italian*)

Kamya B.M. (2012, July) *Bridge Management Systems: Challenge of adopting a bridge management system appropriate to the needs of a local authority: Examples from the United Kingdom*. Proceedings of the 6th International IABMAS Conference on Bridge Maintenance, Safety, Management, Resilience and Sustainability, Stresa 8th-12th July 3162-3169, ISBN 978-0-415-62124-3.

Kuprenas J., Madjidi F., Vidaurrazaga A., Lim C.L. (1998) *Seismic retrofit program for Los Angeles Bridges*. Journal of infrastructure systems, 4 (4): 185-191.

Lee Y.J., Song J., Gardoni P., Lim H.W. (2011) *Post-hazard flow capacity of bridge transportation network considering structural deterioration of bridges*. Structure and Infrastructure Engineering, 7:7-8, 509-521.

Legislative Decree n°112 (1998). *Conferimento di funzioni e compiti amministrativi dello stato alle regioni ed agli enti locali, in attuazione del capo I della legge 15 marzo 1997, n°59*, Central Italian Government. (*in Italian*)

Livio F.A., Berlusconi A., Michetti A.M., Sileo G., Zerboni A., Trombino L., Cremaschi M., Mueller K., Vittori E., Carcano C., Rogledi S. (2009) *Active fault-folding in the epicentral area of the December 25, 1222 (Io = IX MCS) Brescia earthquake (Northern Italy): seismotectonic implications*. Tectonophysics, 476: 320-335.

Lupoi G., Franchin P., Lupoi A., Pinto P.E. (2006) *Seismic fragility analysis of structural systems.* Journal of Engineering Mechanics-Asce; 132(4): 385-395.

Mander J.B., Priestley M.J.N., Park R. (1988) *Theoretical stress-strain model for confined concrete*. Journal of Structural Engineering, 114(8): 1804-1826.

Markow M.J. (1995) *Highway management systems: state of the art*. Journal of Infrastructure Systems, 1 (3), 186– 191.

Marone C., Scholz H. (1988) *The depth of seismic faulting and the upper transition from stable to unstable slip regimes*. Geophisical Research Letters 15, 6: 621-624.

MATLAB. version 7.14.0 (r2012a). The Mathworks, Inc., 2012.

Melchers R.E., Li C.Q., Lawanwisut W. (2008) *Probabilistic modelling of structural deterioration of reinforced concrete beams under saline environment corrosion*. Structural Safety, 30: 447-460.

Meletti C., Galadini F., Valensise G., Stucchi M., Basili R., Barba S., Vannucci G., Boschi E. (2008) *A seismic source zone model for the seismic hazard assessment of the Italian territory*. Tectonophysics, doi: 10.1016/j.tecto.2008.01.003.

Meletti C., Patacca E., Scandone P. (2000) *Construction of a seismotecnotic model: the case of Italy*. Pure and Applied Geophysics 157, 11-35.

Mendonça, T., Brito, V. (2014). *Bridge management in Portugal: the past, the present and the future*. Proceedings of the 7th International IABMAS Conference on Bridge Maintenance, Safety, Management, Resilience and Sustainability, Shanghai 7th-11th July 2014, ISBN 978-1-138-00103-9.

MidasFEA v2.9.6 (2009) *Nonlinear and detail FE Analysis System for Civil Structures*. Midas Information Technology Co. Ltd.

Modena C., Castegini C., De Zuccato L., Stoppa M. (2004) *Seismic repair and retrofitting: the example of the Albaredo d'Adige Bridge*. Proc. National Conference Giornate AICAP 2004, 26-29 May 2004, Verona.

Modena C., Tecchio G., Pellegrino C., Da Porto F., Donà M., Zampieri P., Zanini M.A. (2015). *Typical deficiencies and strategies for retrofitting RC and masonry arch bridges in seismic areas*. Structure and Infrastructure Engineering, 11(4): 415-442.

Monti G., Nisticò N. (2002) *Simple Probability-Based Assessment of Bridges under Scenario Earthquakes*. Journal of Bridge Engineering; 7(2): 104-114.

Morbin R., Pellegrino C., Grendene M., Modena C. (2010) *Strategies for seismic vulnerability evaluation of common RC bridges typologies*. In Proc. of 14ECEE - 14th European Conference on Earhtquake Engineering 2010. Ohrid, Republic of Macedonia: 30th August – 3rd September.

Morbin R., Zanini M.A., Pellegrino C., Zhang H., Modena C. (2015). *A probabilistic strategy for seismic assessment and FRP retrofitting of existing bridges*. Bulletin of Earthquake Engineering, DOI: 10.1007/s10518-015-9725-2.

Nielson B., DesRoches R. (2007) *Analytical seismic fragility curves for typical bridges in the central and south eastern United States*. Earthquake Spectra, 3(23): 615-633.

OPCM 3362/04 (2004). *Modalità di attivazione Fondo per investimenti straordinari della Presidenza del Consiglio dei Ministri istituito ai sensi dell'art. 32-bis del decreto legge 30 settembre 2003, n°269, convertito, con*

modificazioni, dalla legge 24 novembre 2003, n°326, Ordinancy of the President of the Ministry Council, Rome (*in Italian*).

OpenSees (2001) *Open System for Earthquake Engineering Simulation* – PEER, University of California, Berkeley.

Ordinance of the Presidency of the Council of Ministers n. 3274 of 20 March 2003. *Initial elements on the general criteria for classifying national seismic zones and technical standards for construction*. Official Gazette of the Italian Republic (*in Italian*).

Padgett J.E., DesRoches R. (2008) *Methodology for the development of analytical fragility curves for retrofitted bridges*. Earthquake Engineering & Structural Dynamics; 37 (8): 1157-1174.

Pellegrino C., Franchetti P., Soffiato A., Modena C., Bruno D. (2004) *Evaluation criteria for bridge maintenance*. 2nd International Conference on Bridge Maintenance, Safety and Management, IABMAS '04, 19–22 October 2004, Kyoto, Japan.

Pellegrino C., Modena C. (2010) *Analytical model for FRP confinement of concrete columns with and without internal steel reinforcement*. Journal of Composites for Construction, 14(6): 693-705.

Pellegrino C., Pipinato A., Modena C. (2011) *A simplified management procedure for bridge network maintenance*. Structure and Infrastructure Engineering, 7 (5), 341-351.

Pellegrino C., Zanini M.A., Zampieri P., Modena C. (2014) *Contribution of in situ and laboratory investigations for assessing seismic vulnerability of existing bridges*. Structure and Infrastructure Engineering, DOI: 10.1080/15732479.2014.938661.

Peresan A., Zuccolo E., Vaccari F., Gorshkov A., Panza G.F. (2011) *Neo-deterministic seismic hazard and pattern recognition techniques: Time-dependent scenarios for north-eastern Italy*. Pure and Applied Geophysics, 168:583–607.

Poli M.E., Burrato P., Galadini F., Zanferrari A. (2008) *Seismogenic sources responsible for destructive earthquakes in north-eastern Italy*. Bollettino di Geofisica Teorica ed Applicata, 49: 301-313.

Powers N., Hinkeesing S. (2014) *Deterioration modelling using condition inspection data and engineering judgment.* Proceedings of the 7th International IABMAS Conference on Bridge Maintenance, Safety, Management, Resilience and Sustainability, Shanghai 7th-11th July 2014, ISBN 978-1-138-00103-9.

Rasheeduzzafar J., Al-Saadoun S.S., Al-Gahtani A.S. (1992) *Corrosion cracking in relation to bar diameter, cover and concrete quality*. Journal of Materials in Civil Engineering, 4 (4).

Rebez A., Slejko D. (2004) *Introducing epistemic uncertanties into seismic hazard assessment for the broader Vittorio Veneto area*. Bollettino di Geofisica Teorica ed Applicata 45, 305-320.

RILEM (1996) Durability design of concrete structures. Rep14, E&FN Spon, London.

Risk-UE (2004) *An advanced approach to earthquake risk scenarios with applications to different European Town*. Risk-UE 2004, EVK4,CT 2000-00014.

Roberts J. (2004) *Caltrans structural control for bridges in high-seismic zones*. Earthquake Engineering and Structural Dynamics. 34: 449-470.

Rodriguez J., Ortega L.M., Casal J. (1997) *Load carrying capacity of concrete structures with corroded reinforcement*. Construction and Building Materials, 11(4): 239-248.

Romeo R., Pugliese A. (2000) *Seismicity, seismotectonics and seismic hazard of Italy*. Eng. Geol. 55, 241-266.

Rota M., Pecker A., Bolognini D., Pinho R. (2005) *A methodology for seismic vulnerability of masonry arch bridges walls*. Journal of Earthquake Engineering, 9(2): 331–353.

S.A.MA.R.I.S. (2005) *Sustainable and advanced materials for road infrastructure*. Final report, VI Framework Programme, Brussels.

Sabetta F., Pugliese A. (1996) *Estimation of response spectra and simulation of non-stationary earthquake ground motions*. Bulletin of the Seismological Society of America 86, 2:337-352.

Saydam D., Bocchini P., Frangopol D.M. (2013) *Time-dependent risk associated risk with deterioration of highway bridges*. Engineering Structures, 54: 221-233.

SB-ICA (2007) *Guideline for Inspection and Condition Assessment of Railway Bridges*. [Online] Prepared by Sustainable Bridges – a project within EU FP6. Available from: www.sustainablebridges.net.

Scandone P., Patacca E., Meletti C., Bellatalla M., Perilli N., Santini U. (1992) *Struttura geologica, evoluzione cinematica e schema sismotettonico della penisola italiana*, GNDT, Atti del Convegno 1990 "Zonazione e Riclassificazione Sismica", 1, 119-135. (*in Italian*)

Sgaravato M., Banerjee S., Shinozuka M. (2008) *Seismic risk assessment of highway transportation network and cost-benefit analysis for bridge retrofitting*. Proc. of the 14th World Conference on Earthquake Engineering October 12-17, Beijing, China.

Shahrooz B., Boy S. (2004) *Retrofit of a Three-Span Slab Bridge with Fiber Reinforced Polymer Systems – Testind and Rating*. Journal of Composites for Constructions. 8 (3): 241-247. DOI: 10.1061/(ASCE)1090-0268(2004)8:3(241).

Shinozuka M., Feng M.Q., Lee J., Naganuma T. (2000) *Statistical analysis of fragility curves*. Journal of Engineering Mechanics-Asce; 126 (12): 1224-1231.

Shinozuka M., Kim S.H., Kushiyama S., Yi J.H. (2002) *Fragility Curves of Concrete Bridges Retrofitted by Column Jacketing*. Journal of Earthquake Engineering and engineering vibration; 1 (2): 195-206.

Shinozuka M., Murachi Y., Dong X., Zhou Y., Orlikowsky M. (2003) *Effect of seismic retrofit of bridges on trasportation networks*. Earthquake engineering and engineering vibration; 2 (2): 169-179.

Shinozuka M., Zhou Y., Banerjee S. (2006) *Cost-effectiveness of seismic bridge retrofit*. Proceedings of the IABMAS'06 Conference - Third International Conference on Bridge Maintenance, Safety and Management July 16-19, Porto, Portugal.

Sleijko D., Rebez A. (2002) *Probabilistic seismic hazard assessment and deterministic ground shaking scenarios for Vittorio Veneto (N.E. Italy)*. Bollettino di Geofisica Teorica e Applicata, 43(3-4):263-280.

Slejko D., Rebez A., Santulin M. (2008) *Seismic hazard estimates for Vittorio Veneto boarder area (N.E. Italy)*. Boll. Geof. Teor. Appl. 49: 329-356.

Söderqvist M.K., Veijola M. (2012) *The new management system of engineering structures in Finland*. Proceedings of the 6th International IABMAS Conference on Bridge Maintenance, Safety, Management, Resilience and Sustainability, Stresa 8th-12th July 3162-3169, ISBN 978-0-415-62124-3.

Strand 7 v2.4 (2010) *Strand7 Finite Element System Release 2.4.* Strand 7 Pty Ltd.

Sustainable Bridges (2006). *Guideline for load and resistance assessment of existing European railway bridges – advices on the use of advanced methods*. European research project under the EU 6th framework programme (http://www.sustainablebridges.net/).

Thoft-Christensen P. (1995) *Advanced bridge management systems*. Structural Engineering Review, 7(3), 151–163.

Torkkeli M., Lämsä, J. (2012) *Guidelines and policy for maintaining and managing all engineering structures of the Traffic Agency*. Proceedings of the 6th International IABMAS Conference on Bridge Maintenance, Safety, Management, Resilience and Sustainability, Stresa 8th-12th July 3162-3169, ISBN 978-0-415-62124-3.

I.Br.I.D. Italian Bridge Interactive Database Project (2006) [Online] University of Padua. Available from: http://ibrid.dic.unipd.it /.

Vanmarcke E.H. (1976) *Structural response to earthquakes, in Seismic risk and engineering decisions*. Elsevier Scientific Pub. Co.: distributions for the United States and Canada, Elsevier/North Holland; p. 287-337.

Vidal T., Castel A., François R. (2004) *Analyzing crack width to predict corrosion in reinforced concrete*. Cement and Concrete Research, 34(1): 165-174.

Viganò A., Bressan G., Ranalli G., Martin S. (2008) *Focal mechanism inversion in the Giudicarie-Lessini seismotectonic region (Southern Alps, Italy): insights on tectonic stress and strain*. Tectonophysics, 460: 106-115.

Wang X.H., Liu X.L. (2004) *Modelling effects of corrosion on cover cracking and bond in reinforced concrete*. Magazine of Concrete Research, 4: 191-199.

Yue Y.C., Pozzi M., Zonta D., Zandonini, R. (2012) *Bayesian networks for post-earthquake assessment of bridges*. Proceedings of the 6th International IABMAS Conference on Bridge Maintenance, Safety, Management, Resilience and Sustainability, Stresa 8th-12th July 3162-3169, ISBN 978-0-415-62124-3.

Zanini M.A., Pellegrino C., Morbin R., Modena C. (2013) *Seismic vulnerability of bridges in transport networks subjected to environmental deterioration*. Bulletin of Earthquake Engineering, 11(2):561-579.

Zhang R., Castel A., François R. (2009) *The corrosion pattern of reinforcement and its influence on serviceability of reinforced concrete members in chloride environment*. Cement and Concrete Research, 39(11): 1077-1086.

Zonta D., Zandonini R., Bortot F. (2007) *A reliability-based bridge management concept*. Structure and Infrastructure Engineering, 3(3): 215-235.